



# INVESTIGATING THE FEASIBILITY OF ENERGY HARVESTING USING POTENTIAL ENERGY AT THE TIDAL LOCK IN HEUSDEN AND USING KINETIC ENERGY AT SEVERAL LOCATIONS IN THE SCHELDT RIVER

SECTION REPORT 1: INVESTIGATING THE FEASIBILITY OF ENERGY HARVESTING FROM POTENTIAL ENERGY AT THE LOCK IN HEUSDEN

**VERSION 3.0 - 13 MARCH 2014**

Toon Goormans, Jeroen Verbelen, Cleo Pandelaers, Steven Smets, Roeland Notelé



---

## Colophon

---

Waterwegen en Zeekanaal nv – Afdeling Zeeschelde

Address: Vlaams Administratief Centrum, Anna-Bijnsgebouw, Lange Kievitstraat 111-113, bus 44, 2018 Antwerp, Belgium

☎: + 32 3 224 67 11

📠: + 32 3 224 67 05

Email: [zeeschelde@wenz.be](mailto:zeeschelde@wenz.be)

Website: [www.wenz.be](http://www.wenz.be)

International Marine & Dredging Consultants

Address: Coveliersstraat 15, 2600 Antwerp, Belgium

☎: + 32 3 270 92 95

📠: + 32 3 235 67 11

Email: [info@imdc.be](mailto:info@imdc.be)

Website: [www.imdc.be](http://www.imdc.be)

## Document Identification

Title	Section report 1: Investigating the feasibility of energy harvesting from potential energy at the lock in Heusden
Project	Investigating the feasibility of energy harvesting using potential energy at the tidal lock in Heusden and using kinetic energy at several locations in the Scheldt river
Client	Waterwegen en Zeekanaal NV - Afdeling Zeeschelde
Tender	16EI/11/76
Document ref	I/RA/11407/12.318/TGO
Document name	K:\PROJECTS\11\11407 - Getijden Energie\10-Rap\DO-1 - Potentiële energie\RA12318_Detailed_Feasibility_Tidal_Lock_Heusden\RA12318_Detailed_Feasibility_Tidal_Lock_Heusden_v3.0.docx

## Revision

Version	Date	Description	Author	Checked	Approved	
1.0	28/06/13	Concept report	TGO, JVB	SME	BND	
2.0	04/11/13	Additions after review (10/09/13)	TGO, CPA	SME	BND	
3.0	13/03/14	Change of target power generation time ratio	TGO	SME	BND	3

## Contact within IMDC

<b>Name</b>	<b>Steven Smets</b>
Phone number	+32 3 287 25 03
E-mail	steven.smets@imdc.be

## Distribution List

	Hard copy	
1	Electronic	ir. R. Notelé (W&Z)

## Abstract

Waterwegen en Zeekanaal NV – Department Sea Scheldt is investigating the feasibility of tidal energy harvesting in the Sea Scheldt, on the one hand using potential energy at the to-be-constructed tidal lock in Heusden, and on the other hand using kinetic energy at different locations in the Sea Scheldt. This report describes the results of the detailed feasibility study of tidal energy harvesting using potential energy at the tidal lock in Heusden. A high pressure on the water use, combined with a relatively small head, that moreover varies strongly due to the tide of the Scheldt, make energy harvesting at this location challenging. However, applying suitable technology and controlling the surrounding hydraulic structures makes energy harvesting feasible. Purely financially speaking, it will be very difficult to obtain a profitable project. Nonetheless, other factors could lead to the decision of continuing the efforts for energy harvesting at this location.



## Table of Contents

<b>0</b>	<b>INTRODUCTION.....</b>	<b>10</b>
0.1	THE ASSIGNMENT.....	10
0.2	AIM OF THE STUDY.....	10
0.3	OVERVIEW OF THE STUDY.....	10
0.4	STRUCTURE OF THE REPORT.....	10
<b>1</b>	<b>STUDY AREA.....</b>	<b>12</b>
1.1	THE TIDAL LOCK AT HEUSDEN.....	12
1.2	WATER SCARCITY AROUND GHENT.....	16
<b>2</b>	<b>METHODOLOGY FOR ESTIMATING THE ENERGY YIELD.....</b>	<b>17</b>
2.1	HYDRO POWER GENERATION.....	17
2.2	DIRECT INTEGRATION METHOD.....	17
2.3	LONG-TERM AVERAGE METHOD.....	19
2.3.1	<i>Principle.....</i>	19
2.3.2	<i>Implementation of additional operational rules.....</i>	21
2.3.3	<i>Discussion.....</i>	22
2.4	EXTENDED LONG-TERM AVERAGE METHOD.....	23
2.5	SMALLER HYDRAULIC HEAD RANGE.....	26
<b>3</b>	<b>AVAILABLE DATA.....</b>	<b>27</b>
3.1	WATER LEVEL DATA.....	27
3.2	FLOW DATA.....	29
<b>4</b>	<b>CONSIDERED FLOW SCENARIOS.....</b>	<b>32</b>
4.1	S0: ONLY HYDROLOGICAL RUNOFF.....	32
4.2	S2: EXTRA VOLUME THROUGH THE WEIR CHANNELS.....	35
4.3	DRAINAGE FROM FLOW PASSING EVERGEM.....	38
4.3.1	<i>S3: Daily power generation.....</i>	39
4.3.2	<i>S4: Active recharge of KGT.....</i>	46
4.3.3	<i>S5: Compromise between power generation and water usage.....</i>	55
<b>5</b>	<b>ENERGY YIELD.....</b>	<b>63</b>
5.1	TYPE OF TURBINE.....	63
5.2	CALCULATIONS.....	63
5.3	RESULTS.....	63
5.4	DISCUSSION.....	66
<b>6</b>	<b>CONCEPTUAL DESIGN.....</b>	<b>68</b>
6.1	HYDRAULIC DESIGN.....	68
6.1.1	<i>Geometric boundary conditions.....</i>	68
6.1.2	<i>Elements of the hydraulic circuit.....</i>	68
6.1.3	<i>Hydraulic considerations.....</i>	69
6.2	GEOMETRIC DESIGN.....	71

6.2.1	<i>Layout</i> .....	71
6.2.2	<i>Higher design flow</i> .....	73
6.2.3	<i>Cost estimate</i> .....	73
6.3	RECOMMENDATIONS FOR DETAILED DESIGN .....	75
<b>7</b>	<b>FISH MIGRATION ASPECTS</b> .....	<b>76</b>
7.1	INTRODUCTION .....	76
7.2	SPECIES TO CONSIDER.....	76
7.3	FISH PASSAGE ROUTES AT THE LOCK IN HEUSDEN .....	79
7.3.1	<i>Passage in the landward direction</i> .....	79
7.3.2	<i>Passage in the seaward direction</i> .....	80
7.4	BARRIERS .....	80
7.4.1	<i>Physical barriers</i> .....	80
7.4.2	<i>Behavioural barriers</i> .....	81
7.4.3	<i>Louvre screens</i> .....	87
7.5	CONCLUSION AND RECOMMENDATION.....	87
<b>8</b>	<b>COST-BENEFIT ANALYSIS</b> .....	<b>89</b>
8.1	IDENTIFICATION OF THE COSTS AND BENEFITS .....	89
8.1.1	<i>Costs</i> .....	89
8.1.2	<i>Benefits</i> .....	91
8.2	ECONOMIC EVALUATION.....	94
8.3	RESULTS.....	94
8.3.1	<i>Full implementation</i> .....	95
8.3.2	<i>Phased implementation</i> .....	97
8.3.3	<i>Without governmental support</i> .....	96
8.3.4	<i>Levelized cost of electricity</i> .....	98
8.3.5	<i>Conclusion</i> .....	99
<b>9</b>	<b>CONCLUSIONS</b> .....	<b>100</b>
<b>10</b>	<b>REFERENCE LIST</b> .....	<b>101</b>
<b>11</b>	<b>ANNEXES</b> .....	<b>104</b>
	ANNEX 1 BILL OF QUANTITIES CONCEPTUAL DESIGN - CIVIL WORKS 4 AND 8 m <sup>3</sup> /s .....	104

## List of Tables

TABLE 3-1: CHARACTERISTIC WATER LEVELS OF THE TIDE AT MELLE. ....	29
TABLE 4-1: AVERAGE DAILY RECHARGE FLOW THROUGH ONE WEIR CHANNEL. ....	35
TABLE 4-2: WATER BALANCE PARAMETERS FOR THE SCENARIOS WITH DRAINAGE, WITHOUT PUTTING ADDITIONAL PRESSURE ON THE WATER SUPPLY TO KGT. ....	41
TABLE 4-3: WATER BALANCE PARAMETERS FOR THE SCENARIOS WITH ACTIVE RECHARGE OF KGT, WITHOUT PUTTING ADDITIONAL PRESSURE ON THE WATER SUPPLY TO KGT. ....	48
TABLE 4-4: WATER BALANCE PARAMETERS FOR THE SCENARIOS WITH ACTIVE RECHARGE OF KGT, WITH INCREASE OF THE EXCEEDANCE FREQUENCY OF 13 M <sup>3</sup> /S. ....	56
TABLE 5-1: OVERVIEW OF AVERAGE YEARLY ENERGY YIELD OF THE CONSIDERED SCENARIOS. ....	65
TABLE 6-1: ESTIMATE OF INITIAL INVESTMENT COST. ....	74
TABLE 7-1 : CATCH FREQUENCY FOR FISH SPECIES, EXPRESSED AS PERCENTAGE, FOR THE FRESHWATER ZONE OF THE ZEESCHELDE BETWEEN 1997 AND 2008 (BREINE, 2009) AND SPRINT SPEED (KROES & MONDEN, 2005). ....	78

## List of Figures

FIGURE 1-1: LOCATION OF THE STUDY AREA ZGM, AT THE UPSTREAM END OF THE SEA SCHELDT. ....	13
FIGURE 1-2: MORE DETAILED VIEW OF THE STUDY AREA, AND THE FUTURE LOCK AT HESUDEN. ....	14
FIGURE 1-3: TOP VIEW OF THE CURRENT PRELIMINARY DESIGN OF THE LOCK AT HEUSDEN. THE UPPER REACH IS ON THE LEFT, THE LOWER REACH ON THE RIGHT (IMDC IN ASSOCIATION WITH TRITEL, TECHNUM AND ECOBE, 2011). ....	15
FIGURE 1-4: SIMULATED TIME SERIES OF THE FLOW PASSING THE WEIR STRUCTURE IN EVERGEM, WHICH IS CONSIDERED REPRESENTATIVE FOR THE FLOW TOWARDS KGT. ....	16
FIGURE 2-1: EXAMPLE OF WATER LEVEL DIFFERENCE AND DISCHARGE TIME SERIES AS USED IN THE PREVIOUS STUDY (ADAPTED FROM IMDC, 2011). ....	18
FIGURE 2-2: EXAMPLE OF EFFICIENCY CURVES AS USED IN THE PREVIOUS STUDY (ADAPTED FROM IMDC, 2011). ....	18
FIGURE 2-3: FREQUENCY DISTRIBUTION OF THE FULL HYDRAULIC HEAD TIME SERIES. ....	20
FIGURE 2-4: FREQUENCY DISTRIBUTION OF THE SIMULATED RUNOFF TO THE ZGM REACH, FOR THE ENTIRE SIMULATED PERIOD. ....	21
FIGURE 2-5: FREQUENCY DISTRIBUTION OF THE HYDRAULIC HEAD AFTER APPLYING A THRESHOLD OF 1 M. ONLY THE BLACK PART IS CONSIDERED. ....	22
FIGURE 2-6: FREQUENCY DISTRIBUTION OF THE POWER GENERATION TIME RATIO WHEN DERIVING THE AVAILABLE VOLUMES FROM THE SIMULATED HYDROLOGICAL FLOW. ....	24
FIGURE 2-7: EFFECT OF DECREASING THE DESIGN FLOW ON THE FREQUENCY DISTRIBUTION OF THE POWER GENERATION TIME RATIO. ....	24
FIGURE 3-1: A DETAIL OF THE CALCULATED TIMES SERIES OF THE WATER LEVEL DIFFERENCE BETWEEN UPPER AND LOWER REACH, CONSIDERED REPRESENTATIVE AT THE FUTURE LOCK IN HEUSDEN. ....	28

FIGURE 3-2: DURATION CURVE OF THE CALCULATED WATER LEVEL DIFFERENCE BETWEEN THE UPPER AND LOWER REACH, CONSIDERED REPRESENTATIVE AT THE FUTURE LOCK IN HEUSDEN. ....29

FIGURE 3-3: SKETCH OF THE WATER DISTRIBUTION AROUND GHENT. THE NUMBERS GIVE THE TARGET LEVEL IN MTAW (DE BOECK ET AL., 2012). ....30

FIGURE 3-4: THE AVERAGE DISCHARGE FOR THE SIMULATION WITH THE WATER BALANCE MODEL FOR THE PERIOD 1969-2009 (DE BOECK ET AL., 2012). ....31

FIGURE 3-5: SIMULATED FLOW PASSING IN EVERGEM, AND SIMULATED RUNOFF FLOW TO THE REACH OF THE SEA SCHELDT BETWEEN GENTBRUGGE AND MELLE (ZGM), AND THE SIMULATED FLOW IN EVERGEM. ....31

FIGURE 4-1: TIME SERIES OF THE AVAILABLE FLOW FROM THE SIMULATED HYDROLOGICAL FLOW (S0).32

FIGURE 4-2: FREQUENCY DISTRIBUTION OF THE AVAILABLE FLOW FROM THE SIMULATED HYDROLOGICAL FLOW (S0). ....33

FIGURE 4-3: DURATION CURVE OF THE AVAILABLE FLOW FROM THE SIMULATED HYDROLOGICAL FLOW (S0). ....33

FIGURE 4-4: FREQUENCY DISTRIBUTION OF THE POWER GENERATION TIME RATIO FROM THE SIMULATED HYDROLOGICAL FLOW (S0), FOR DESIGN FLOWS  $Q_d = 2$  AND  $4 \text{ m}^3/\text{s}$ . ....34

FIGURE 4-5: TIME SERIES OF THE AVAILABLE FLOW WHEN CONSIDERING THE RECHARGE FLOW FROM TWO WEIR CHANNELS (S2A AND S2B). ....36

FIGURE 4-6: DURATION CURVE OF THE AVAILABLE FLOW WHEN USING THE RECHARGE FLOW FROM TWO WEIR CHANNELS (S2A AND S2B). ....36

FIGURE 4-7: FREQUENCY DISTRIBUTION OF THE POWER GENERATION TIME RATIO WHEN USING THE RECHARGE FLOW FROM ONE WEIR CHANNEL, THAT IS CLOSED ON 5.5 MTAW (S2A), FOR DESIGN FLOWS  $Q_d = 2, 4$  AND  $8 \text{ m}^3/\text{s}$ . ....37

FIGURE 4-8: FREQUENCY DISTRIBUTION OF THE POWER GENERATION TIME RATIO WHEN USING THE RECHARGE FLOW FROM ONE WEIR CHANNEL, THAT IS CLOSED ON 6.5 MTAW (S2B), FOR DESIGN FLOWS  $Q_d = 2, 4$  AND  $8 \text{ m}^3/\text{s}$ . ....38

FIGURE 4-9: TIME SERIES OF THE AVAILABLE FLOW WHEN CONSIDERING THE RECHARGE FLOW FROM TWO WEIR CHANNELS, WITH AN ADDITIONAL FLOW DRAINED FROM KGT WHEN NECESSARY AND POSSIBLE, FOR A DESIGN FLOW OF  $2 \text{ m}^3/\text{s}$  (S3A.2). ....42

FIGURE 4-10: TIME SERIES OF THE AVAILABLE FLOW WHEN CONSIDERING THE RECHARGE FLOW FROM TWO WEIR CHANNELS, WITH AN ADDITIONAL FLOW DRAINED FROM KGT WHEN NECESSARY AND POSSIBLE, FOR A DESIGN FLOW OF  $4 \text{ m}^3/\text{s}$  (S3A.4). ....42

FIGURE 4-11: TIME SERIES OF THE AVAILABLE FLOW WHEN CONSIDERING THE RECHARGE FLOW FROM TWO WEIR CHANNELS, WITH AN ADDITIONAL FLOW DRAINED FROM KGT WHEN NECESSARY AND POSSIBLE, FOR A DESIGN FLOW OF  $8 \text{ m}^3/\text{s}$  (S3A.8). ....43

FIGURE 4-12: DURATION CURVES OF THE AVAILABLE FLOW WHEN USING THE RECHARGE FLOW FROM TWO WEIR CHANNELS, WITH AN ADDITIONAL FLOW DRAINED FROM KGT WHEN NECESSARY AND POSSIBLE. ....43

FIGURE 4-13: FREQUENCY DISTRIBUTION OF THE POWER GENERATION TIME RATIO WHEN USING THE RECHARGE FLOW FROM TWO WEIR CHANNELS, WITH AN ADDITIONAL DIVERTED FLOW FROM KGT WHEN NECESSARY AND POSSIBLE (S3A.2, S3A.4 AND S3A.8). ....44

FIGURE 4-14: FREQUENCY DISTRIBUTION OF THE POWER GENERATION TIME RATIO WHEN USING THE RECHARGE FLOW FROM TWO WEIR CHANNELS, WITH AN ADDITIONAL DIVERTED FLOW FROM KGT WHEN NECESSARY AND POSSIBLE (S3B.2, S3B.4 AND S3B.8). ....45



FIGURE 4-15: DURATION CURVE OF THE DRAINED FLOW, DAILY AVERAGED, FROM KGT TO ZGM WHEN GENERATING POWER ON A DAILY BASIS (S3A AND S3B). .....46

FIGURE 4-16: TIME SERIES OF THE AVAILABLE FLOW WHEN COMBINING FLOW DIVERSION FROM AND ACTIVE RECHARGE TO KGT, FOR A DESIGN FLOW OF 2 M<sup>3</sup>/S (S4A.2 AND S4B.2). .....49

FIGURE 4-17: TIME SERIES OF THE AVAILABLE FLOW WHEN COMBINING FLOW DIVERSION FROM AND ACTIVE RECHARGE TO KGT, FOR A DESIGN FLOW OF 4 M<sup>3</sup>/S (S4A.4 AND S4B.4).....49

FIGURE 4-18: TIME SERIES OF THE AVAILABLE FLOW WHEN COMBINING FLOW DIVERSION FROM AND ACTIVE RECHARGE TO KGT, FOR A DESIGN FLOW OF 8 M<sup>3</sup>/S (S4A.8 AND S4B.8).....50

FIGURE 4-19: DURATION CURVE OF THE AVAILABLE FLOW WHEN COMBINING FLOW DRAINAGE FROM AND ACTIVE RECHARGE TO KGT, AND A GATE CLOSURE LEVEL OF 5.5 MTAW (S4A.2, S4A.4 AND S4A.8). .....51

FIGURE 4-20: DURATION CURVE OF THE AVAILABLE FLOW WHEN COMBINING FLOW DRAINAGE FROM AND ACTIVE RECHARGE TO KGT, AND A GATE CLOSURE LEVEL OF 6.5 MTAW (S4B.2, S4B.4 AND S4B.8). .....51

FIGURE 4-21: FREQUENCY DISTRIBUTION OF THE POWER GENERATION TIME RATIO WHEN COMBINING FLOW DRAINAGE FROM AND ACTIVE RECHARGE TO KGT, AND A GATE CLOSURE LEVEL OF 5.5 MTAW (S4A.2, S4A.4 AND S4A.8). .....52

FIGURE 4-22: FREQUENCY DISTRIBUTION OF THE POWER GENERATION TIME RATIO WHEN COMBINING FLOW DRAINAGE FROM AND ACTIVE RECHARGE TO KGT, AND A GATE CLOSURE LEVEL OF 6.5 MTAW (S4B.2, S4B.4 AND S4B.8). .....52

FIGURE 4-23: DURATION CURVE OF THE DIVERTED FLOW, DAILY AVERAGED, FROM KGT TO ZGM WHEN COMBINING FLOW DRAINAGE FROM AND ACTIVE RECHARGE TO KGT (S4).....53

FIGURE 4-24: TWO-MONTHLY AVERAGED SIMULATED DAILY FLOW PASSING EVERGEM, FOR THE CURRENT SITUATION (WITHOUT RECHARGE OR DRAINAGE) AND THE SITUATION WITH ACTIVE RECHARGE AND DRAINAGE (AND A CLOSURE LEVEL OF THE WEIR CHANNELS GATES OF 5.5 MTAW, S4A.4), FOR THE YEARS 1996-1998.....54

FIGURE 4-25: TWO-MONTHLY AVERAGED SIMULATED DAILY FLOW PASSING EVERGEM, FOR THE CURRENT SITUATION (WITHOUT RECHARGE OR DRAINAGE) AND THE SITUATION WITH ACTIVE RECHARGE AND DRAINAGE (AND A CLOSURE LEVEL OF THE WEIR CHANNELS GATES OF 5.5 MTAW, S4A.4), FOR THE PERIOD APRIL–OCTOBER 1997.....55

FIGURE 4-26: TIME SERIES OF THE AVAILABLE FLOW WHEN COMBINING FLOW DIVERSION FROM AND ACTIVE RECHARGE TO KGT, WHILST ALSO IMPROVING THE WATER BALANCE, FOR A DESIGN FLOW OF 2 M<sup>3</sup>/S (S5A.2 AND S5B.2). .....57

FIGURE 4-27: TIME SERIES OF THE AVAILABLE FLOW WHEN COMBINING FLOW DIVERSION FROM AND ACTIVE RECHARGE TO KGT, WHILST ALSO IMPROVING THE WATER BALANCE, FOR A DESIGN FLOW OF 4 M<sup>3</sup>/S (S5A.4 AND S5B.4). .....57

FIGURE 4-28: TIME SERIES OF THE AVAILABLE FLOW WHEN COMBINING FLOW DIVERSION FROM AND ACTIVE RECHARGE TO KGT, WHILST ALSO IMPROVING THE WATER BALANCE, FOR A DESIGN FLOW OF 8 M<sup>3</sup>/S (S5A.8 AND S5B.8). .....58

FIGURE 4-29: DURATION CURVE OF THE AVAILABLE FLOW WHEN COMBINING FLOW DIVERSION FROM AND ACTIVE RECHARGE TO KGT, WHILST ALSO IMPROVING THE WATER BALANCE, AND A GATE CLOSURE LEVEL OF 5.5 MTAW (S5A.2, S5A.4 AND S5A.8).....59

FIGURE 4-30: DURATION CURVE OF THE AVAILABLE FLOW WHEN COMBINING FLOW DIVERSION FROM AND ACTIVE RECHARGE TO KGT, WHILE ALSO IMPROVING THE WATER BALANCE, AND A GATE CLOSURE LEVEL OF 6.5 MTAW (S5B.2, S5B.4 AND S5B.8).....59



FIGURE 4-31: FREQUENCY DISTRIBUTION OF THE POWER GENERATION TIME RATIO WHEN COMBINING FLOW DIVERSION FROM AND ACTIVE RECHARGE TO KGT, WHILST ALSO IMPROVING THE WATER BALANCE, AND A GATE CLOSURE LEVEL OF 5.5 MTAW (S5A.2, S5A.4 AND S5A.8). .....60

FIGURE 4-32: FREQUENCY DISTRIBUTION OF THE POWER GENERATION TIME RATIO WHEN COMBINING FLOW DIVERSION FROM AND ACTIVE RECHARGE TO KGT, WHILST ALSO IMPROVING THE WATER BALANCE, AND A GATE CLOSURE LEVEL OF 6.5 MTAW (S5B.4 AND S5B.8).....60

FIGURE 4-33: DURATION CURVE OF THE DIVERTED FLOW, DAILY AVERAGED, FROM KGT TO ZGM WHEN COMBINING FLOW DIVERSION FROM AND ACTIVE RECHARGE TO KGT, WHILST ALSO IMPROVING THE WATER BALANCE (S5). THE GREEN LINES ARE THE CURVES OF THE CORRESPONDING S4-SCENARIOS.....61

FIGURE 4-34: TWO-MONTHLY AVERAGED SIMULATED DAILY FLOW PASSING EVERGEM, FOR THE CURRENT SITUATION (WITHOUT RECHARGE OR DRAINAGE), THE SITUATION WITH ACTIVE RECHARGE AND DRAINAGE (S4B.4), AND THE COMPROMISE BETWEEN POWER GENERATION AND WATER USAGE (S5B.4), FOR THE PERIOD APRIL–OCTOBER 1997. ....62

FIGURE 5-1: AVERAGE YEARLY ENERGY YIELD FOR THE DIFFERENT CONSIDERED SCENARIOS.....66

FIGURE 5-2: VARIATION OF THE AVERAGE YEARLY ENERGY YIELD WITH DESIGN FLOW, IN SCENARIO S2B.67

FIGURE 6-1 : INTEGRATION OF THE HYDROPOWER STATION INTO THE DESIGN OF THE LOCK. ....71

FIGURE 6-2: GEOMETRIC DESIGN OF THE HYDROPOWER STATION – TOP VIEW. ....72

FIGURE 6-3: GEOMETRIC DESIGN OF THE HYDROPOWER STATION – SIDE VIEW. ....72

FIGURE 7-1 : CONCEPT DIAGRAM OF THE GRADUATED OUTPUT OF A GFFB ELECTRIC DETERRENCE ARRAY TO GUIDE UPSTREAM-MOVING FISH INTO A DIVERSION CHANNEL. THE GRADIENT [V/CM] INCREASES AS FISH MOVE UPSTREAM (TAKEN FROM BURGER ET AL., 2012). .....82

FIGURE 7-2: PICTORIAL DIAGRAM OF THE ELECTRODE SPACING (TOP LEFT), A SINGLE ELECTRODE (TOP RIGHT) AND AN EXAMPLE OF A POSSIBLE SET UP (UNDER) (TAKEN FROM FISHWAYS GLOBAL, 2013).83

FIGURE 7-3: BIO-ACOUSTIC FISH FENCE (TAKEN FROM OVIVO, 2013).....86

FIGURE 8-1: SPECIFIC COST OF INSTALLED POWER AS A FUNCTION OF HEAD. ....90

FIGURE 8-2: TYPICAL TURN-KEY INVESTMENT COSTS FOR SMALL HYDROPOWER PLANTS. ....90

FIGURE 8-3: EVOLUTION OF THE PRICE OF ELECTRICITY [€/MWH] BETWEEN 30/03/2013 AND 28/06/2013, ON THE BELGIAN STOCK EXCHANGE AND THAT OF ITS NEIGHBOURING COUNTRIES THE NETHERLANDS (APX), FRANCE (EPEX SPOT FR) AND GERMANY (EPEX SPOT DE) (BELPEX, 2013A).....92

FIGURE 8-4: MONTHLY AVERAGE OF THE DAILY AVERAGED BELPEX INDEX [€/MWH], FOR THE YEAR 2013 (SOURCE: BELPEX, 2013B).....92

FIGURE 8-5 : EVOLUTION OF THE AVERAGE MONTHLY PRICE PER GREEN POWER CERTIFICATE (GPC) (VREG, 2014). ....93

FIGURE 8-6: RATIO OF NET PRESENT VALUE TO INITIAL INVESTMENT THROUGH TIME, FOR S2B.4 AND S4B.8. ....95

FIGURE 8-7: RATIO OF NET PRESENT VALUE TO INITIAL INVESTMENT THROUGH TIME, FOR S2B.4 AND S4B.8, WHEN ONLY THE COSTS FOR INTAKE, ENERGY PRODUCTION AND OUTLET ARE CONSIDERED.97

FIGURE 8-8: RATIO OF NET PRESENT VALUE TO INITIAL INVESTMENT THROUGH TIME, FOR S2B.4 AND S4B.8, WITHOUT GREEN POWER CERTIFICATES. ....96

FIGURE 8-9: ESTIMATED LEVELIZED COST OF NEW ELECTRIC GENERATING TECHNOLOGIES IN 2018 [2011 \$/MWH]. ....98

## 0 INTRODUCTION

### 0.1 THE ASSIGNMENT

This assignment concerns the investigation of energy harvesting possibilities using potential energy at the tidal lock in Heusden and using kinetic energy at several locations in the Sea Scheldt river.

Waterwegen en Zeekanaal nv is participating in the European project PRO-TIDE, funded by the Interreg IVB North-West Europe program. The main goal of this project is “to increase the use of renewable energy by promoting innovative, sustainable and cost effective solutions for tidal energy through research, development, testing and comparison of different forms of tidal energy at different locations and circumstances, in coastal zones and estuaries”.

### 0.2 AIM OF THE STUDY

In a previous study the feasibility of harvesting tidal energy on the Sea Scheldt was considered in more general terms. Different techniques were described, that are applicable at several types of locations, such as tidal measuring stations, inlet-outlet structures or the lock to be constructed in Heusden, that has a downstream water level influenced by the tide (IMDC, 2011).

10

Harvesting tidal energy at the lock appeared to be feasible, given certain assumptions and conditions. In this study the feasibility is studied in more detail, taking additionally into account the water availability around Ghent and the hydraulics of the inlet to and outlet from the turbine. Also a conceptual design is developed so as to estimate the civil costs in more detail.

### 0.3 OVERVIEW OF THE STUDY

This section report 1 is part of a series of reports which together describe the complete study:

Section report 1: Investigating the feasibility of energy harvesting from potential energy at the lock in Heusden (I/RA/11407/12.318/TGO).

Section report 2: Current measurements in the Sea Scheldt (I/RA/11407/13.217/KVT).

Section report 3: Feasibility of harvesting tidal current energy in the Sea Scheldt (I/RA/11407/13.168/TGO).

### 0.4 STRUCTURE OF THE REPORT

The report starts with a brief description of the study area, together with the governing issues related to the water balance around Ghent (Chapter 1). Then, the methodology that has been developed to estimate the energy yield for different scenarios, is explained in detail in Chapter 2, after which the available data are described. Once the methodology

is made clear and the available data are illustrated, the report elaborates on the considered scenarios in terms of water usage and possible redistribution (Chapter 4).

Then, the developed methodology is applied to the different scenarios, to calculate the yearly average energy yield (Chapter 5). Chapter 6 explains the conceptual design of the hydropower station, with a focus on the hydraulic aspects. Also, a cost estimate is made in this chapter, for two different sizes of turbines. In Chapter 7 the impact of a hydropower plant at Heusden on fish migration is discussed, as well as mitigating measures. Finally, the cost estimates from Chapter 6 serve as input to the cost-benefit analysis in Chapter 8, that investigates the financial feasibility of energy harvesting at the lock in Heusden.

## 1 STUDY AREA

*This chapter describes the study area in more detail. First, an overview is given on why it was decided to construct a lock, where it will be implemented and how the preliminary design looks like. After that, the issue of water scarcity around Ghent is explained briefly.*

### 1.1 THE TIDAL LOCK AT HEUSDEN

The Sea Scheldt is that part of the Scheldt river in Flanders that is influenced by the tides. The construction of the lock at Heusden fits in a multidisciplinary project to redevelop the most upstream part of the Sea Scheldt. Currently, the tidal influence in the 8 km long upstream stretch of the Sea Scheldt between Melle and Gentbrugge reaches up to the existing weir complex in Gentbrugge, in the eastern part of the city of Ghent. Throughout the text, this reach is referred to as ZGM ("Zeeschelde Gentbrugge-Melle"). Its location relative to the Sea Scheldt is indicated in Figure 1-1.

The redevelopment project is part of the Sigmoplan, a large multidisciplinary project approved in 2005 by the Flemish Government to enhance the protection against flooding on the Sea Scheldt and at the same time to obtain a robust self-conserving ecosystem. In addition, the Sigmoplan integrates the recreational and economical functions of the Sea Scheldt.

A significant increase in traffic is expected on the shipping route between Antwerp and Ghent via the river Sea Scheldt and the Ringvaart, part of the TEN-T (Trans-European Transport Network), due to the upgrade of the inland waterways network connecting the Seine and the Scheldt basin. Re-enabling navigability of the Sea Scheldt towards Gentbrugge for recreational shipping will offer a solution for capacity and safety issues on the Ringvaart. Currently there is interference of commercial shipping (ship class CEMT IV) and recreational shipping.

12

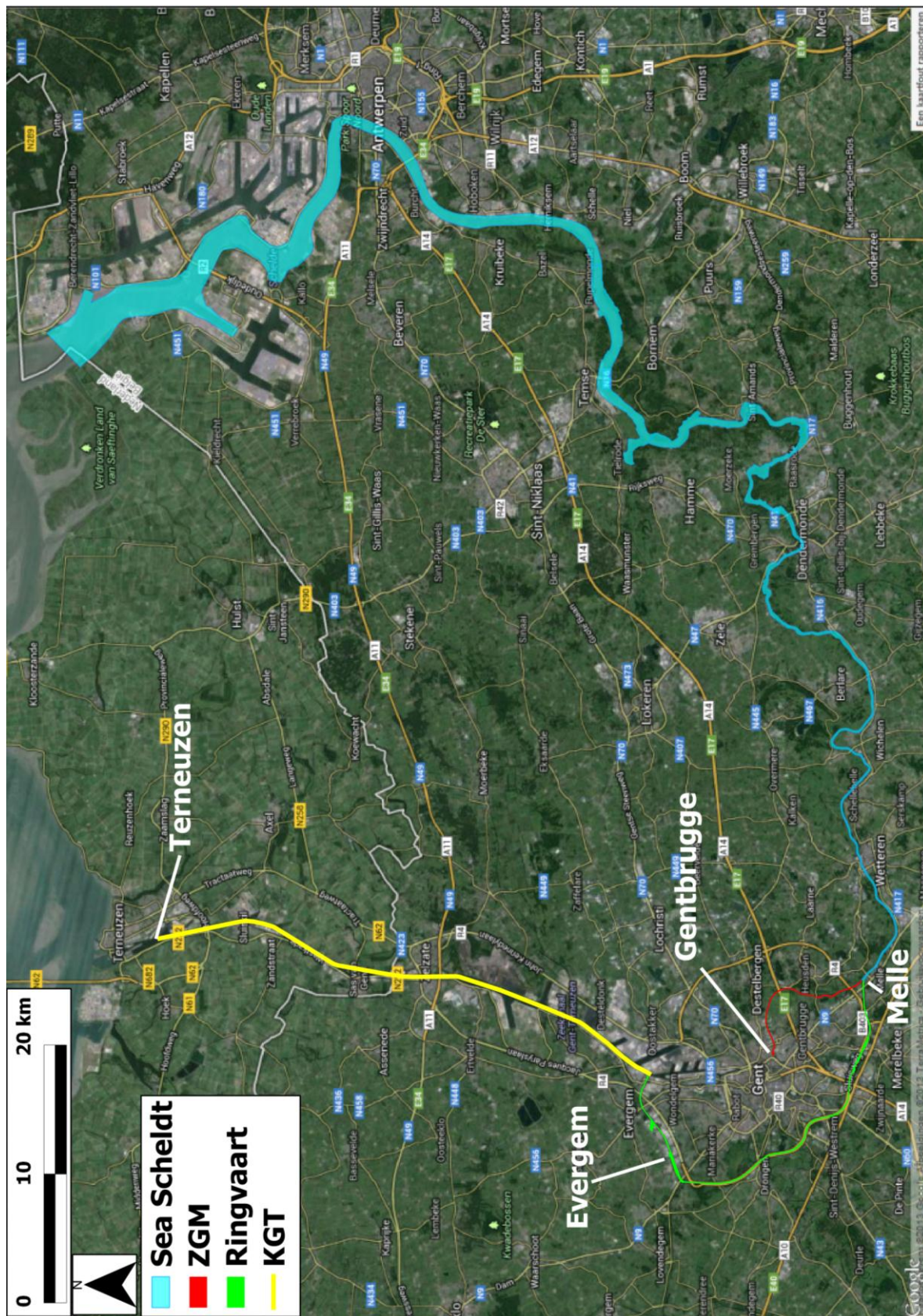


Figure 1-1: Location of the study area ZGM, at the upstream end of the Sea Scheldt<sup>1</sup>.

<sup>1</sup> Source satellite image: Google Maps.

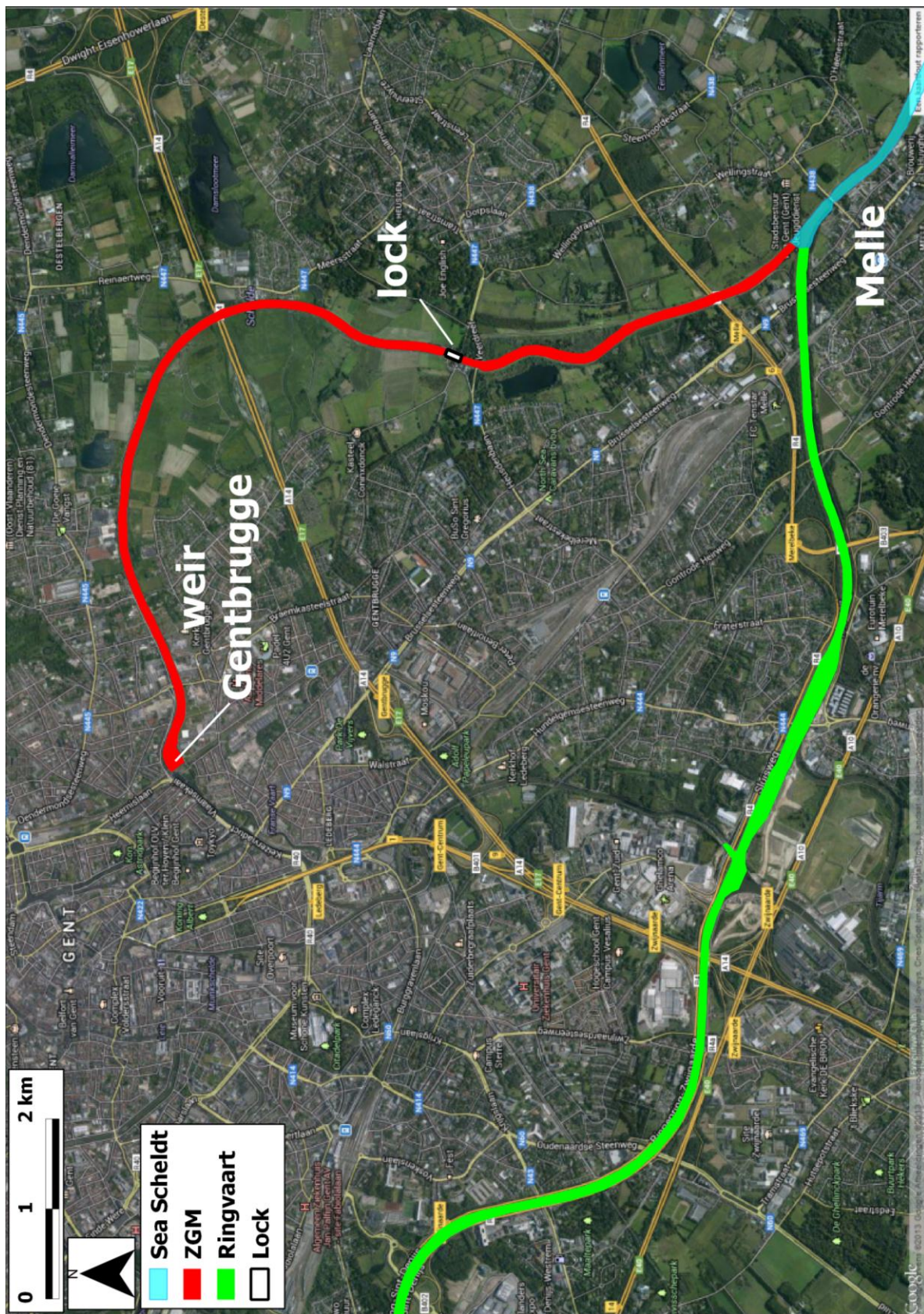


Figure 1-2: More detailed view of the study area, and the future lock at Hesuden<sup>2</sup>.

<sup>2</sup> Source satellite image: Google Maps.

Figure 1-3 shows a plan view of the current preliminary design of the lock. Given a lock width of 8 m, an almost equal positive and negative water level difference of 3 m and the specific location of the new lock, a single leaf pivoting gate in combination with a latching frame to resist negative hydraulic loads is proposed. It can be noted that this type of gate has never been used before in Flanders. An intermediate gate is foreseen as well, and will benefit the waiting time in low season and reduce water use in dry periods.

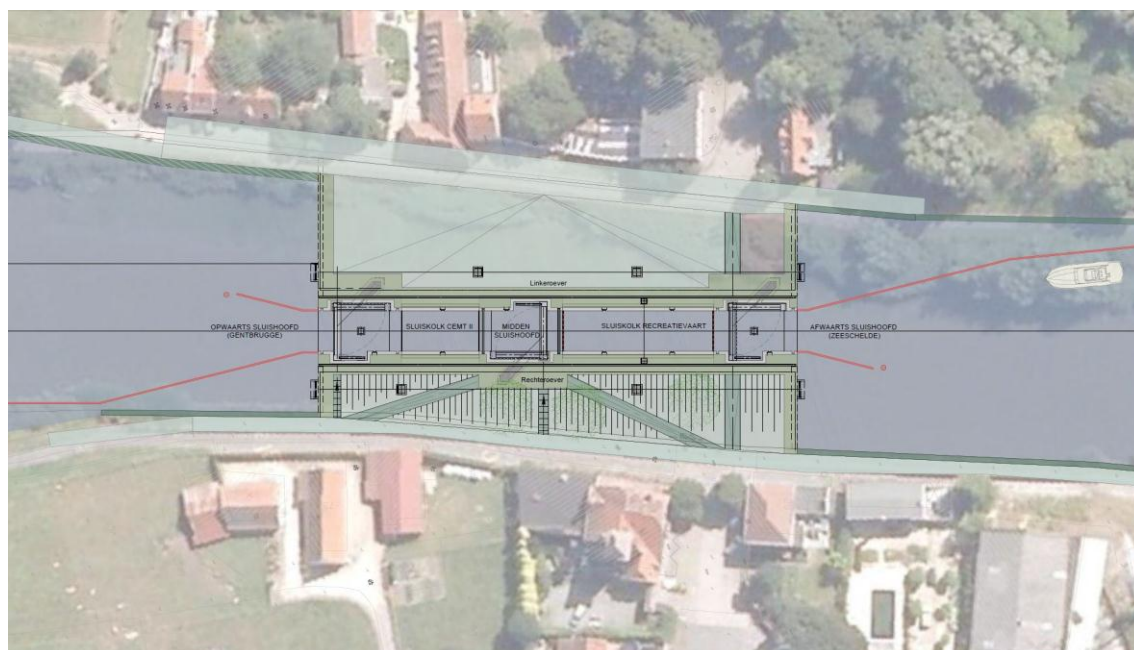


Figure 1-3: Top view of the current preliminary design of the lock at Heusden. The upper reach is on the left, the lower reach on the right (IMDC in association with Tritel, Technum and Ecobe, 2011).

Two weir channels are foreseen through the lock system, (i) to enable flow from the upstream reach to the Sea Scheldt during periods with high rainfall amounts, (ii) to enable flow from the Sea Scheldt to the upstream reach at high tide to alleviate water scarcity during dry periods (see below) and, (iii) to guarantee fish passage in both directions, depending on the tide. In the preliminary design, these weir channels are each 3 m wide and 2.2 m high, with both invert levels at 3.85 mTAW<sup>3</sup>. Stop logs are foreseen at the downstream end of each weir channel to create a backwater effect that results in the target water level in the upstream reach.

During periods of extreme high water levels in the Sea Scheldt, the weir channels will be closed to protect the landward areas. For this, the downstream end of the weir channels will be fitted with automatic gates. The Sea Scheldt water level at which the gates should close, is not yet determined.

<sup>3</sup> TAW = 'Tweede Algemene Waterpassing'. It is the reference level at which elevation values are expressed in Belgium. Zero meters TAW (mTAW) corresponds to the mean sea level at low tide in Ostend.

## 1.2 WATER SCARCITY AROUND GHENT

The harbour of Ghent is connected to the Westerscheldt, and hence the North Sea, via the channel between Ghent and the lock complex in Terneuzen (The Netherlands), as indicated on Figure 1-1. This channel will often be referred to as KGT ("kanaal Gent-Terneuzen") in the remainder of this report. Since the lock complex in Terneuzen connects a fresh water system with the salt water in the Westerscheldt, inland salt intrusion occurs.

In order to keep this salinisation within acceptable boundaries, a minimal flow towards the lock complex of Terneuzen is required. Belgium and The Netherlands signed a treaty stating that Belgium will provide KGT with a minimal flow of 13 m<sup>3</sup>/s, after applying a moving average with a time window of 2 months. For this study, the flow passing the weir in Evergem is considered as representative flow towards KGT. As can be seen in Figure 1-4, the threshold of 13 m<sup>3</sup>/s cannot always be reached. After performing long-term simulations with the water balance model around Ghent, De Boeck et al. (2012) concluded that, in the current situation, the threshold is not exceeded during about 3.5 months per year, on average.

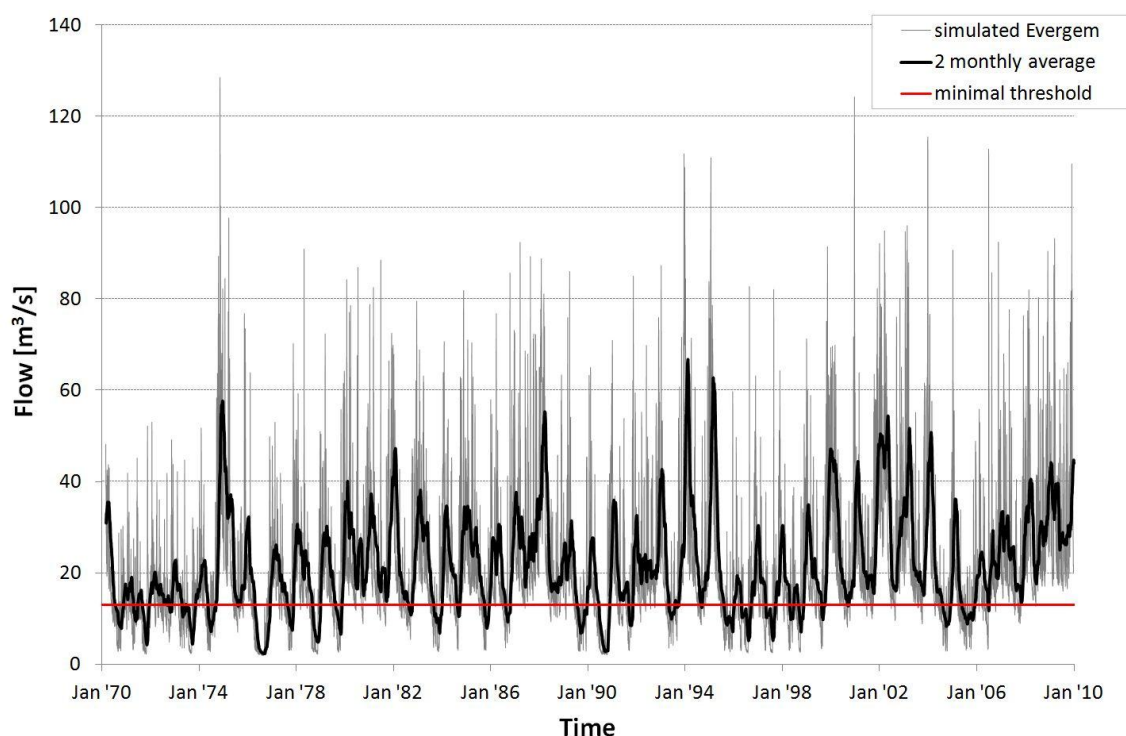


Figure 1-4: Simulated time series of the flow passing the weir structure in Evergem, which is considered representative for the flow towards KGT.

## 2 METHODOLOGY FOR ESTIMATING THE ENERGY YIELD

*This chapter describes the methodology used to calculate the expected energy yield at the lock. It starts with a brief explanation of the method used in the previous study (IMDC, 2011), in which the energy yield is calculated from a direct integration of generated power. After that, the method used in this study is described more elaborately. It is based on duration curves of both discharge and water level.*

### 2.1 HYDRO POWER GENERATION

It can be shown that the power generated by a turbine  $P$  [W] can be calculated as:

$$P = \eta \cdot \rho \cdot g \cdot Q \cdot \Delta H \quad (1)$$

in which:

$\eta$	= combined efficiency of all electromechanical components required for electricity generation	[-]
$\rho$	= density of water	[kg/m <sup>3</sup> ]
$g$	= gravitational acceleration	[m/s <sup>2</sup> ]
$Q$	= discharge passing the turbine	[m <sup>3</sup> /s]
$\Delta H$	= head over the turbine	[m]

The efficiency depends on the flow conditions, hence  $\eta(Q, \Delta H_{net})$ . The energy yield  $E$  [J] during a certain time period with duration  $T$  [s] hence is easily calculated by integrating the generated power over time:

$$E = \int_0^T P(t) \cdot dt = \rho \cdot g \cdot \int_0^T \eta(Q(t), \Delta H(t)) \cdot Q(t) \cdot \Delta H(t) \cdot dt \quad (2)$$

Mostly,  $E$  is expressed in kWh, 1 kWh being the amount of energy corresponding to a power source of 1 kW active during 1 hour; 1 kWh = 3.6 x 10<sup>6</sup> J. In Flanders, the average amount of energy consumed by a household is 3500 kWh per year (VREG, 2014)<sup>4</sup>.

### 2.2 DIRECT INTEGRATION METHOD

In IMDC (2011) the average yearly energy yield was calculated by directly applying Equation (2). First, the time series  $Q(t)$  was derived from  $\Delta H(t)$  using basic hydraulic considerations, resulting in the time series depicted in Figure 2-1. The variability of  $\eta$  was taken into account by allowing a variation with discharge, depending on turbine type, as shown in Figure 2-2. A variation with head was not considered.

<sup>4</sup> Not taking electrical heating into account.

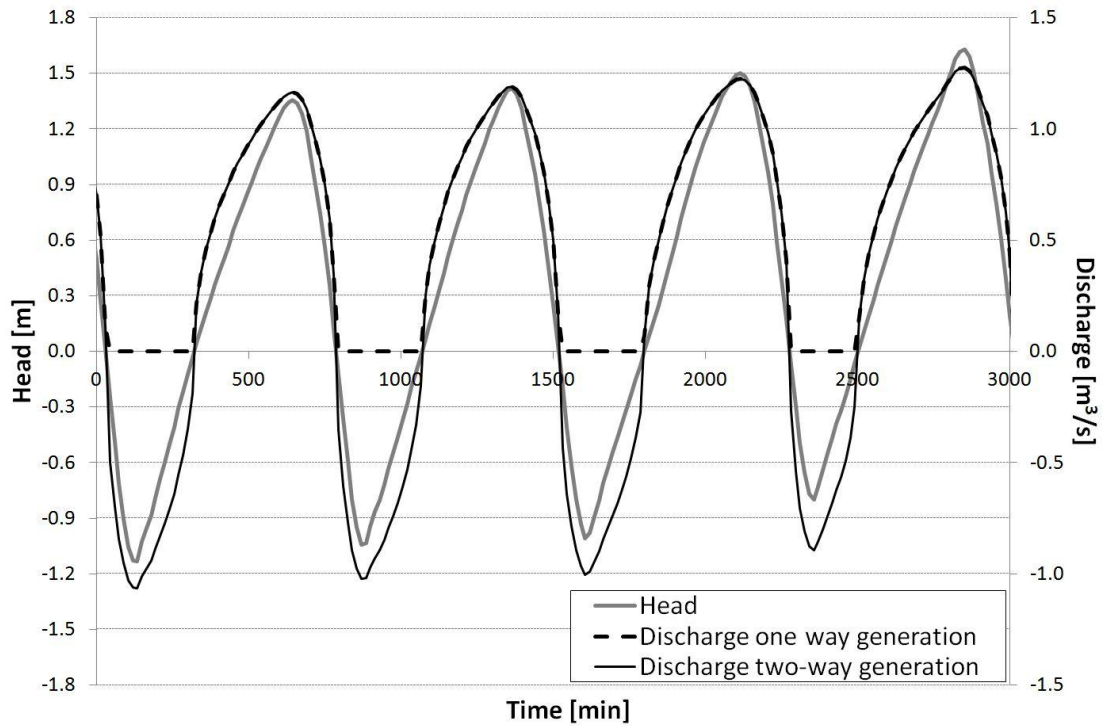


Figure 2-1: Example of water level difference and discharge time series as used in the previous study (adapted from IMDC, 2011).

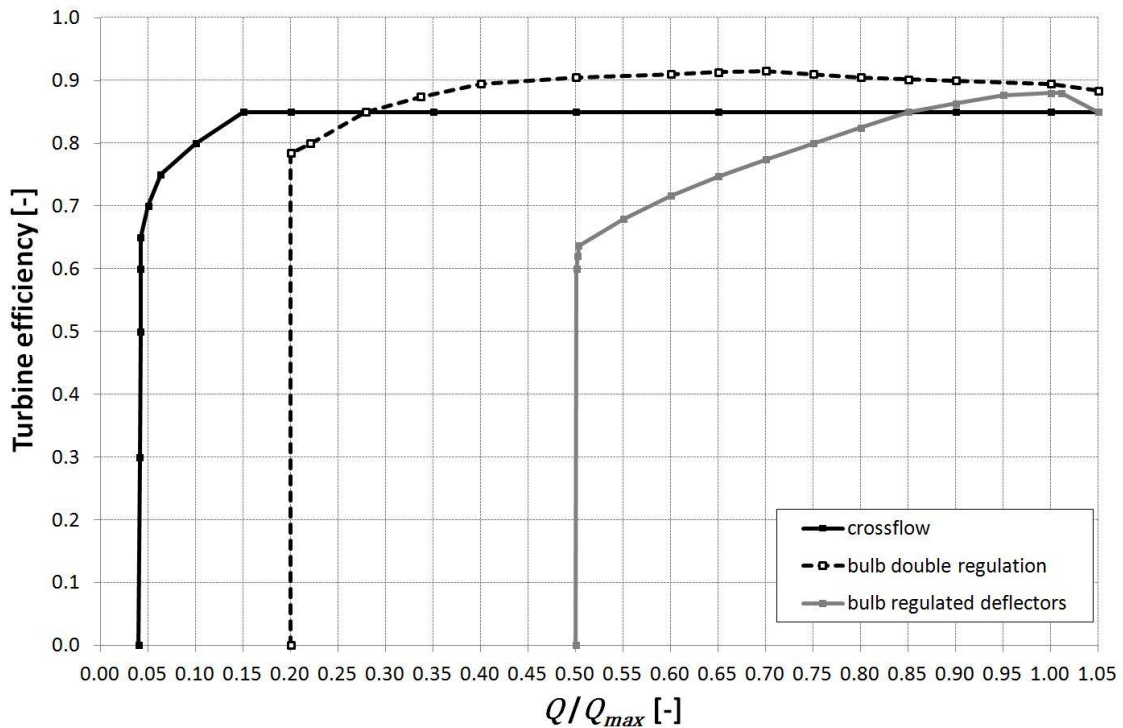


Figure 2-2: Example of efficiency curves as used in the previous study (adapted from IMDC, 2011).

Then,  $P(t)$  was calculated using Equation (1), resulting in time series of generated power for the considered turbine types and turbine configurations. Finally, these series were

integrated (Equation (2)) and averaged over a year to obtain the average yearly energy yield  $E_{year}$ . For time series with a time resolution  $\Delta t$ :

$$E_{year} = \frac{1}{Y} \sum_{i=1}^N P_i \cdot \Delta t = \rho \cdot g \cdot \frac{\Delta t}{Y} \cdot \sum_{i=1}^N \eta_i \cdot Q_i \cdot \Delta H_i \quad (3)$$

in which:

$Y$	=	number of years in the considered time period	[years]
$N$	=	number of time steps in the considered time period	[-]
$P_i$	=	power generated during the time interval $t_i - t_{i-1}$	[W]
$\eta_i$	=	turbine efficiency for a discharge $Q_i$	[-]
$Q_i$	=	discharge passing the turbine during the time interval $t_i - t_{i-1}$	[m <sup>3</sup> /s]
$\Delta H_i$	=	head over the turbine during the time interval $t_i - t_{i-1}$	[m]

## 2.3 LONG-TERM AVERAGE METHOD

### 2.3.1 PRINCIPLE

The direct integration method is relatively straightforward to apply. Moreover, certain operation rules, such as setting threshold levels of minimum head or discharge below which no power generation will take place, are easily considered. However, its application in the previous study had one major drawback: the implicit assumption that there were no restrictions regarding the available flow that could be used for power generation. After all, the flow times series was derived from the time series of the available head, without considering whether this flow is available.

The water balance model can deliver time series of *available* flow. However, the time resolution of these series are daily based, while the head strongly varies during one day, so it is not possible to apply Equation (3) directly. In this section, another method is described, to cope with flow and head time series with different time resolutions. *The method's major assumption is that  $\Delta H$  and  $Q$  are uncoupled – i.e. that the flow  $Q$  can be used for power generation throughout the entire day regardless of  $\Delta H$ .*

If this assumption holds, then the average yearly energy yield can be calculated using the average values for  $\Delta H$  and  $Q$ . These values can be determined from the frequency distributions of both parameters. For  $\Delta H$  with a frequency distribution  $f(\Delta H)$ , and after discretization in classes  $\Delta H_j$  each with a frequency of occurrence  $f_j$ , this gives:

$$\Delta H_{avg} = \sum_{j=1}^n f_j \cdot \Delta H_j \quad (4)$$

in which  $n$  is the number of head classes. The sum of all frequencies should equal to 1. For  $Q$  with a frequency distribution  $g(Q)$ , and after discretization in classes  $Q_k$  each with a frequency of occurrence  $g_k$ , this gives:

$$Q_{avg} = \sum_{k=1}^m g_k \cdot Q_k \quad (5)$$

in which  $m$  is the number of flow classes. Actually, since the efficiency is varying with the discharge passing the turbine, it should be included in the summation. Hence Equation (7) should be rewritten as:

$$(\eta \cdot Q)_{avg} = \sum_{k=1}^m g_k \cdot \eta_k \cdot Q_k \quad (6)$$

As an example, Figure 2-3 shows the frequency distribution of the water level difference, based on the entire available time series as described in §3.1, while Figure 2-4 shows the frequency distribution of the runoff to the ZGM reach, as simulated by the hydrological submodel of the water balance model, for the entire period, as described in §3.2. Each bar in the graph hence represents a value  $f_j$  or  $g_k$  as used in Equations (6) and (8).

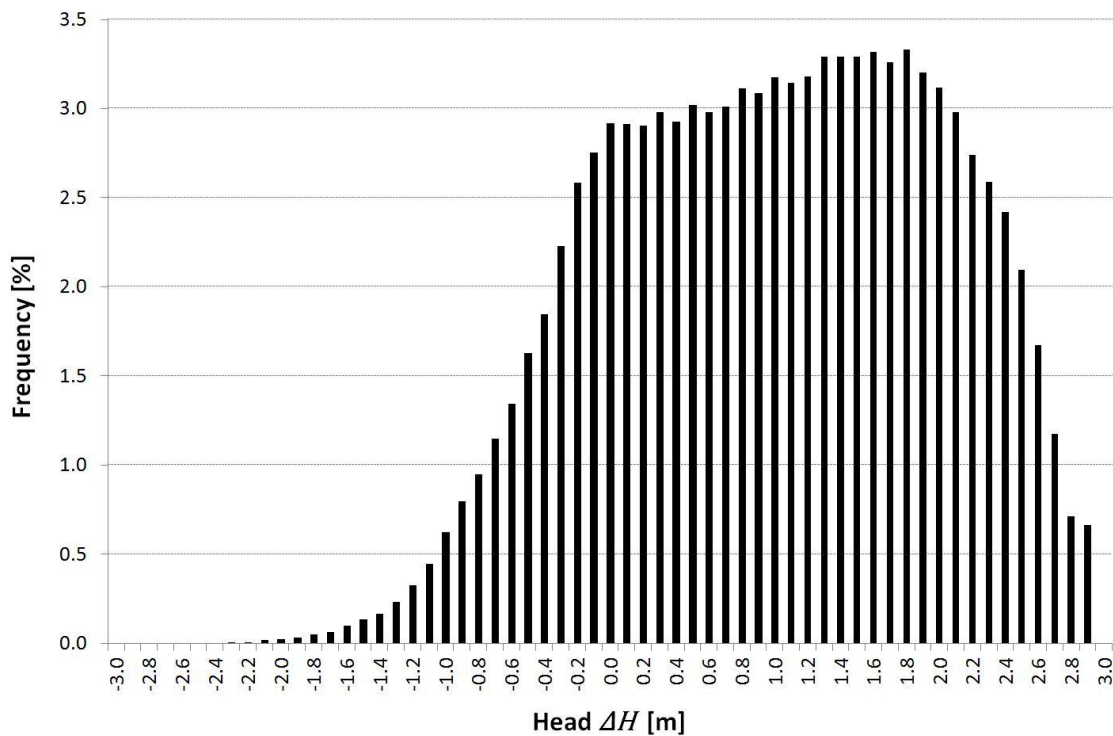


Figure 2-3: Frequency distribution of the full hydraulic head time series.

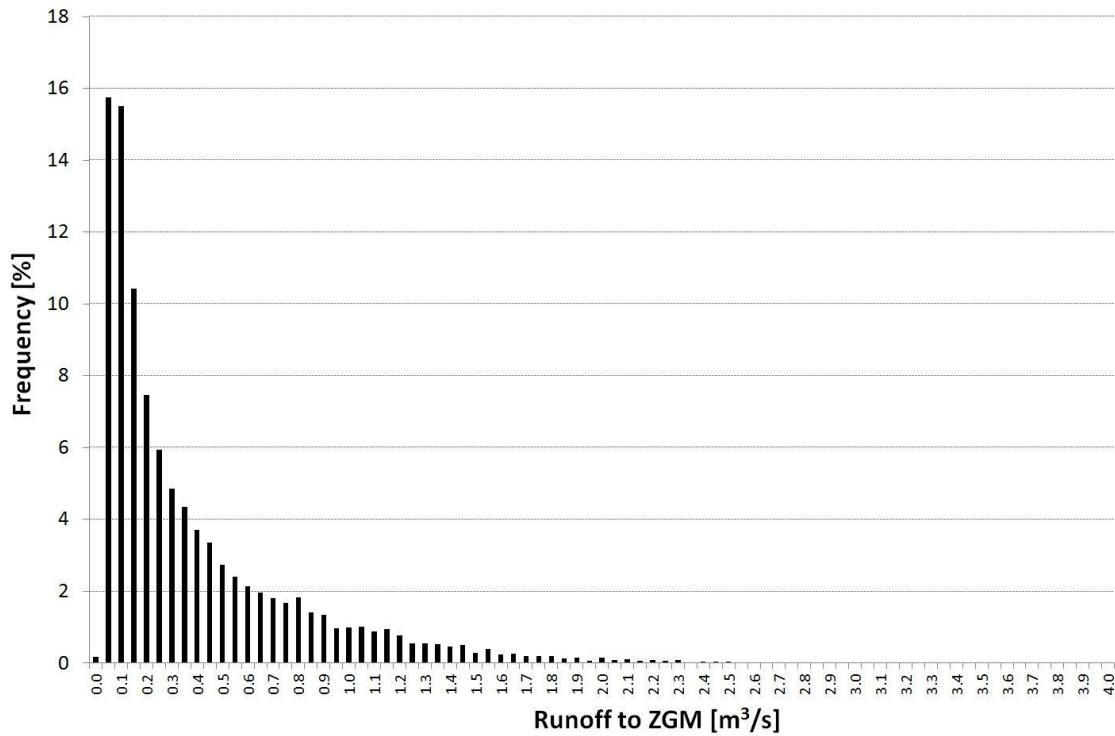


Figure 2-4: Frequency distribution of the simulated runoff to the ZGM reach, for the entire simulated period.

The average yearly energy yield, expressed in kWh/year, then can be calculated as:

21

$$E_{year} = \rho \cdot g \cdot (\eta \cdot Q)_{avg} \cdot \Delta H_{avg} \cdot \left( \frac{24}{1000} \right) \quad (7)$$

Finally, when taking into account not only turbine efficiency, but also the efficiency of other electromechanical components, such as the generator and the transmission, Equation (7) becomes:

$$E_{year} = \rho \cdot g \cdot \eta_{gen} \cdot \eta_{trans} \cdot (\eta \cdot Q)_{avg} \cdot \Delta H_{avg} \cdot \left( \frac{24}{1000} \right) \quad (8)$$

In principle  $\eta_{gen}$  and  $\eta_{trans}$  also depend on the operating conditions, i.e. rotational speed, and hence the discharge. However constant values  $\eta_{gen} = 0.90$  and  $\eta_{trans} = 0.97$  are assumed here (ANRE & ODE-Vlaanderen, 1999).

### 2.3.2 IMPLEMENTATION OF ADDITIONAL OPERATIONAL RULES

Some operational rules need to be implemented as well, such as a lower threshold value for the head  $\Delta H_{low}$  below which no power generation is possible, e.g. due to the electromechanical resistance of the turbine. To consider this rule in the proposed method, it suffices to limit the calculation of the weighted average of the head (Equation (4)) to the values above the predefined threshold, while the frequency of occurrence values  $f_i$  remains the same. This way, a turbine that does not start below e.g. 1 m head, can be considered. Also the negative head can be disregarded, since during these periods, no power generation is possible (with a unidirectional turbine). As an example, Figure 2-5

shows the frequency distribution after applying a threshold of 1 m. Since the frequencies  $f_i$  remain the same, the average value of  $\Delta H$  – and hence the energy yield – will be lower (Equation (8)).

The same could be applied to the discharge.

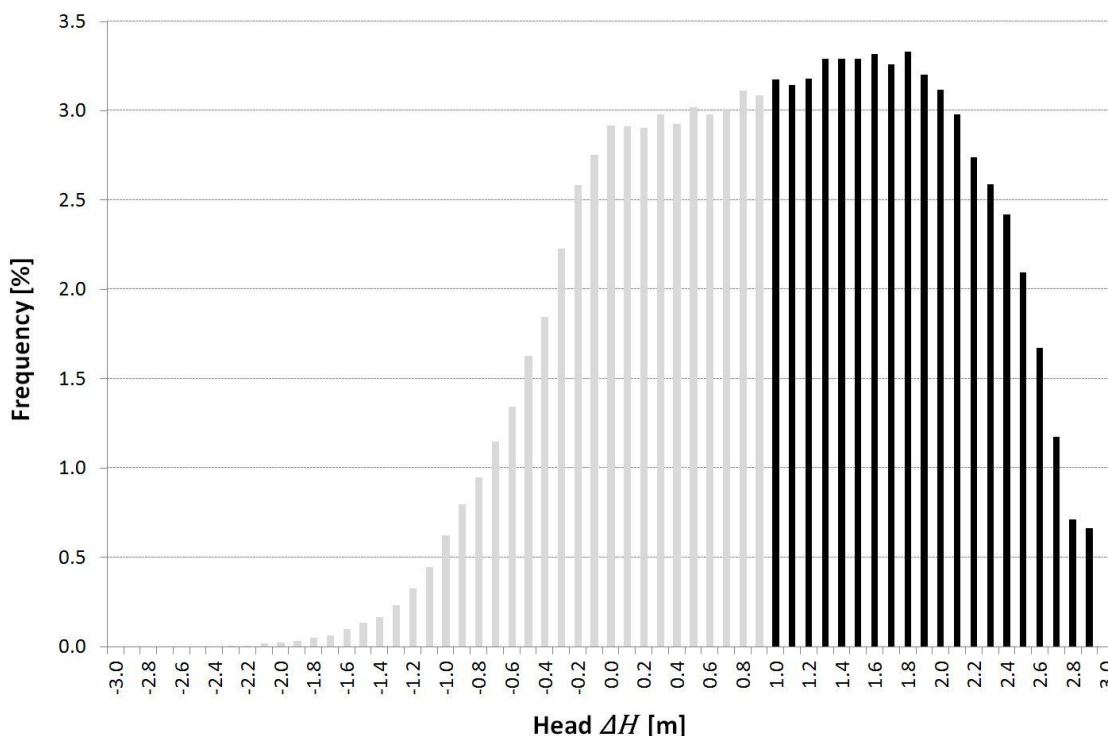


Figure 2-5: Frequency distribution of the hydraulic head after applying a threshold of 1 m. Only the black part is considered.

### 2.3.3 DISCUSSION

The main advantage of using the long-term average method over the direct integration method, is that it can cope with time series of different length and different time resolution. Of course, the longer the time series the more representative the frequency distribution and the corresponding average will be for estimating the average yearly energy yield. In fact, the actual time series are not even required as long as the frequency distributions are available, e.g. as part of a previous study.

One major drawback is the required assumption of independence between the hydraulic head and the flow passing the turbine. Hence, it is (implicitly) assumed that the *available volume* is used uniformly throughout the day for power generation. This is not a realistic assumption, since after applying a threshold for the hydraulic head, not all available volume is used for power generation *if* the same daily averaged flow is used. In other words, part of the volume is 'lost'. The basic method is not able to cope with this inefficient use of water. Therefore, the method has to be extended.

## 2.4 EXTENDED LONG-TERM AVERAGE METHOD

Suppose the available daily averaged flow for a certain day is  $Q$  [m<sup>3</sup>/s]. Then this flow could be recalculated to an available volume  $V$  [m<sup>3</sup>] for that day:

$$V = Q \cdot \Delta T \quad (9)$$

with  $\Delta T = 1 \text{ day} = 86400 \text{ s}$ .

And suppose a turbine with a design flow  $Q_d$  is installed to generate power. Then the amount of time for that day, during which the available volume can be conveyed along the turbine, let's say the power generation time using the design flow,  $\Delta t_d$ , is:

$$\begin{aligned} \Delta t_d &= \frac{V}{Q_d} = \frac{Q \cdot \Delta T}{Q_d} \quad \text{if } Q < Q_d \\ \Delta t_d &= \Delta T \quad \text{if } Q \geq Q_d \end{aligned} \quad (10)$$

And so the relative amount of time during that day, called the power generation time ratio  $x_d$  is:

$$\begin{aligned} \frac{\Delta t_d}{\Delta T} &= x_d = \frac{Q}{Q_d} \quad \text{if } Q < Q_d \\ \frac{\Delta t_d}{\Delta T} &= x_d = 1 \quad \text{if } Q \geq Q_d \end{aligned} \quad (11)$$

In the above equations it is assumed that any surplus discharge – in case  $Q > Q_d$  – is not conveyed along the turbine but along an alternative route, e.g. the other weir channel. For all  $Q$ -values larger than  $Q_d$ , these  $x_d$ -values have the same frequency distribution as the original available flow, since  $Q_d$  is a constant value:

$$g(x_d) = g(Q) \quad (12)$$

For instance, when the hydrological runoff to ZGM, simulated with the hydrological submodel of the water balance model, is considered as available flow and the design flow is taken equal to 4 m<sup>3</sup>/s, the frequency distribution of the power generation time ratio will look exactly like the one depicted in Figure 2-4. To exemplify, this distribution is shown in Figure 2-6.

The distribution given in Figure 2-6 would only result in a limited amount of days that the turbine operates for a substantial amount of time. By lowering the design flow of the turbine, or by providing additional available flow, e.g. from the water system around Ghent, it is possible to increase the frequency of the higher values of the power generation time ratio. As an example, Figure 2-7 shows this effect when considering half and quart of the original design flow. At this point, no attention is given to whether turbines with such small design flows exist for the given circumstances.

Also, when a negative head is present during a considerable amount of time during the day,  $x_d = 100\%$  should not be the target. When accounting for a lower limit of the head for the turbine to operate,  $\Delta H_{low}$ ,  $x_d$  can even be lower.

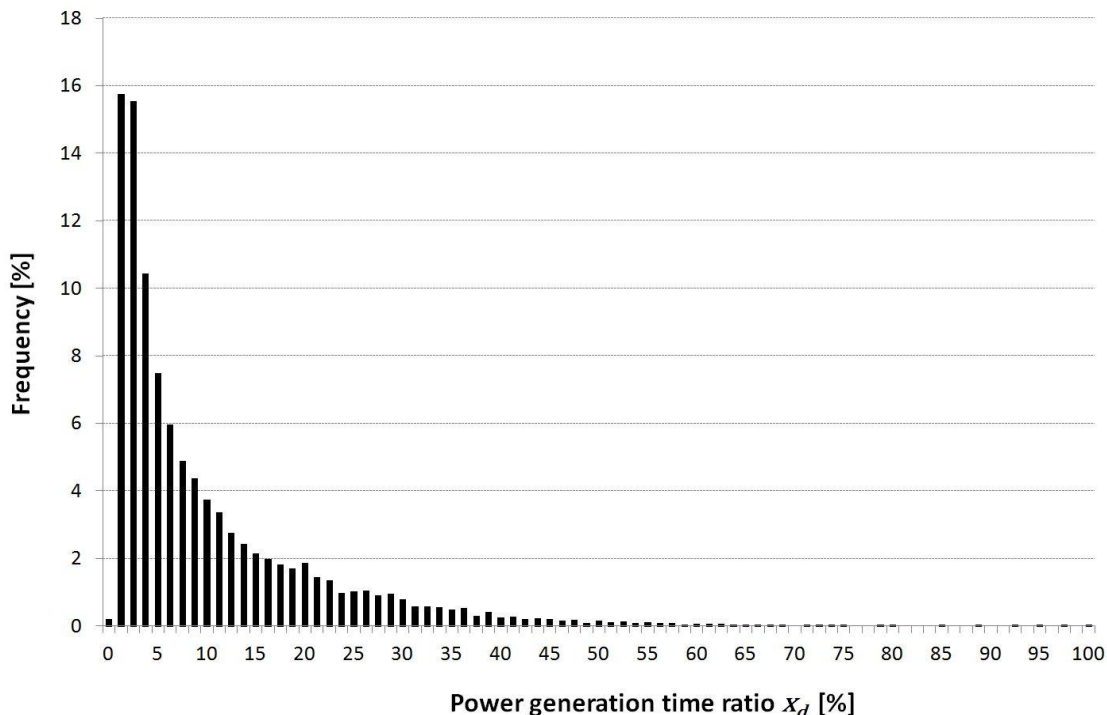


Figure 2-6: Frequency distribution of the power generation time ratio when deriving the available volumes from the simulated hydrological flow.

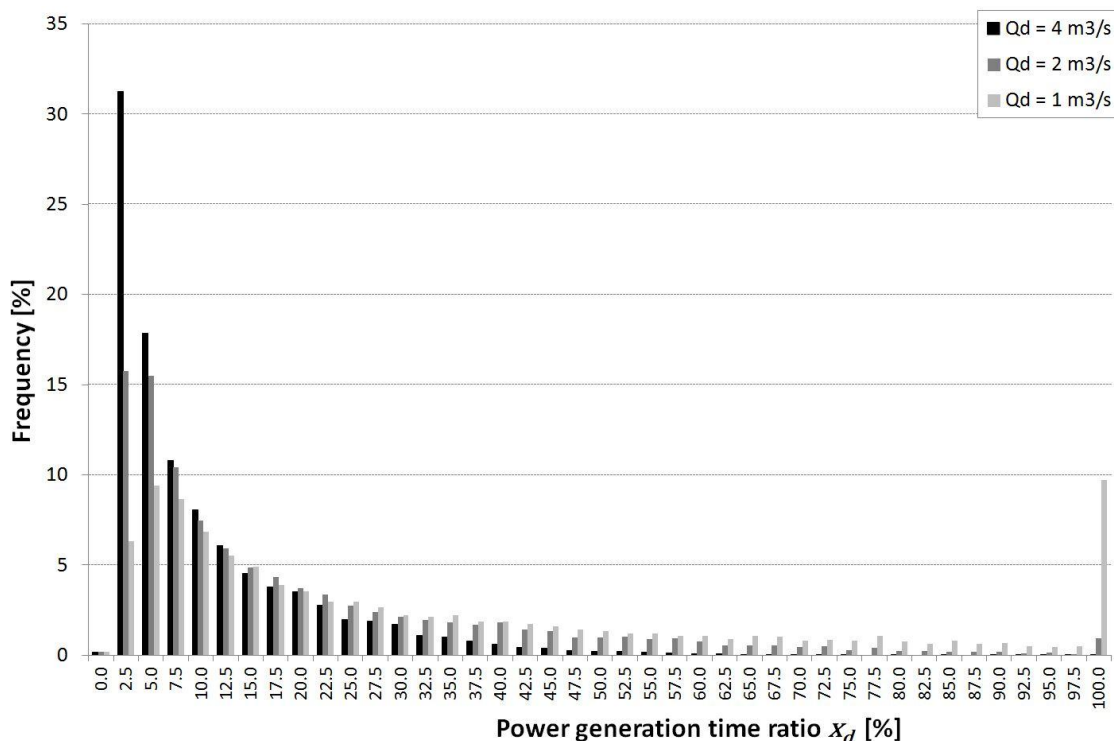


Figure 2-7: Effect of decreasing the design flow on the frequency distribution of the power generation time ratio.

Now, the objective is to maximize the generated energy yield, in other words, to generate power using the design discharge when the hydraulic head is largest. Suppose the power generation time ratio to be  $x_d$  for a certain day under consideration. In order to maximize

the energy yield, the available volume is first used during the time period of the day with the highest hydraulic head,  $\Delta H_1$ . The generated energy during this period would be:

$$E_1 = \rho \cdot g \cdot \eta(Q_d) \cdot Q_d \cdot \Delta H_1 \cdot f_1 \cdot \Delta T \quad (13)$$

Now, if  $x_d > f_1$ , water is still available, and power can be generated during the period with the second highest hydraulic head,  $\Delta H_2$ :

$$E_2 = \rho \cdot g \cdot \eta(Q_d) \cdot Q_d \cdot \Delta H_2 \cdot f_2 \cdot \Delta T \quad (14)$$

This continues up to the point where all available volume has been used, i.e. when the power generation time is fully considered. Or, mathematically, when:

$$\sum_{i=1}^{n_d} f_i \cdot \Delta T = \Delta t_d \quad (15)$$

with  $n_d$  the number of head classes that can be considered. Or, after applying Equation (11):

$$\sum_{i=1}^{n_d} f_i = x_d \quad (16)$$

The summation on the left side of the above equation, is equal to the exceedance frequency of  $\Delta H_{nd}$ , since the summation starts at the highest hydraulic head. The 25 exceedance frequency can be derived from the duration curve depicted in Figure 3-2.

So, the total energy yield for the considered day, that has a power generation time ratio  $x_d$ ,  $E_{x_d}$ , is:

$$E_{x_d} = \sum_{i=1}^{n_d} E_i = \rho \cdot g \cdot \eta(Q_d) \cdot Q_d \cdot \Delta T \cdot \sum_{i=1}^{n_d} f_i \cdot \Delta H_i \quad (17)$$

or, when considering the efficiencies of other electromechanical components as well:

$$E_{x_d} = \rho \cdot g \cdot \eta_{gen} \cdot \eta_{trans} \cdot \eta(Q_d) \cdot Q_d \cdot \Delta T \cdot \sum_{i=1}^{n_d} f_i \cdot \Delta H_i \quad (18)$$

When calculating the average energy yield, the average frequency distribution can be considered for each day throughout the year. In the final step, the average yearly energy yield  $E_{year}$  can be easily calculated, since the frequency distribution of the flow  $g(Q)$ , and hence of the power generation time ratio  $g(x_d)$ , is known:

$$E_{year} = 365 \cdot \sum_{g=1}^m g_k \cdot E_{x_d} \quad (19)$$

It should be noted that in the above derived calculation, it is implicitly assumed that the water level – for  $f_i$  and  $\Delta H_i$  – and flow – for  $x_d$  and hence  $n_d$  – are predictable on a daily basis. After all, using the volume of water available for power generation between  $\Delta H_1$  and  $\Delta H_{nd}$  when  $\Delta H$  has a tidal variation, means that the turbine must start operating at  $\Delta H_{nd}$

through  $\Delta H_1$  and back to  $\Delta H_{nd}$ . For this, both  $\Delta H(t)$  and  $Q(t)$  should be known beforehand, e.g. by means of a prediction model. Predicting  $\Delta H(t)$  is relatively straightforward, since the tidal variation of the Sea Scheldt is well known and the water levels are monitored constantly at several locations. For  $Q(t)$ , the prediction depends on the flow distribution around Ghent and hence the position of the surrounding control structures.

Here, no attention is given to the practical implementation on how to distribute the available volume. A proper set of control rules can probably approximate the theoretical yield, but nevertheless a perfect optimization will not be possible. Consequently, the energy yields calculated with Equation (19) should be considered upper values, given the distribution of hydraulic head and flow. Nevertheless the values will enable the identification of substantial differences between different scenarios,

## 2.5 SMALLER HYDRAULIC HEAD RANGE

In the above, power is generated starting from the maximum head difference each day. This results in an overestimation, since this maximum head does not occur every day. Suppose power on a certain day can only be generated between a lower and upper limit of the head,  $\Delta H_{low}$  and  $\Delta H_{up}$ . The lower limit exists because there is an electromechanical resistance of the turbine that has to be overcome, and the upper limit is the maximum head of that day, which occurs at low tide.  $\Delta H_{low} = 1$  m seems to be an appropriate choice, considering the available technology.

26

An upper limit  $\Delta H_{up}$  can be considered as well, e.g. when the water level in the Sea Scheldt is too low for vessels to navigate safely in the lock while the turbine is discharging in the lower reach. Instead of making the summation in Equation (18) from  $i = 1$  to  $i = n_d$ , it should start from  $i = n_{up}$  to  $i = n_{low}$ :

$$E_{x_d} = \rho \cdot g \cdot \eta_{gen} \cdot \eta_{trans} \cdot \eta(Q_d) \cdot Q_d \cdot \Delta T \cdot \sum_{i=n_{up}}^{n_{low}} f_i \cdot \Delta H_i \quad (20)$$

with:

$$\sum_{i=n_{up}}^{n_{low}} f_i = x_d \quad (21)$$

If a certain day has an  $x_d$ -value larger than the target value, this means not all available volume can be utilized to generate power, because the hydraulic head is too small or too large; the surplus volume is considered lost e.g. spilled through the weir channel.

However in this study, an upper limit is not considered. Because the method takes the frequency of  $\Delta H$  into account, the summation in Equation (20) can be evaluated from  $i = 1$  to  $i = n_{low}$ .

### 3 AVAILABLE DATA

*In calculating the energy generated power, two hydraulic variables are important: the water level difference over the turbine, i.e. the hydraulic head, and the discharge that passes the turbine. In this chapter, the data that are considered for these hydraulic variables are discussed.*

#### 3.1 WATER LEVEL DATA

The available hydraulic head is calculated using the water levels in the upper and lower reach, being the inner waterways around Ghent and the Sea Scheldt respectively.

The *water level in the upper reach* is assumed equal to the target level of the inner waterways around Ghent. In the previous study (IMDC, 2011) a target level of 4.45 mTAW was used. In the course of the lock's design process this value is currently set to 4.50 mTAW. In reality variations occur: in the measurements in Wondelgem, somewhere in Ghent, taken from 1991 to 2011, the level of 4.50 mTAW is exceeded during about 50% of time, the values 4.45 mTAW and 4.40 mTAW respectively around 25% and 5% of time. These variations however are limited, so the influence on the calculated yearly energy yield can be assumed to be negligible.

The water level in the lower reach is assumed equal to the level in the Sea Scheldt as measured at the tidal station in Melle. For this location, Flanders Hydraulics Research made a times series available from 23/06/2006 09:15 to 18/03/2011 09:15<sup>5</sup>, i.e. almost 4 years and 9 months. The tidal station in Melle is located almost 3 km further downstream, so it can be questioned whether these data are suitable for this study. In the current situation, the mean high water in Gentbrugge, a tidal gauge located about 8 km further upstream along ZGM, is about 5 cm higher, while the mean low water is about 17 cm higher (Afdeling Kust – Vlaamse Hydrografie, 2012). Higher water levels in Heusden compared to Melle are to be expected in the future situation as well, with the lock constructed. So using the level time series of Melle would result, in principle, in an underestimation of the occurring low water values, and so in an overestimation of the energy yield. Conversely, the construction of the lock at the proposed location, combined with the planned dredging works on the Sea Scheldt on the stretch between Melle and Heusden, will result in an increase of the high water values in Heusden with about 15 to 20 cm, and a decrease of the low water values with about 10 to 15 cm, compared to the current situation (Coen et al., 2012). This way, the measured time series of the water level at Melle becomes representative again for the future situation, especially regarding periods of low water. The difference for periods of high water are less relevant, since no power generation is possible then, because of the negative head<sup>6</sup>.

27

<sup>5</sup> Source: Flanders Hydraulics Research (Waterbouwkundig Laboratorium).

<sup>6</sup> Unless a bi-directional turbine is foreseen, that is capable of power generation in both directions. This scenario is not considered any further in this study.

A detail of the level difference, as used for the calculations, can be seen in Figure 3-1, while Figure 3-2 shows the corresponding duration curve. During about 50% of time, the head is larger or equal to 1 m. During slightly more than 20% of time, a negative head exists, i.e. the water level of the Scheldt is higher than the level in the upper reach.

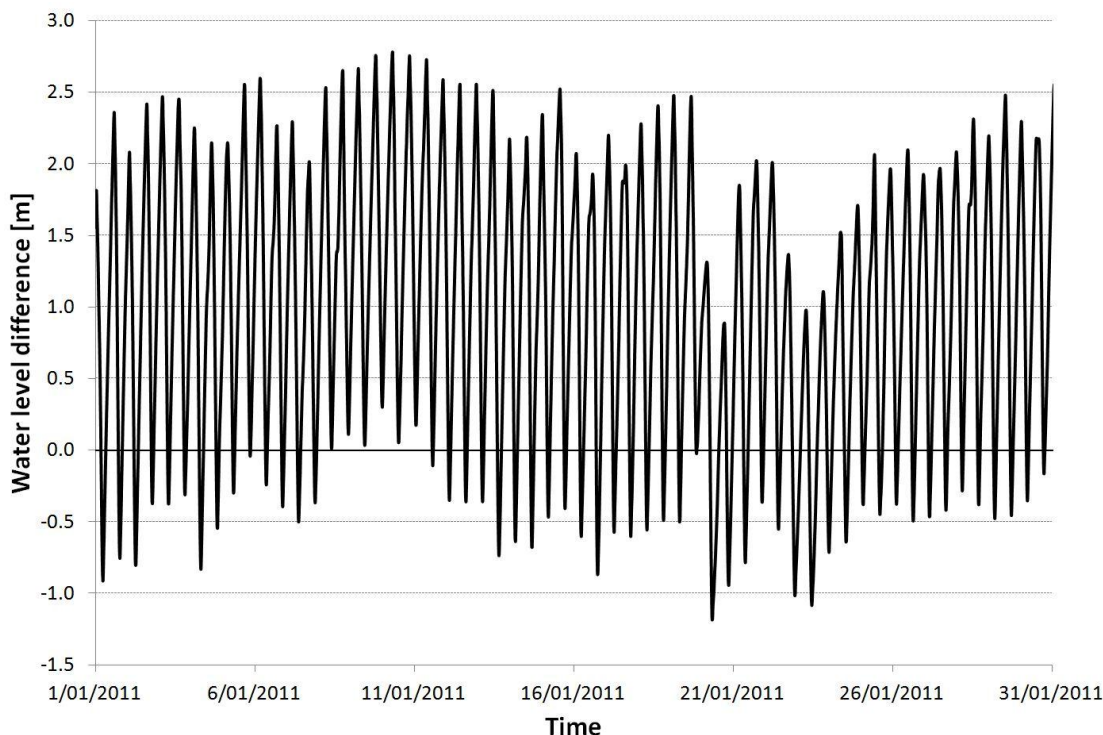


Figure 3-1: A detail of the calculated times series of the water level difference between upper and lower reach, considered representative at the future lock in Heusden.

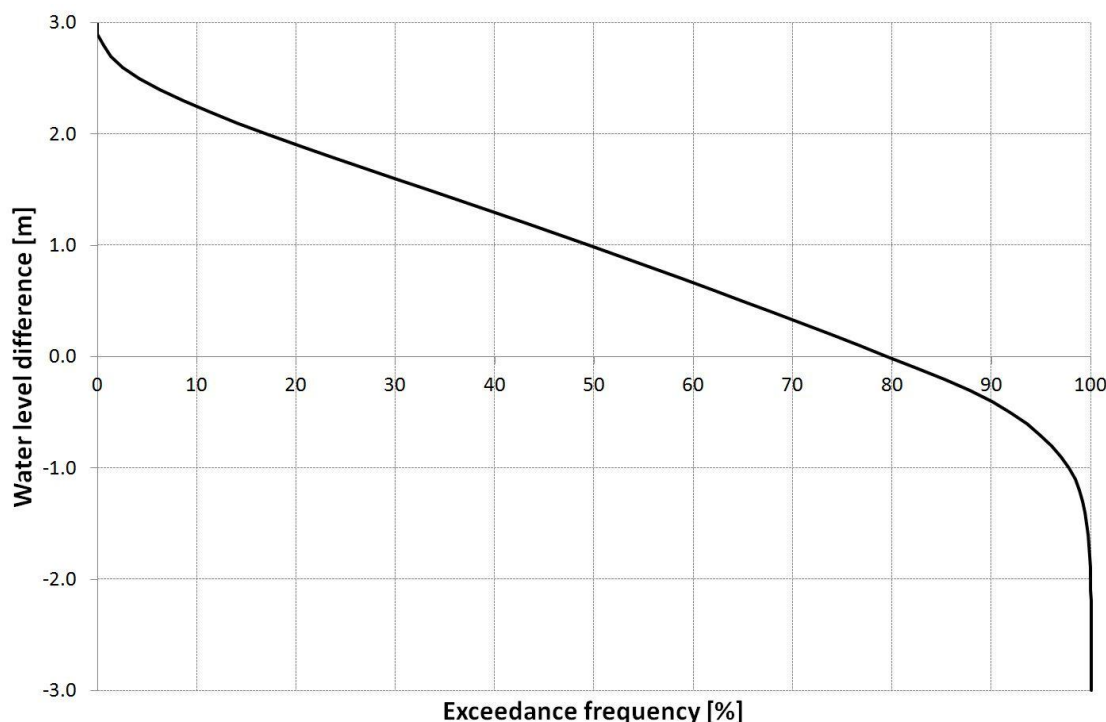


Figure 3-2: Duration curve of the calculated water level difference between the upper and lower reach, considered representative at the future lock in Heusden.

Finally, Table 3-1 gives the values of the characteristic water levels of the tide at Melle (Afdeling Kust – Vlaamse Hydrografie, 2012).

Table 3-1: Characteristic water levels of the tide at Melle.

CHARACTERISTIC WATER LEVELS OF THE TIDE AT MELLE		
Characteristic water level	Value [mTAW]	Corresponding head [m]
Mean low water during neap tide	2.45	2.05
Mean low water during average tide	2.55	1.95
Mean low water during spring tide	2.62	1.88
Mean high water during neap tide	4.68	-0.18
Mean high water during average tide	4.93	-0.43
Mean high water during spring tide	5.14	-0.64

(Source: Afdeling Kust – Vlaamse Hydrografie, 2012)

### 3.2 FLOW DATA

Data on the discharge, available for power generation, are made available by Flanders Hydraulics Research. The discharge time series around Ghent are the result of long-term simulations (1969-2009) using a water balance model. This model is described in detail by De Boeck et al. (2012), and accounts for all sources of water supply and water demand.

Figure 3-3 shows the situation of the different channel reaches around Ghent, while Figure 3-4 illustrates the average discharge distribution for the entire considered period.

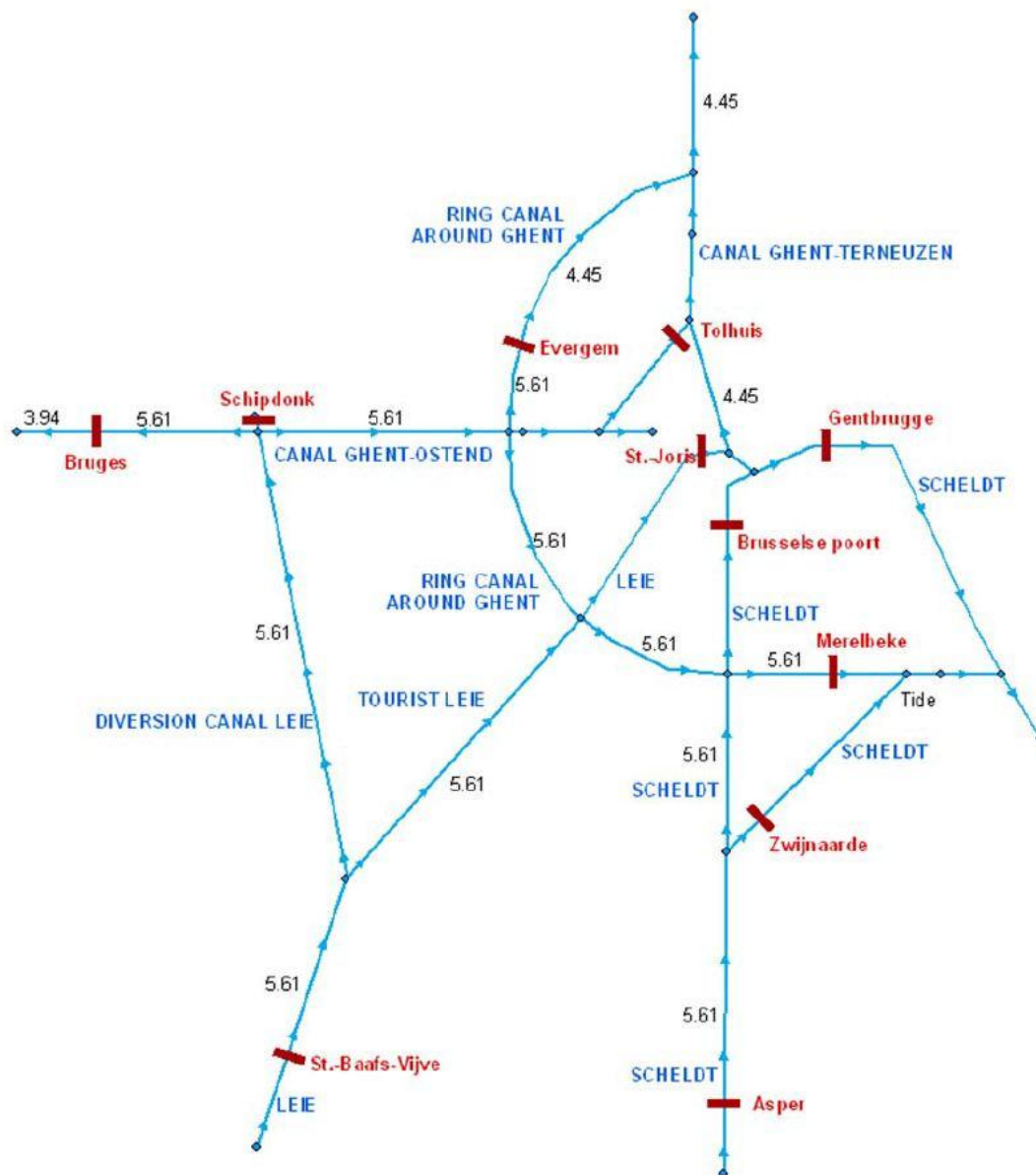


Figure 3-3: Sketch of the water distribution around Ghent. The numbers give the target level in mTAW (De Boeck et al., 2012).

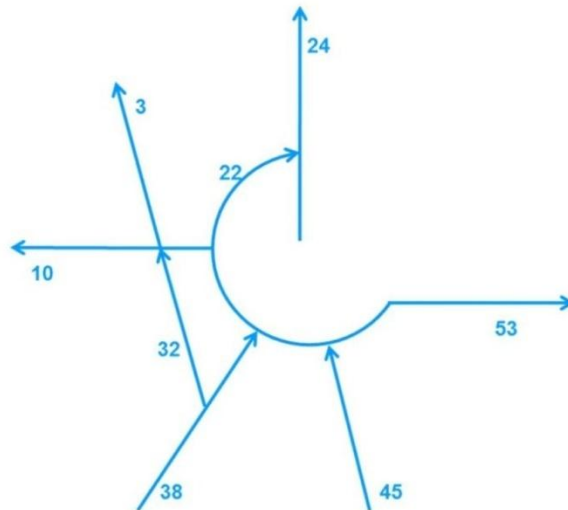


Figure 3-4: The average discharge for the simulation with the water balance model for the period 1969-2009 (De Boeck et al., 2012).

The new tidal lock will be constructed on the reach of the Sea Scheldt between Gentbrugge-Melle (ZGM). For this reach, the hydrological submodel of the water balance model returns the runoff flow time series as depicted in Figure 3-5. In the figure, the simulated flow passing the structure in Evergem is shown as well. The difference in order of magnitude is clear.

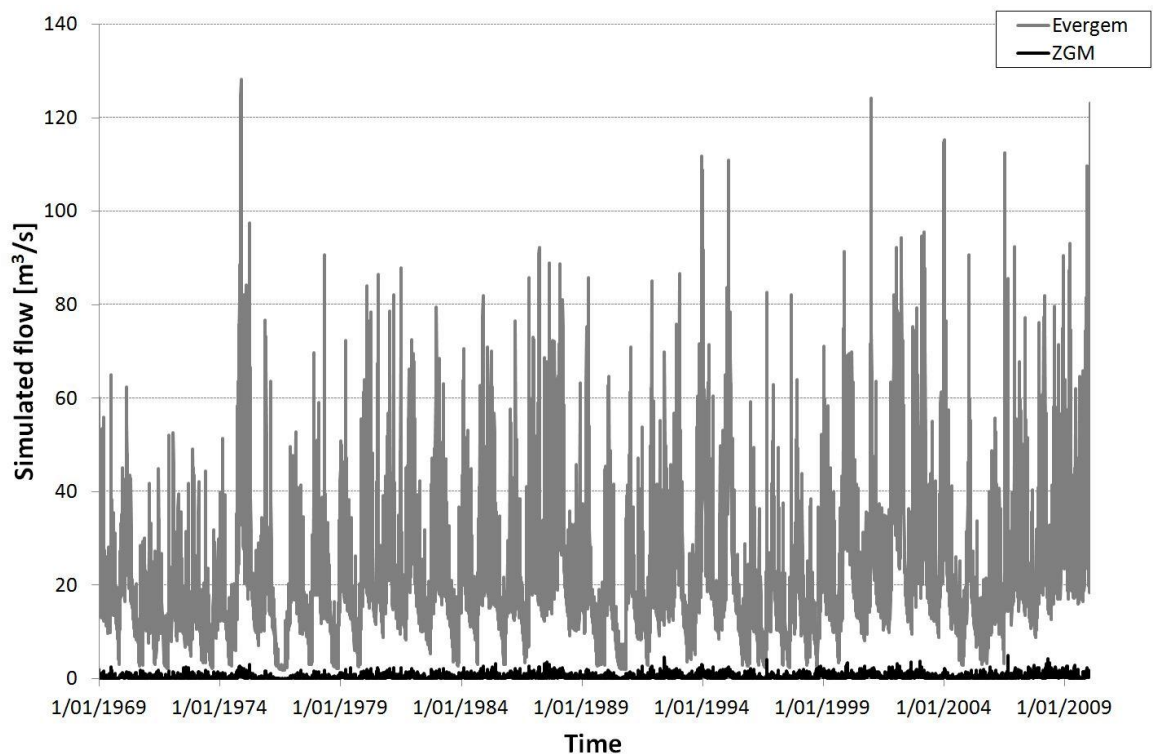


Figure 3-5: Simulated flow passing in Evergem, and simulated runoff flow to the reach of the Sea Scheldt between Gentbrugge and Melle (ZGM), and the simulated flow in Evergem<sup>7</sup>.

<sup>7</sup> Source: Flanders Hydraulics Research.

## 4 CONSIDERED FLOW SCENARIOS

*Since the magnitude in head is limited – it even becomes negative during a considerable amount of time, making power generation impossible with a unidirectional turbine –, the flow passing the turbine should be maximized in order to reach acceptable levels of power generation. This however can be challenging, due to the issues of water scarcity during prolonged dry periods, mostly in summer.*

*In this chapter, different flow scenarios are considered, with increasing complexity in terms of required control strategy, in order to find a compromise between power generation and water supply. Due to the method used for estimating the energy yield, a flow scenario is fully characterized by its frequency distribution.*

### 4.1 S0: ONLY HYDROLOGICAL RUNOFF

In Scenario 0 (S0), only the hydrological runoff, coming from the catchments draining to ZGM, is considered as available flow. This scenario can be considered as the 'baseline' scenario: only the flow that is currently passing the location of the future lock is used for power generation.

The frequency distribution of the flow is calculated from the simulated runoff time series from the water balance model. Figure 4-1 shows this time series, while Figure 4-2 shows the derived frequency distribution. The more this curve is situated towards the upper right, the higher the energy yield will be. After all, a shift in this direction corresponds to higher flows being available for a longer period of time.

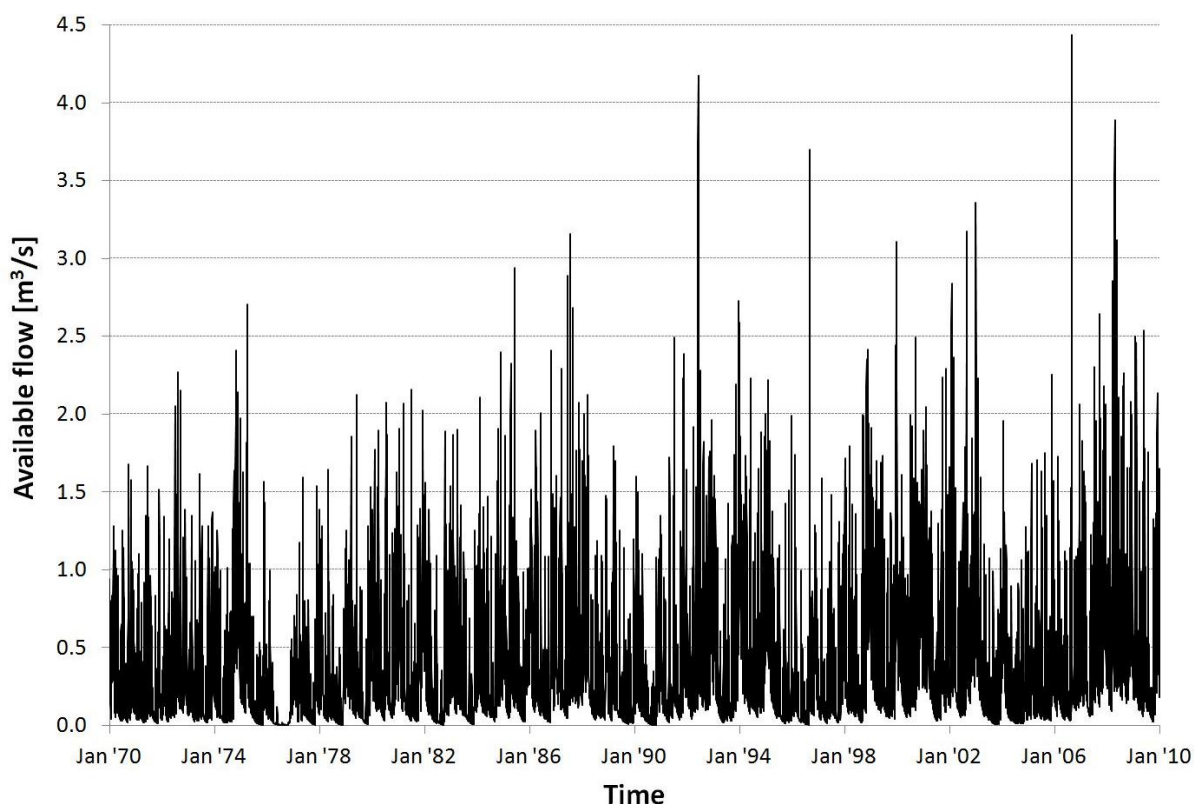


Figure 4-1: Time series of the available flow from the simulated hydrological flow (S0).



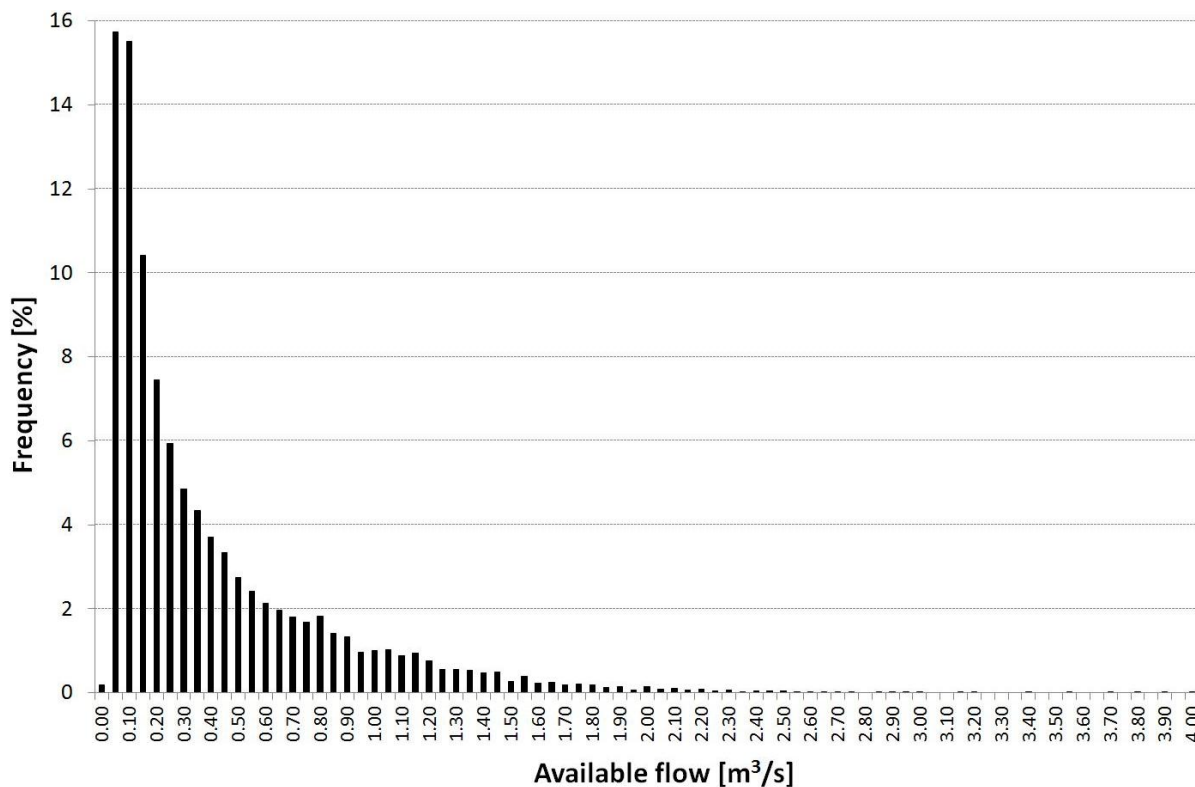


Figure 4-2: Frequency distribution of the available flow from the simulated hydrological flow (S0).

From the distribution the flow duration curve can be derived, a curve often used in assessing the potential of a certain site for developing hydro power. This curve is given in Figure 4-3.

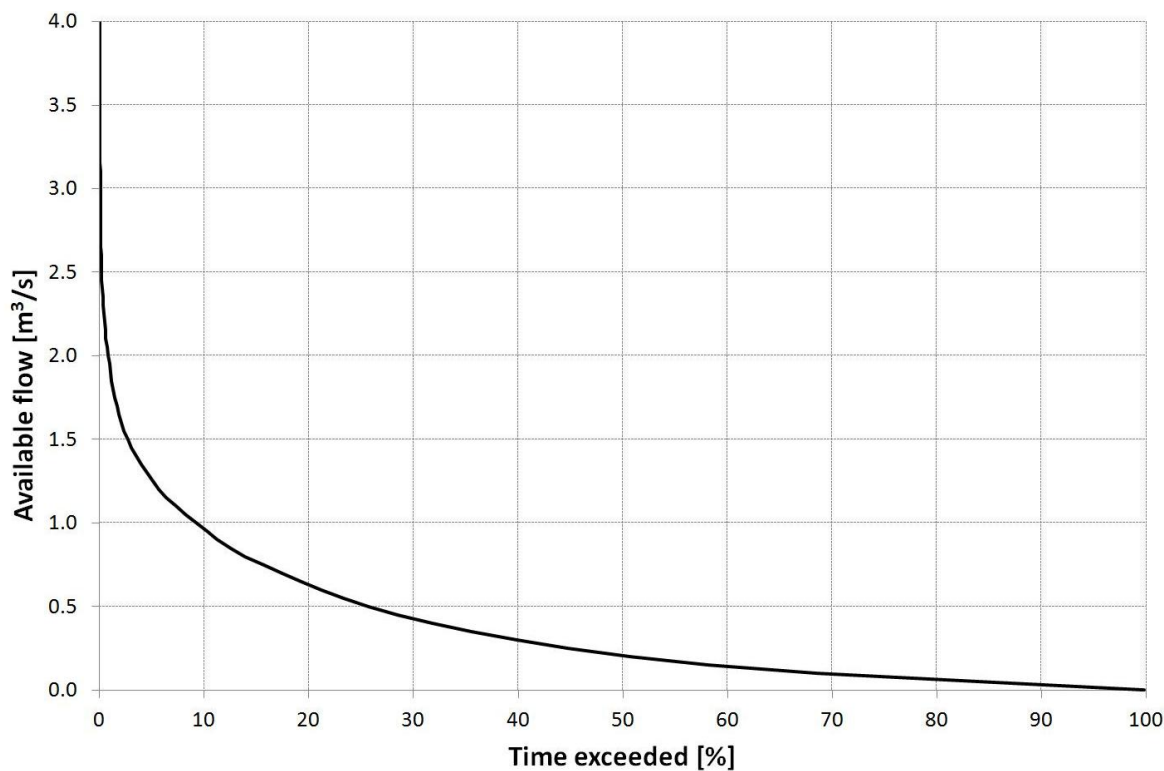


Figure 4-3: Duration curve of the available flow from the simulated hydrological flow (S0).

The frequency distributions of  $x_d$ , for design flows of 2 and 4 m<sup>3</sup>/s are given in Figure 4-4. These subscenarios are denoted S0.2 and S0.4.

Due to the tide, it is not possible to generate power throughout the day – at least not with a unidirectional turbine, which is considered here. So there is a limit to the power generation time ratio, as also explained in §2.5. Only when the head is positive, power can be generated. And even with a positive head, there is a minimum head that has to be taken into account, below which the turbine will not generate power, due to internal resistance of the electromechanical parts. A minimal head of 1 m is used in this study. Even though there are probably turbines capable of power generation below this value, it is considered a reasonable value, especially since the amount of power will not be very high at this head at this location, because of the relatively low discharge. The maximum head difference varies during each average tide; the method takes this into account by considering the frequency distribution of  $\Delta H$ , so no upper limit must be imposed.

Looking at the duration curve of the hydraulic head (Figure 3-2), it can be seen that for  $\Delta H_{low} = 1$  m the exceedance frequency is 49.5%. Hence the target power generation time ratio  $x_d = 49.5\%$ . To maximize energy yield, the frequency distribution of  $x_d$  should be concentrated around this target  $x_d$ -value as much as possible.

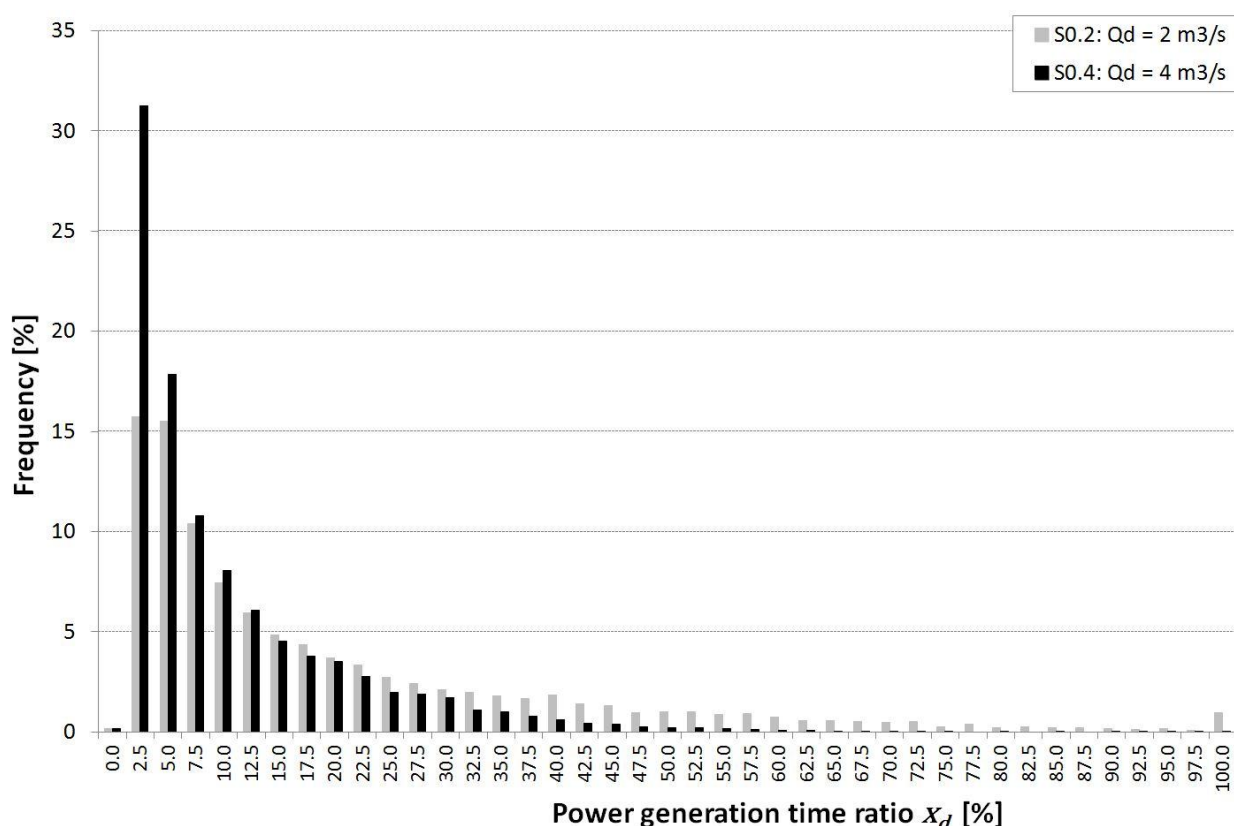


Figure 4-4: Frequency distribution of the power generation time ratio from the simulated hydrological flow (S0), for design flows  $Q_d = 2$  and  $4$  m<sup>3</sup>/s.

## 4.2 S2: EXTRA VOLUME THROUGH THE WEIR CHANNELS

The volume flowing from the Sea Scheldt to the upper reach, through the two weir channels, is considered available for power generation in the following scenario. In a previous study (IMDC, 2012), the average daily discharge passing one weir channel was calculated. This discharge depends on the water level in the Sea Scheldt at which the gates in the weir channel are closed, to protect the landward areas. The results are given in Table 4-1, together with the corresponding volume. These recharge volumes are available on a daily basis.

Table 4-1: Average daily recharge flow through one weir channel.

AVERAGE DAILY RECHARGE FLOW THROUGH ONE WEIR CHANNEL			
Sub-Scenario	Gate closure level [mTAW]	Average daily recharge flow [m <sup>3</sup> /s]	Corresponding volume [m <sup>3</sup> ]
a	5.5	0.23	19872
b	6.5	0.39	33696

(Source: IMDC, 2012)

Two subscenarios will be investigated: an 'a'-scenario with the gate(s) closing at 5.5 mTAW, and a 'b'-scenario with the gate(s) closing at 6.5 mTAW. The flow through both the weir channels is considered, resulting in an S2a and S2b scenario<sup>8</sup>. Both scenarios are investigated, since at the time of this study the gate closure level was not yet decided on.

The average daily flow corresponding to the gate closure level is added to the hydrological flow to ZGM, implying the assumption that all recharge flow is used for power generation. The time series of the flow available for power generation can be seen in Figure 4-5, while Figure 4-6 shows the corresponding duration curves. The graphs of S0 are included as well, to show the effect of the additional flow. The frequency distribution of  $x_d$  is depicted in Figure 4-7 for S2a, and in Figure 4-8 for S2b. Note how the mode – the value with the highest frequency – shifts towards higher  $x_d$ -values with decreasing design discharge, meaning that the turbine is used more effectively in relation to its design discharge.

<sup>8</sup> The scenarios S1a and S1b, in which the flow through only one weir channel was considered, were initially investigated as well. In those scenarios the other half of the amount of volume, recharged through the second weir channel, was regarded as additional flow to KGT, to help decrease the time of non-exceedance of the threshold of 13 m<sup>3</sup>/s. It is chosen to keep the original scenario numbers throughout the remainder of the study.

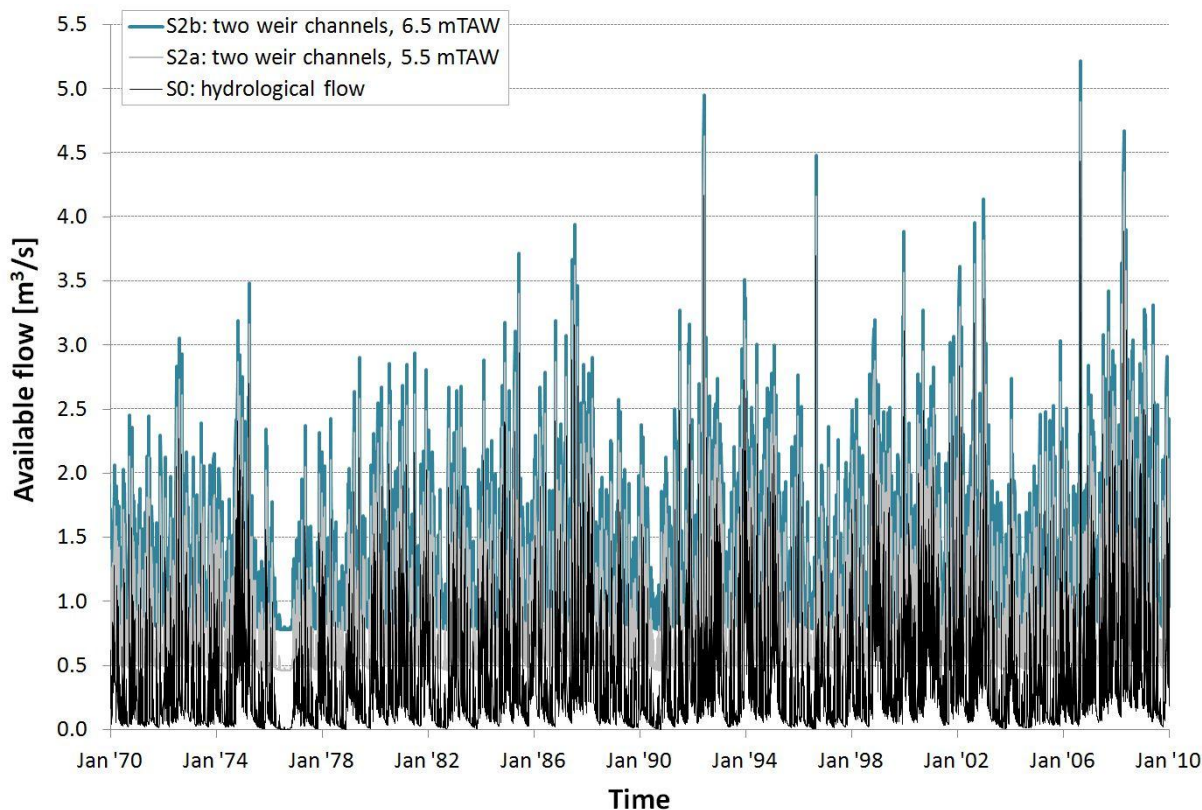


Figure 4-5: Time series of the available flow when considering the recharge flow from two weir channels (S2a and S2b). 36

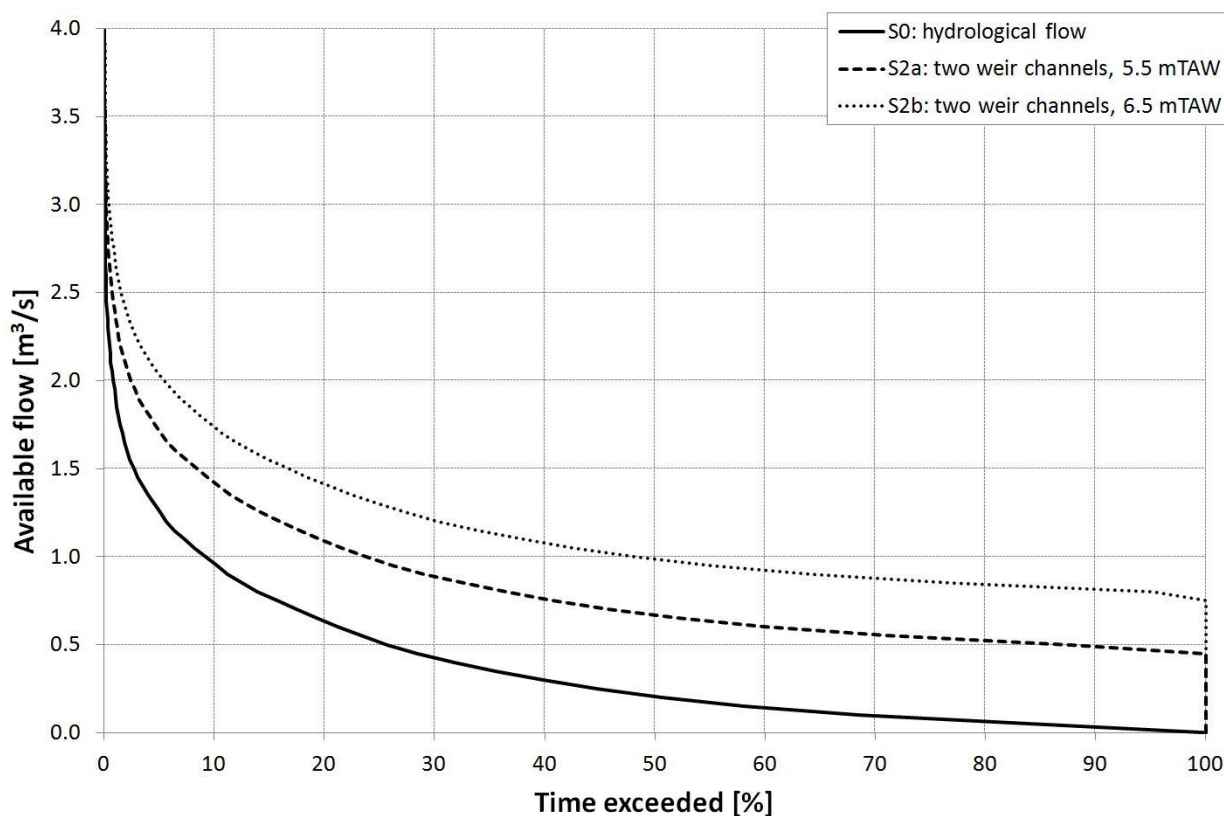


Figure 4-6: Duration curve of the available flow when using the recharge flow from two weir channels (S2a and S2b).

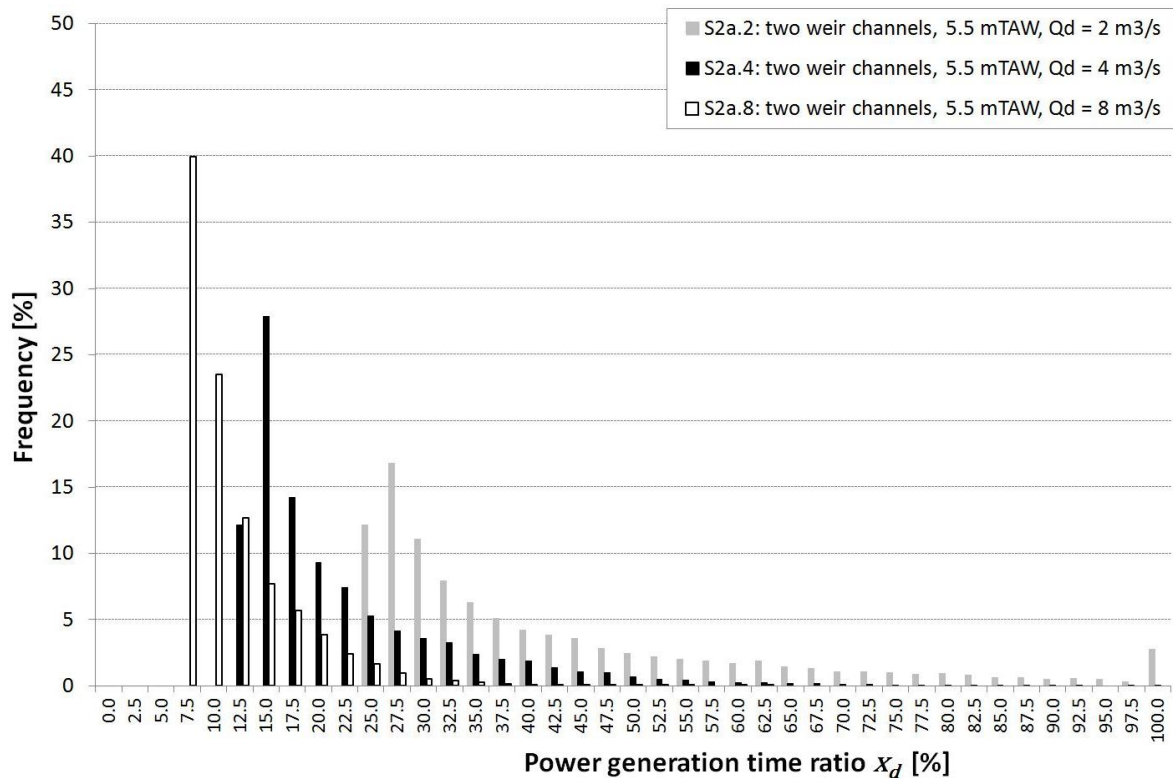


Figure 4-7: Frequency distribution of the power generation time ratio when using the recharge flow from one weir channel, that is closed on 5.5 mTAW (S2a), for design flows  $Q_d = 2, 4$  and  $8 \text{ m}^3/\text{s}$  37

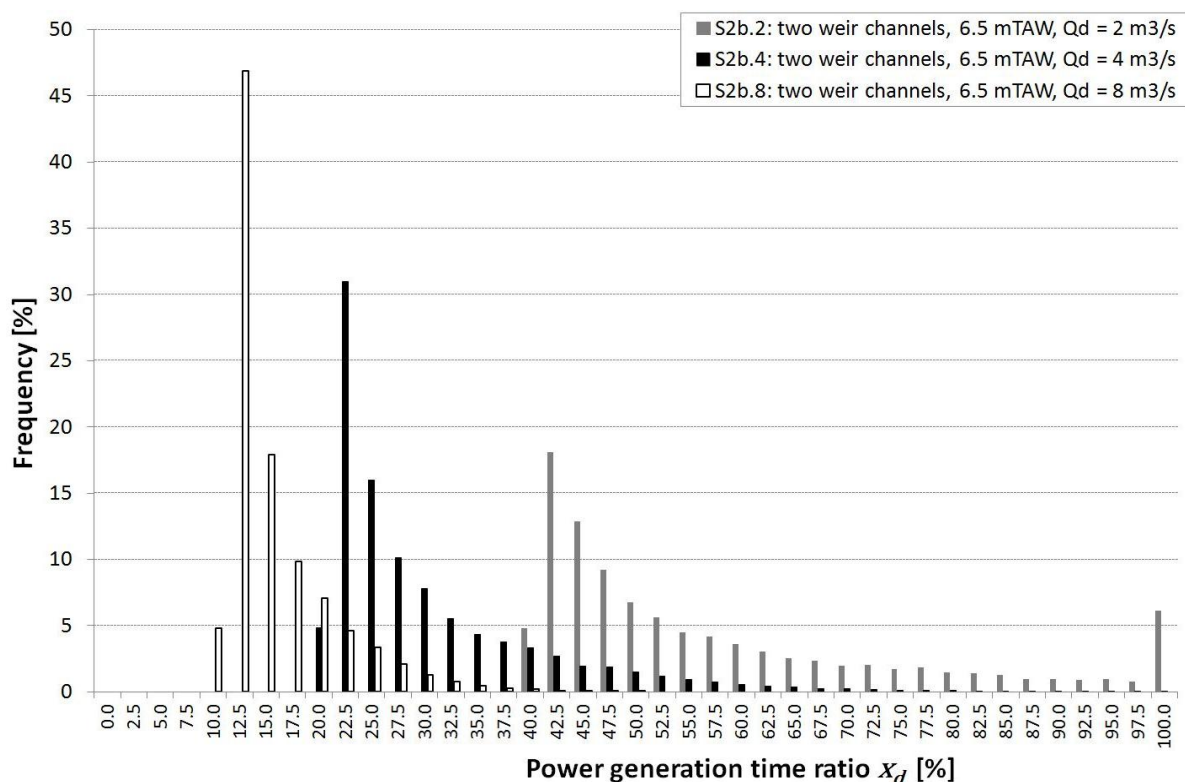


Figure 4-8: Frequency distribution of the power generation time ratio when using the recharge flow from one weir channel, that is closed on 6.5 mTAW (S2b), for design flows  $Q_d = 2, 4$  and  $8$  m<sup>3</sup>/s. 38

### 4.3 DRAINAGE FROM FLOW PASSING EVERGEM

The previous scenarios do not impose extra pressure on the total water balance around Ghent; they are neutral regarding the water balance. However, in order to increase the energy yield, the available flow must increase. The most straightforward solution is to divert additional water from the flow going to the channel between Ghent and Terneuzen (KGT). Although there are restrictions due to the governing treaty with The Netherlands (see §1.2), throughout a large part of the year there are no problems meeting the minimal flow of 13 m<sup>3</sup>/s on a 2-monthly average. During that time, it is – at least in principle – possible to direct flow towards the turbine.

The principal restriction when considering drainage from KGT, is that on average the total time period in which the treaty is not met, does not increase. In other words, the frequency of non-exceedance of 13 m<sup>3</sup>/s cannot increase. Thus, the decision to drain will be based on a control rule that verifies whether the average flow of the past two months towards KGT was sufficient.

Three separate scenarios will be investigated:

- 💡 **S3: daily power generation.** The recharge flow through the weir channels is used every day for power generation, i.e. there is no recharge of KGT. Flow from KGT is drained if possible and necessary to meet the demand.

- 💡 *S4: active recharge of KGT.* Use of the recharge flow and possible drained flow from KGT is only allowed when a minimal threshold power generation ratio can be achieved. Due to the active recharge, the periods during which flow is drained from KGT can be extended, maximizing the energy yield.
- 💡 *S5: compromise between power generation and water usage.* Similar to S4, but also alleviates the pressure on the water balance during dry periods. The energy yield of course will be lower.

### 4.3.1 S3: DAILY POWER GENERATION

In scenario 3 (S3), the hydrological flow (S0) and recharge flow through the weir channels (S2) is complemented with flow drained from KGT, albeit without putting additional pressure on the current water balance. The basic available flow, without draining from KGT, consists of the hydrological runoff  $Q_h$  and the recharge flow through both weir channels  $Q_r$ ; the design flow is  $Q_d$ .

Suppose there is a target value for the power generation time ratio  $x_{d,t}$  that is preferably met each day. Now suppose that on a certain day, the power generation time ratio of the basic available flow is less than the target level. Then a *daily* flow should be diverted from KGT,  $Q_{dr}$ , so as to bring  $x_d$  as close to  $x_{d,t}$  as possible. Then the new power generation time ratio, after adding the drained flow,  $x_{d,dr}$  would be:

$$x_{d,dr} = \frac{Q_h + Q_r + Q_{dr}}{Q_d} \quad (22) \quad \underline{39}$$

From this equation, the flow to be drained to reach the target level of the power generation time ratio can be calculated:

$$Q_{dr} = x_{d,t} \cdot Q_d - (Q_h + Q_r) \quad (23)$$

From the above equation the required flow to be drained, in order to reach  $x_{d,t}$ , can be calculated for each day. Of course,  $Q_{dr} > 0$  because otherwise no drainage would be required.

Another important parameter in this scenario is the threshold value for the flow to KGT,  $Q_{KGT,th}$ , below which flow should not be drained. If the current frequency of not meeting the value of 13 m<sup>3</sup>/s, this threshold value, applied to the average flow to KGT of the past two months, will be substantially larger than 13 m<sup>3</sup>/s. After all, if it is decided to stop power generation only when the 2-monthly averaged flow is 13 m<sup>3</sup>/s, the moment this threshold value is exceeded will take place earlier in time than in the situation without drainage, because the past two months flow has been drained, thus lowering the 2-monthly average compared to the situation without diversion. Finding the suitable threshold value is a trial-and-error procedure, in which the duration curve of the flow to KGT with diversion to ZGM is compared to the one without. The frequency of non-exceedance of 13 m<sup>3</sup>/s must be the same in both cases.

The control routine to decide whether to direct flow to ZGM starts with the calculation of the required flow to be drained  $Q_{dr,req}$ , when the target level for  $x_d$  is  $x_{d,req}$ :

$$Q_{dr,req} = x_{d,req} \cdot Q_d - (Q_h + Q_r) \quad (24)$$

If  $Q_{dr,req} \leq 0$ , no additional flow is required for that day. If on the other hand  $Q_{dr,req} > 0$ , flow should be diverted from KGT to ZGM.

Then it should be checked whether it is possible to drain flow. In other words, if  $Q_{KGT,2months} < Q_{KGT,th}$  no flow drainage can occur, since otherwise the frequency of non-exceedance of 13 m<sup>3</sup>/s will increase, and the power generation time ratio for that day cannot be increased. In the comparison,  $Q_{KGT,2months}$  is calculated from the times series to KGT, taking into account previous days with drainage.

If  $Q_{KGT,2months} \geq Q_{KGT,th}$  drainage from KGT to ZGM is allowed, and the required flow can be subtracted from  $Q_{KGT}$  of that day, thus bringing  $x_d$  to the target level  $x_{d,t}$ .

Six different subscenarios are considered:

- 💡 S3a.2: recharge through two weir channels, that close at 5.5 mTAW. The design flow  $Q_d = 2 \text{ m}^3/\text{s}$ .
- 💡 S3a.4: recharge through two weir channels, that close at 5.5 mTAW. The design flow  $Q_d = 4 \text{ m}^3/\text{s}$ .
- 💡 S3a.8: recharge through two weir channels, that close at 5.5 mTAW. The design flow  $Q_d = 8 \text{ m}^3/\text{s}$ .
- 💡 S3b.2: recharge through two weir channels, that close at 6.5 mTAW. The design flow  $Q_d = 2 \text{ m}^3/\text{s}$ .
- 💡 S3b.4: recharge through two weir channels, that close at 6.5 mTAW. The design flow  $Q_d = 4 \text{ m}^3/\text{s}$ .
- 💡 S3b.8: recharge through two weir channels, that close at 6.5 mTAW. The design flow  $Q_d = 8 \text{ m}^3/\text{s}$ .

The corresponding threshold values  $Q_{KGT,th}$  are given in Table 4-2, together with the derived percentage of days during which drainage occurs. The amount of days with drainage increases with increasing design flow, due to the higher demand for water, while an increasing gate closure level will slightly decrease this amount, due to the larger recharge volume through the weir channels. The holds for the mean drained flow: it increases with increasing design flow, and decreases slightly with increasing gate closure level. For S3b.2 the amount of days with drainage is slightly higher than for S3a.2; on the other hand the relative decrease in mean drained flow, compared to its counterpart 'a'-scenario, is most considerable in this case (factor 3). The total drained volume hence is lower, as expected.

Table 4-2: Water balance parameters for the scenarios with drainage, without putting additional pressure on the water supply to KGT.

WATER BALANCE PARAMETERS FOR THE SCENARIOS WITH DRAINAGE, WITHOUT PUTTING ADDITIONAL PRESSURE ON THE WATER SUPPLY TO KGT			
Scenario	$Q_{KGT,th}$ [m <sup>3</sup> /s]	Mean drained flow [m <sup>3</sup> /s]	Percentage of days with drainage [%]
S3a.2	30.6	0.03	10.6
S3a.4	30.1	0.18	17.6
S3a.8	28.5	0.60	20.6
S3b.2	24.2	0.01	11.3
S3b.4	30.3	0.12	16.4
S3b.8	28.8	0.53	20.2

The time series of the available flow in scenarios S3a.2, S3a.4 and S3a.8 are given in Figure 4-9, Figure 4-10 and Figure 4-11 respectively. The *daily averaged* design flow to reach the target level of  $x_d$  is shown as well<sup>9</sup>. When the available flow is larger than this value, no drainage is required; when it is lower, no drainage is allowed. When the available flow has a horizontal course at the design flow value, flow is drained from KGT. The time series for S3b.2, S3b.4 and S3b.8 look very similar (not depicted).

Figure 4-12 shows the duration curves for the six subscenarios, as well as S2a and S2b to show the influence of draining from KGT. The figure clearly shows how the duration curve is extended to the right at the value for the daily averaged design flow for each scenario, and thus extending the total amount of days in which the target level of the power generation time ratio is reached. Around the daily averaged design flow the duration curve is – in principle – horizontal; the mild slope is an artefact due to the discretisation when determining the occurrence frequencies. The length of the horizontal part in the curve corresponds with the percentage of days with drainage in Table 4-2.

<sup>9</sup> This daily averaged design flow is easily calculated as  $x_{d,t} \cdot Q_d$ , see Equation (23).

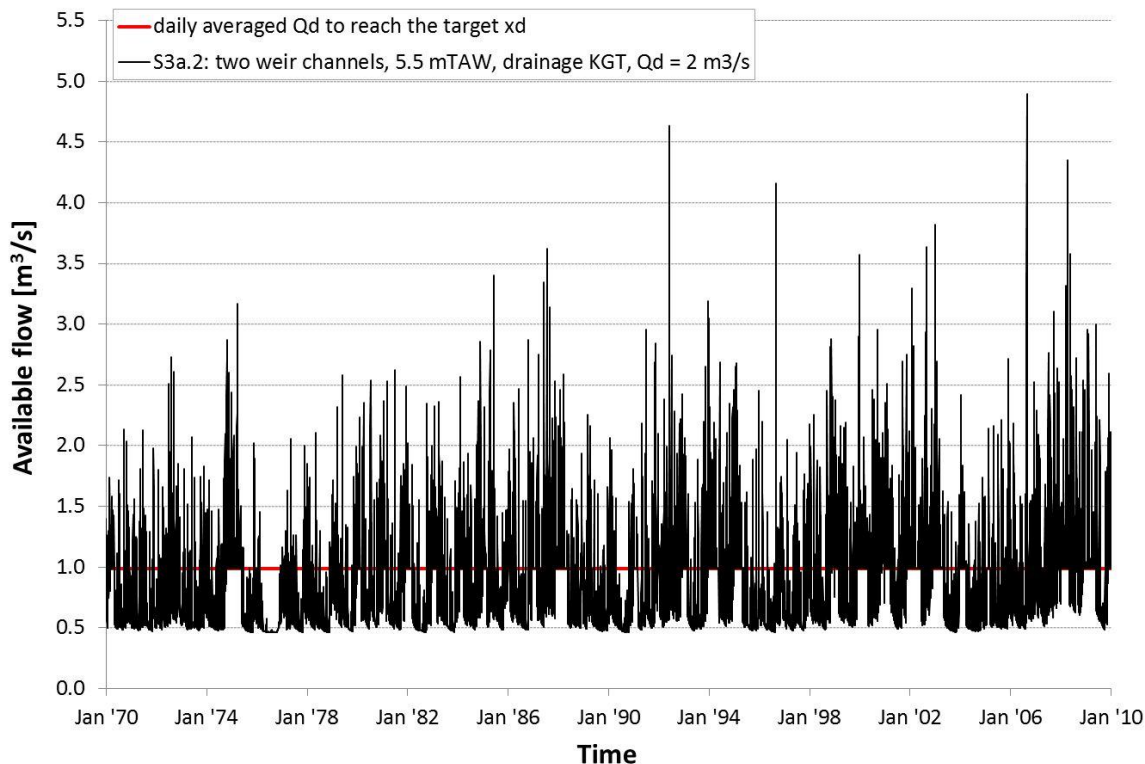


Figure 4-9: Time series of the available flow when considering the recharge flow from two weir channels, with an additional flow drained from KGT when necessary and possible, for a design flow of 2 m<sup>3</sup>/s (S3a.2). 42

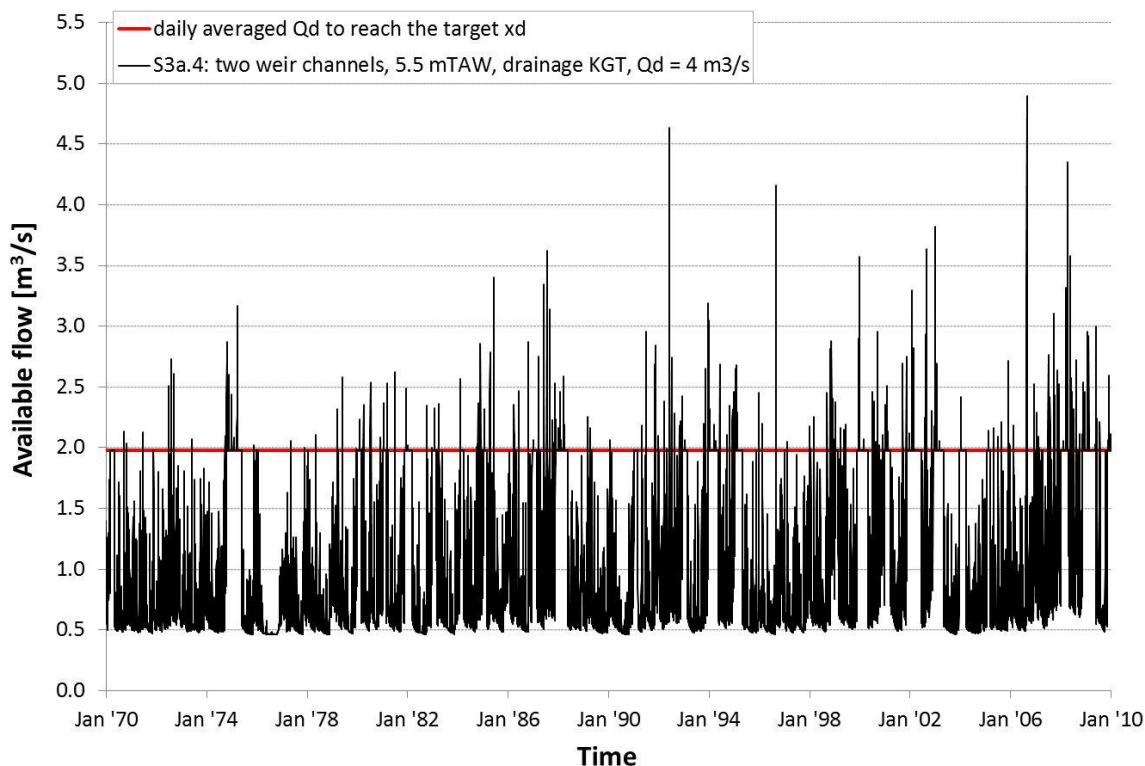


Figure 4-10: Time series of the available flow when considering the recharge flow from two weir channels, with an additional flow drained from KGT when necessary and possible, for a design flow of 4 m<sup>3</sup>/s (S3a.4).

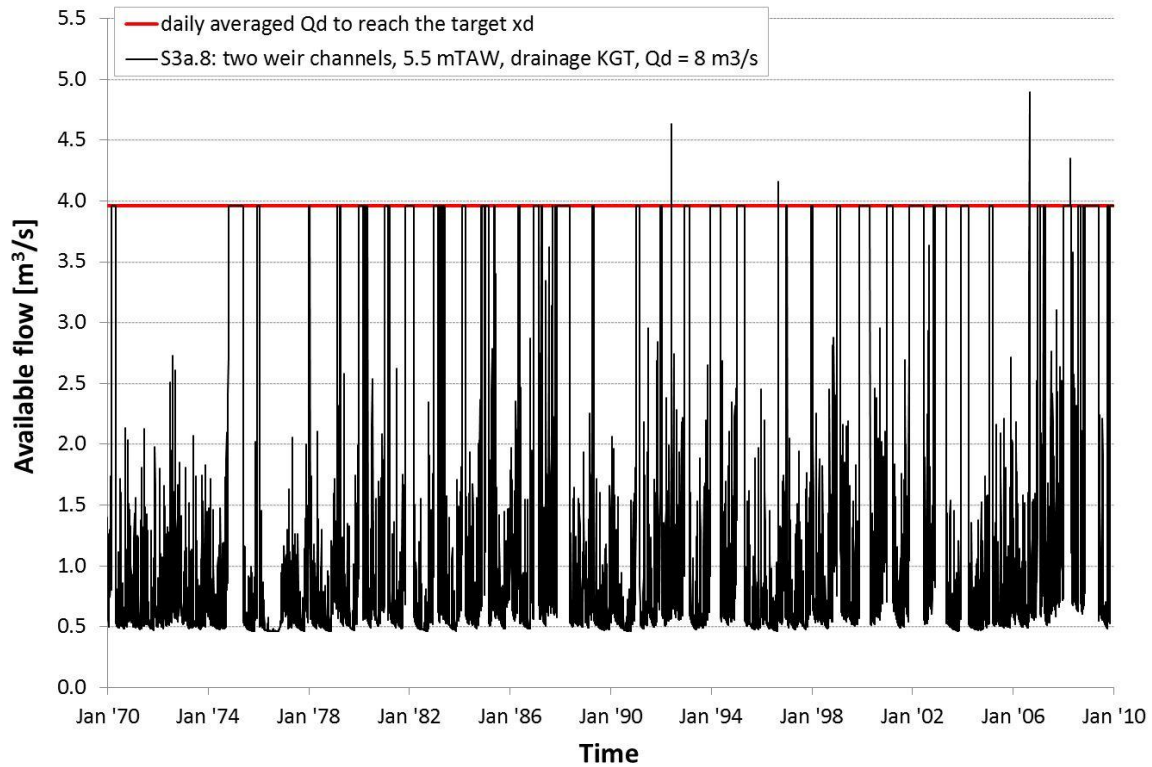


Figure 4-11: Time series of the available flow when considering the recharge flow from two weir channels, with an additional flow drained from KGT when necessary and possible, 43 for a design flow of 8 m³/s (S3a.8).

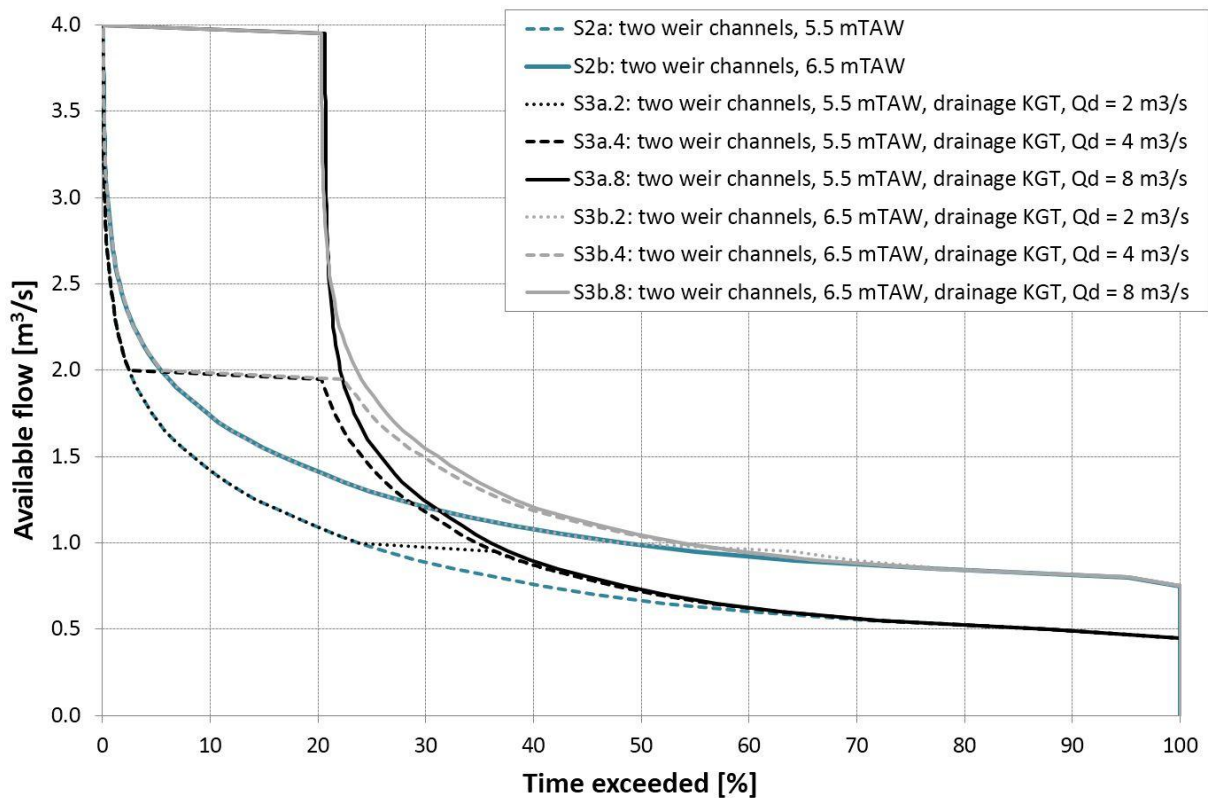


Figure 4-12: Duration curves of the available flow when using the recharge flow from two weir channels, with an additional flow drained from KGT when necessary and possible.

Figure 4-13 shows the frequency distribution of the power generation time ratio for scenarios S3a.2, S3a.4 and S3a.8, Figure 4-14 for scenarios S3b.2, S3b.4 and S3b.8. The frequency increase around the target value can clearly be distinguished. Due to the discrete subdivision in  $x_d$ -classes, the peak is not exactly at 49.5% (but at 50%). For the scenarios considered here, it seems that only 12-20% of days can be obtained with the target  $x_d$ -level. Higher frequencies are not possible without compromising the treaty with The Netherlands.

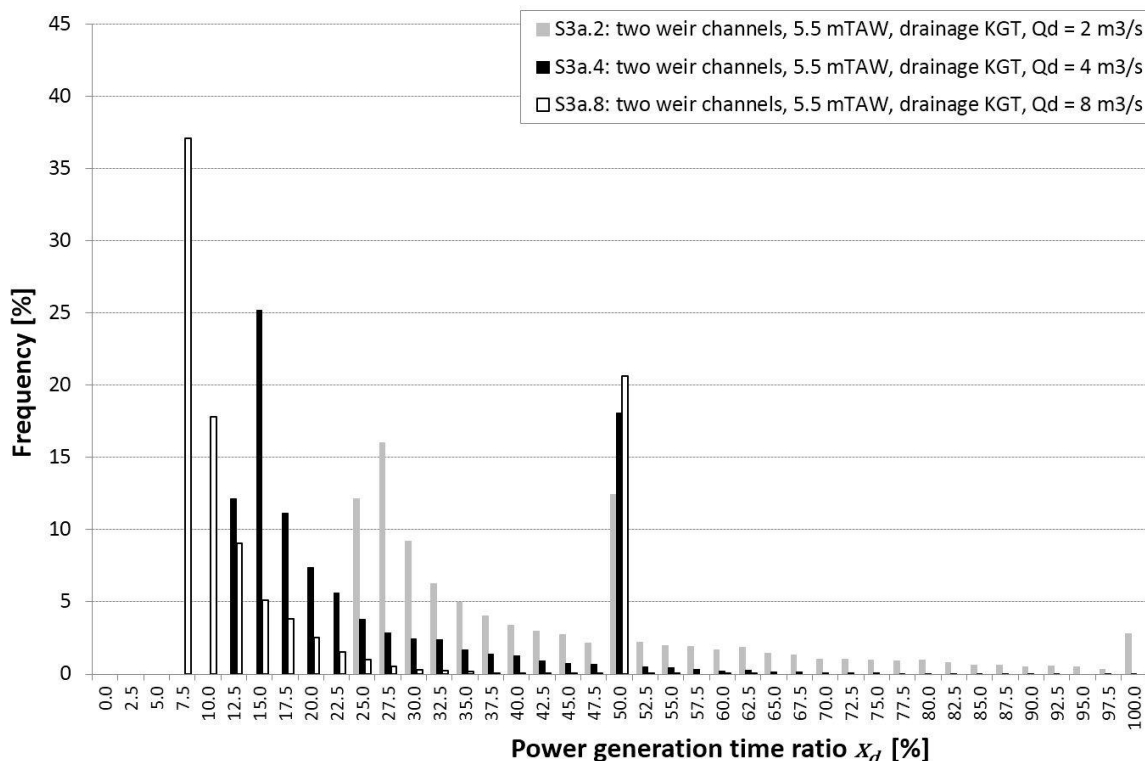


Figure 4-13: Frequency distribution of the power generation time ratio when using the recharge flow from two weir channels, with an additional diverted flow from KGT when necessary and possible (S3a.2, S3a.4 and S3a.8).

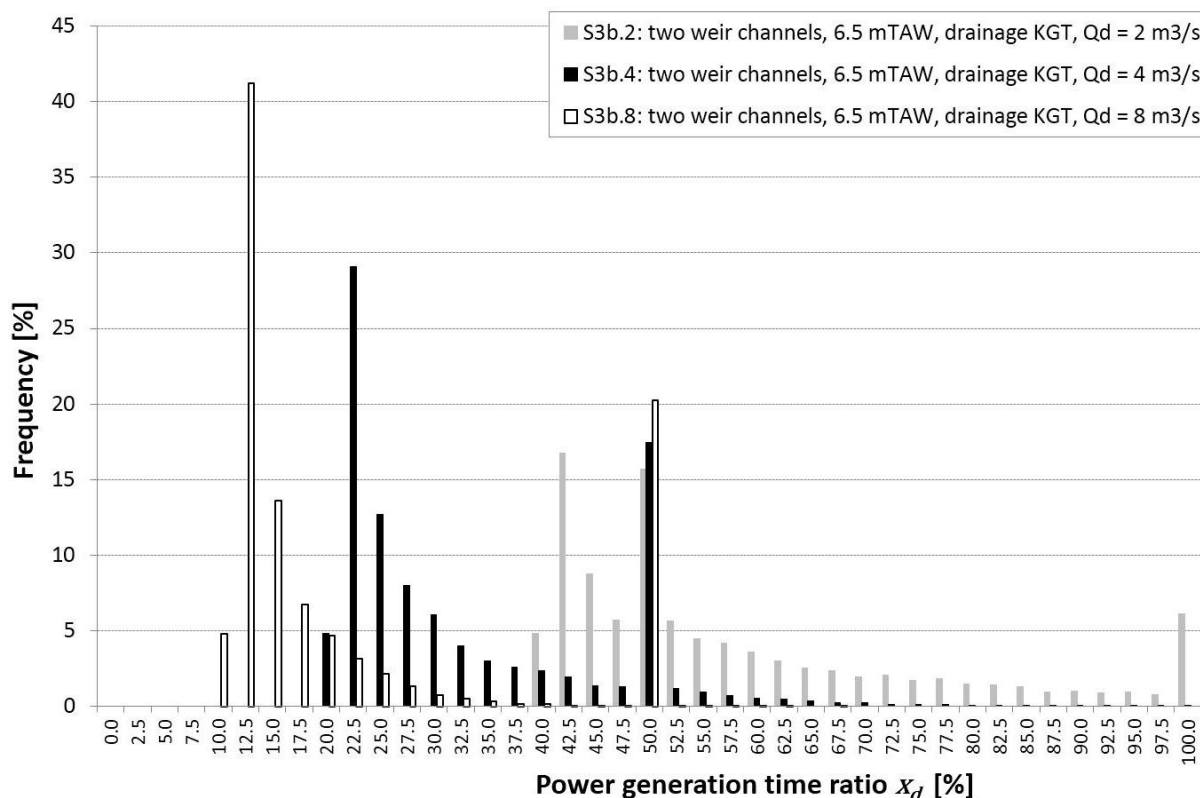


Figure 4-14: Frequency distribution of the power generation time ratio when using the recharge flow from two weir channels, with an additional diverted flow from KGT when necessary and possible (S3b.2, S3b.4 and S3b.8).

Finally it's interesting to look at the duration curves of the flow actually drained from KGT (Figure 4-15). The percentage of days with drainage, as given in Table 4-2, can be found at the crossing of the curve with the x-axis, i.e. it is the exceedance frequency of  $Q_{dr} > 0$ . First, it can be seen that a higher design flow shifts the curve to the upper right corner, meaning more water is drained more often from KGT. Second, it can be noted that in the lower range of time exceedance (0-10%) the difference in drained flow between an 'a'-scenario and 'b'-scenario for the same design flow, remains constant and equal to  $0.32 \text{ m}^3/\text{s}$  ( $= 0.78 \text{ m}^3/\text{s} - 0.46 \text{ m}^3/\text{s}$ ), i.e. the difference in recharge flow between the two scenarios. This makes sense, since the higher values of drained flow correspond to periods in which very little to no hydrological flow is available, and in both scenarios drainage is necessary to meet the demand. The lower values of drained flow correspond to time periods in which the recharge flow in the 'b'-scenario can meet the demand, while this is not true anymore for the 'a'-scenario; therefore the difference between the curves decreases.

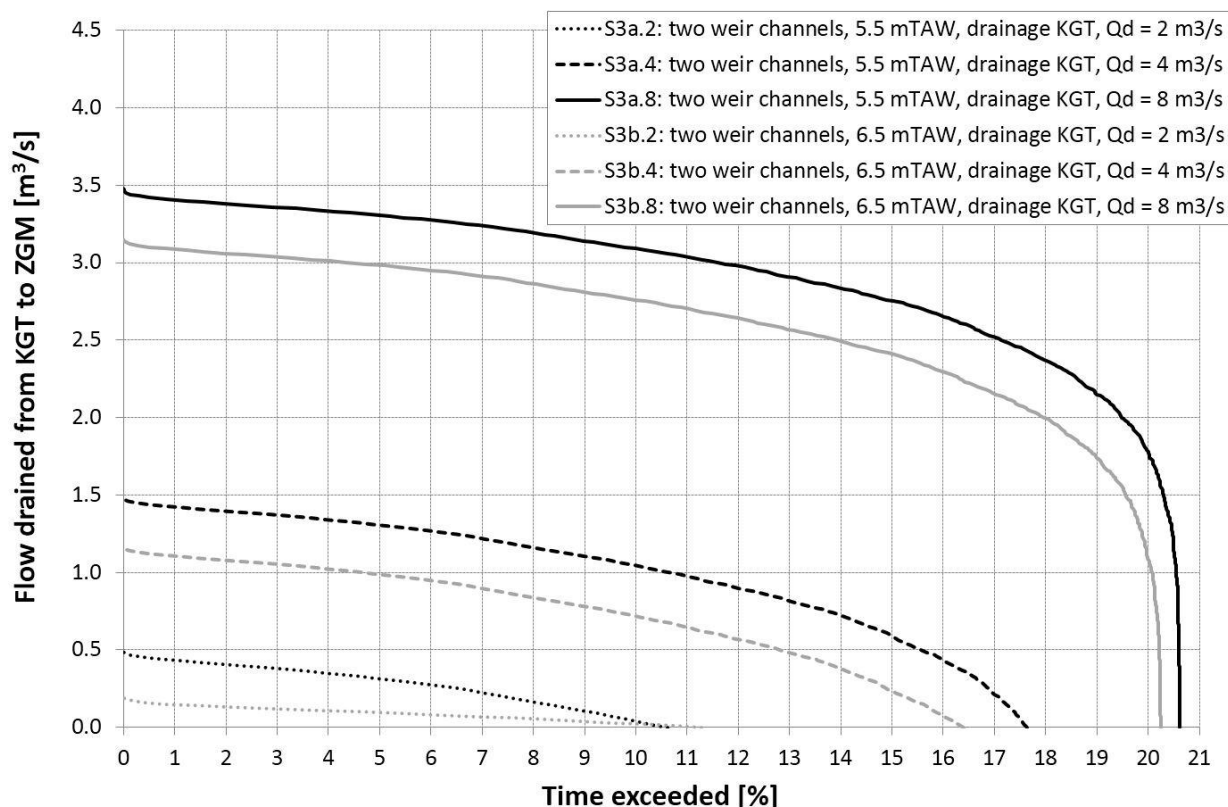


Figure 4-15: Duration curve of the drained flow, daily averaged, from KGT to ZGM when generating power on a daily basis (S3a and S3b).

#### 4.3.2 S4: ACTIVE RECHARGE OF KGT

In Scenario S3 the recharge volume through the weir channels is used every day, possibly complemented with a drained volume from KGT, albeit without putting extra pressure on the water supply to KGT during dry periods. However, with the construction of the lock and the weir channels, it becomes possible to recharge the channel between Ghent and Terneuzen during long periods of water scarcity to ameliorate the conditions regarding salinisation of the channel. This does not necessarily have to lead to a lower total yearly energy yield, because the recharge positively influences the 2-monthly average, making it possible to divert flow from KGT more often. In other words, the value for  $Q_{KGT,th}$  can be lowered.

To implement this recharge, the previous scenario can be extended with an extra control rule, which verifies whether a minimal power generation time ratio,  $x_{d,min}$ , is met should additional flow be diverted from KGT to ZGM. If  $x_{d,min}$  is not met, no power is generated and the recharge flow through the weir channels can be used to recharge KGT. Abstraction is made of the available hydrological runoff, since this will be low as well when drainage would have been required. In principle this volume could be used for power generation or to recharge KGT further, but this is not considered here.

The control rules as explained in §4.3.1 have to be extended. After checking whether flow can be drained, i.e. whether  $Q_{KGT,2months} < Q_{KGT,th}$ , it is additionally checked whether the  $x_d$ -value, should it be decided to drain, meets the minimal power generation time ratio.

Hence it is checked whether  $x_d \geq x_{d,min}$ . If that is the case, drainage will occur, with  $Q_{dr}$  calculated with Equation (24). If  $x_d < x_{d,min}$ , then no drainage occurs and the recharge flow from the Sea Scheldt to the upper reach through the weir channels is used to recharge KGT. Suitable values for both  $Q_{KGT,th}$  and  $x_{d,min}$  have to be set via trial-and-error, in which the values are set as low as possible without increasing the frequency of non-exceedance of the threshold value of 13 m<sup>3</sup>/s.

The scenario can be summarized as follows: (i) if no drainage is required, the recharge volume through the weir channels is used, together with the hydrological flow, for power generation (ii) if conditions are in favour of drainage, i.e. if the minimal power generation time ratio is met, drainage from KGT will occur and power will be generated using the hydrological flow, the recharge flow from the two weir channels and the drainage flow; (iii) if conditions are in favour of recharging KGT, no power will be generated at all, using the recharge flow through both weir channels to recharge KGT. The hydrological flow is not considered.

The water balance parameters of the scenarios are given in Table 4-3. It is clear that the threshold value for  $Q_{KGT}$  can be lowered significantly. Consequently, the percentage of days with drainage rises extensively. In scenario S4b.2, in which the gates of the weir channels close at 6.5 mTAW, less days with drainage from KGT occur compared to both S4a.2 and S4a.4; also the number of days with active recharge is lower compared to the scenarios where the weir channel gates close at 5.5 mTAW. This is a sensible result, since  $x_{d,min}$  is reached more easily without drainage, due to the larger recharge flow available. In other words, the demand – defined by the design flow – can be met more easily with the recharge flow and the hydrological flow.

For the same reason,  $x_{d,min}$  generally has to be given a higher value in the 'b'-scenarios for the same design flow, otherwise the recharge flow will always be used for power generation, i.e. the scenarios would be the same as in S3b (of course the value for  $Q_{KGT,th}$  would have to be higher). When the design flow increases,  $x_{d,min}$  can be lowered again, because the recharge flow together with the hydrological flow is more often not sufficient to meet the demand, and active recharge is allowed.

In S4b.8, the amount of days with drainage is very high. This is because the demand is high, but also because the recharge flow is high. So it often occurs that with the additional effort from draining,  $x_{d,min}$  is met. And this opportunity offers itself more often in S4b.8 than in S4a.8, because the recharge flow is higher in the former. Conversely, the net value of the mean drained flow is lower. The same holds for S4b.4 and S4a.4.

Finally it can be noted that S4b.2 has a high value for  $x_{d,min}$ . This is because of the low design flow compared to the flow through the weir channels: the flow through the weir channels is on average 0.78 m<sup>3</sup>/s, which already results in an  $x_d$ -value of 39%. So imposing an  $x_{d,min}$ -value lower than this 39% has no effect whatsoever.

*Table 4-3: Water balance parameters for the scenarios with active recharge of KGT, without putting additional pressure on the water supply to KGT.*

WATER BALANCE PARAMETERS FOR THE SCENARIOS WITH ACTIVE RECHARGE OF KGT, WITHOUT PUTTING ADDITIONAL PRESSURE ON THE WATER SUPPLY TO KGT						
Scenario	$Q_{KGT,th}$ [m <sup>3</sup> /s]	$X_{d,min}$ [%]	Mean drained flow <sup>a</sup> [m <sup>3</sup> /s]	Percentage of days		
				with drainage [%]	without drainage or recharge [%]	with active recharge [%]
S4a.2	17.4	24	0.11	39.9	55.4	4.7
S4a.4	16.6	15	0.54	57.3	19.7	23.0
S4a.8	17.5	11	1.34	50.3	10.1	39.6
S4b.2	13.7	40	0.01	34.0	0.62	0.04
S4b.4	16.2	21	0.38	57.8	27.7	14.5
S4b.8	17.2	11	1.24	52.2	24.9	22.9

<sup>a</sup>) Taking into account recharge flow as well. Hence negative would mean a net recharge.

In Figure 4-16, the time series of the available flow in scenario S4a.2 and S4b.2 can be seen, while Figure 4-17 shows the available flow in scenarios S4a.4 and S4b.4. Finally, Figure 4-18 depicts the time series of scenarios S4a.8 and S4b.8. It is interesting to note <sup>48</sup> that in S4b.4, the available flow often is below the daily averaged design flow – meaning that no drainage is allowed in order not to increase the frequency of non-exceedance of the 13 m<sup>3</sup>/s threshold, compared to the current situation – in periods in which drainage does occur in S4a.4. Because of the larger recharge flow in S4b.4, it is more often used directly for power generation. In other words, KGT is less frequently recharged, which means the drainage flow can be addressed less frequently as well in dryer periods. This lower recharge frequency for S4b.4 can also be noted in Table 4-3: the percentage of days with active recharge is 23.0% in S4a.4, while this is only 14.5% in S4b.4.

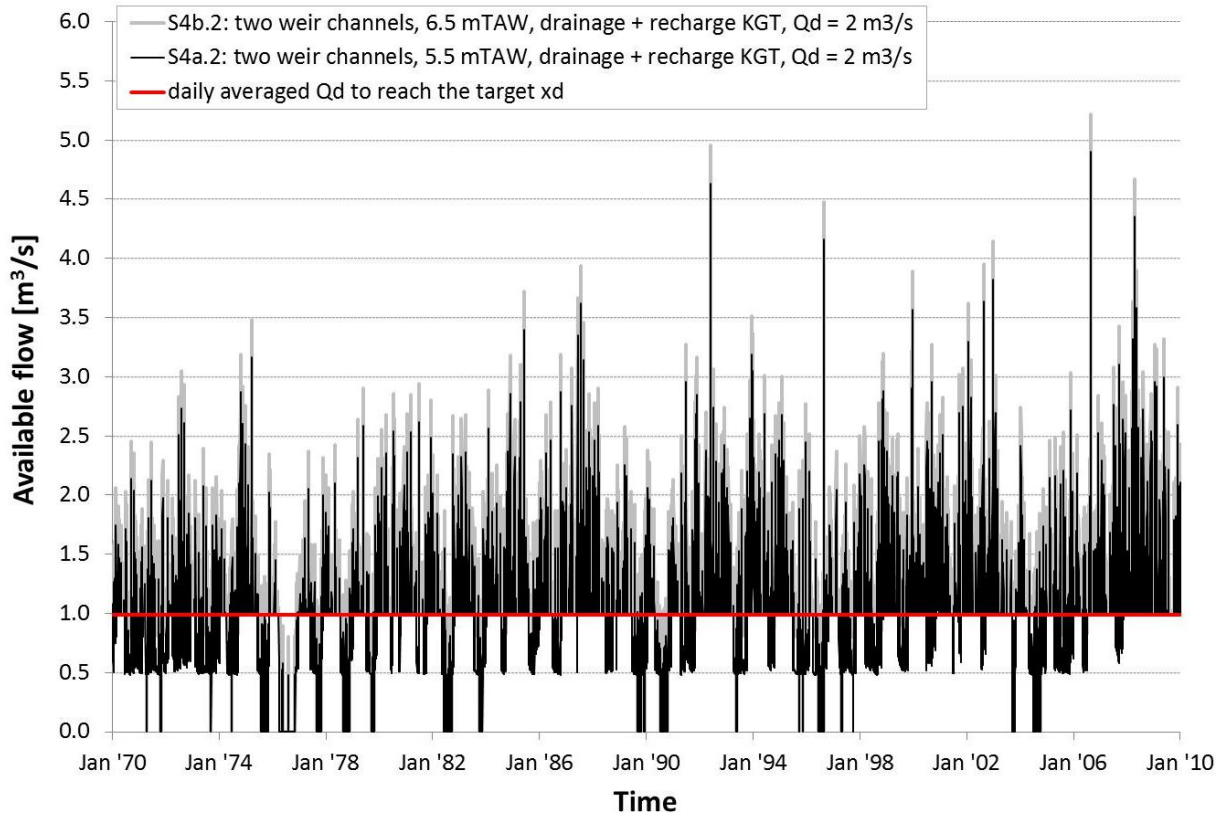


Figure 4-16: Time series of the available flow when combining flow diversion from and active recharge to KGT, for a design flow of 2 m³/s (S4a.2 and S4b.2). 49

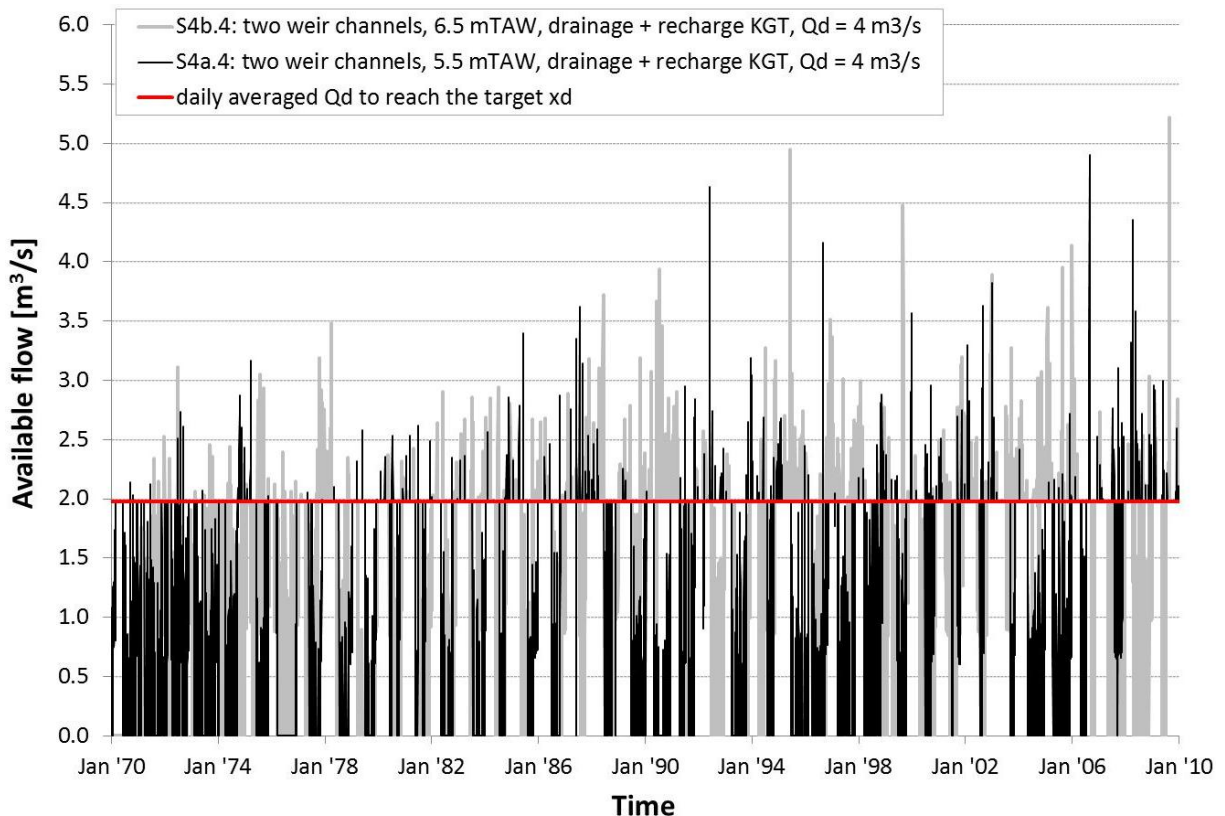


Figure 4-17: Time series of the available flow when combining flow diversion from and active recharge to KGT, for a design flow of 4 m³/s (S4a.4 and S4b.4).

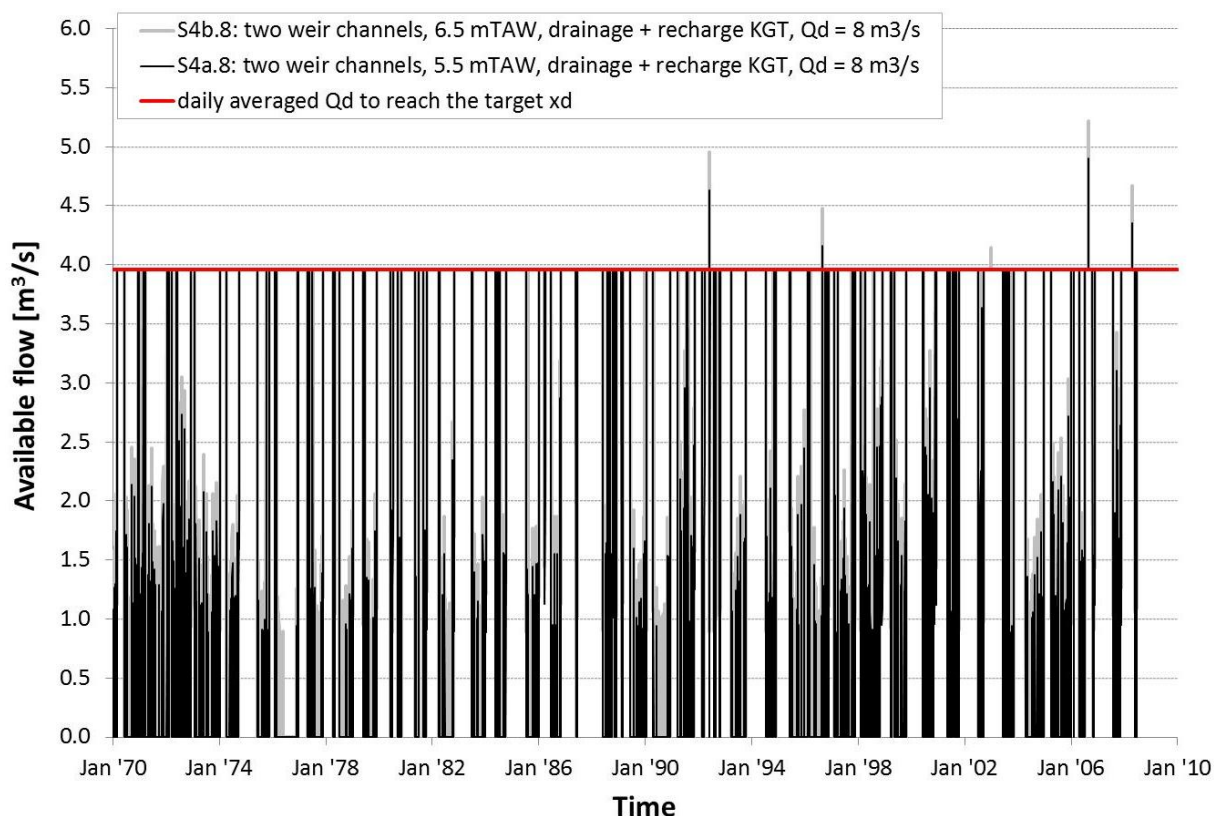


Figure 4-18: Time series of the available flow when combining flow diversion from and active recharge to KGT, for a design flow of 8 m<sup>3</sup>/s (S4a.8 and S4b.8).

The corresponding duration curves of the available flow in the S4a-scenarios can be seen in Figure 4-19. The horizontal part at the daily averaged design flow,  $x_{d,t} \cdot Q_d$ , extends significantly compared to the counterpart S3a scenarios. The same applies for the S4b-scenarios (Figure 4-20). Also, the curve does not span the full 100%: at a percentage of (100 - % of days with active recharge) the curve drops to zero.

This is also visible in the frequency distributions of the power generation ratio, that are shown in Figure 4-21 and Figure 4-22. For instance, for S4a.2 the frequency around the target level of  $x_d = 49.5\%$  is approximately 40%. This means that in about 40% of days, it will be possible to generate power above  $\Delta H_{low}$ , in this case 1 m, while using the full capacity of the turbine. When looking at the percentage of days with drainage (Table 4-3), it is clear that this high percentage can solely be attributed to the drainage. The gain is less pronounced in S4b.2, due to the fact that less active recharge is applied. After all, the recharge volume is larger, resulting in higher  $x_d$ -values. As a result, the minimal value is more easily reached, and power is generated.

In the frequency distribution of e.g. S4a.4, it is also clear that there are more than 20% of days that no power is generated ( $x_d = 0\%$ ). To be more precise, it is 23.0%, as tabulated in Table 4-3, i.e. the percentage of days with active recharge. For S4a.8, this mounts up to 40% of days without power generation. Figure 4-21 and Figure 4-22 also clearly show that for values of  $x_d$  between 0% and  $x_{d,min}$ , the frequency is zero, also meaning that no power is generated.

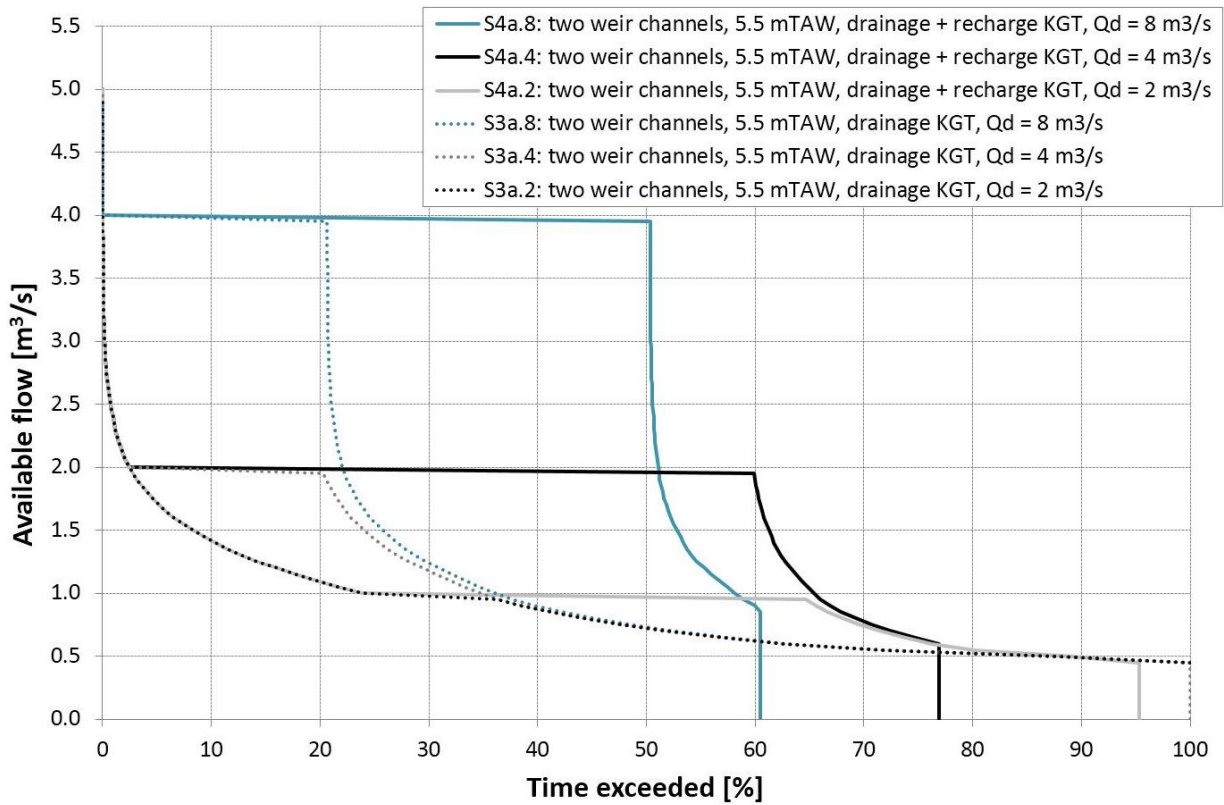


Figure 4-19: Duration curve of the available flow when combining flow drainage from and active recharge to KGT, and a gate closure level of 5.5 mTAW (S4a.2, S4a.4 and S4a.8).

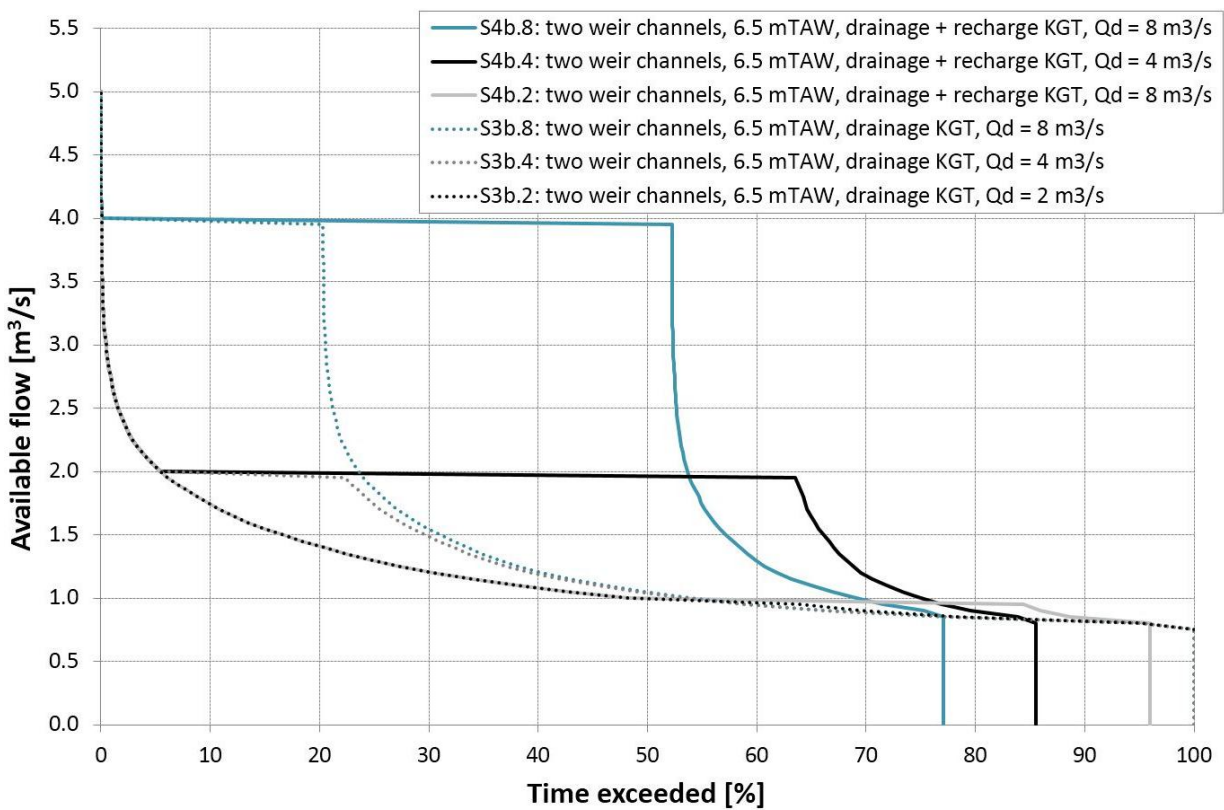


Figure 4-20: Duration curve of the available flow when combining flow drainage from and active recharge to KGT, and a gate closure level of 6.5 mTAW (S4b.2, S4b.4 and S4b.8).

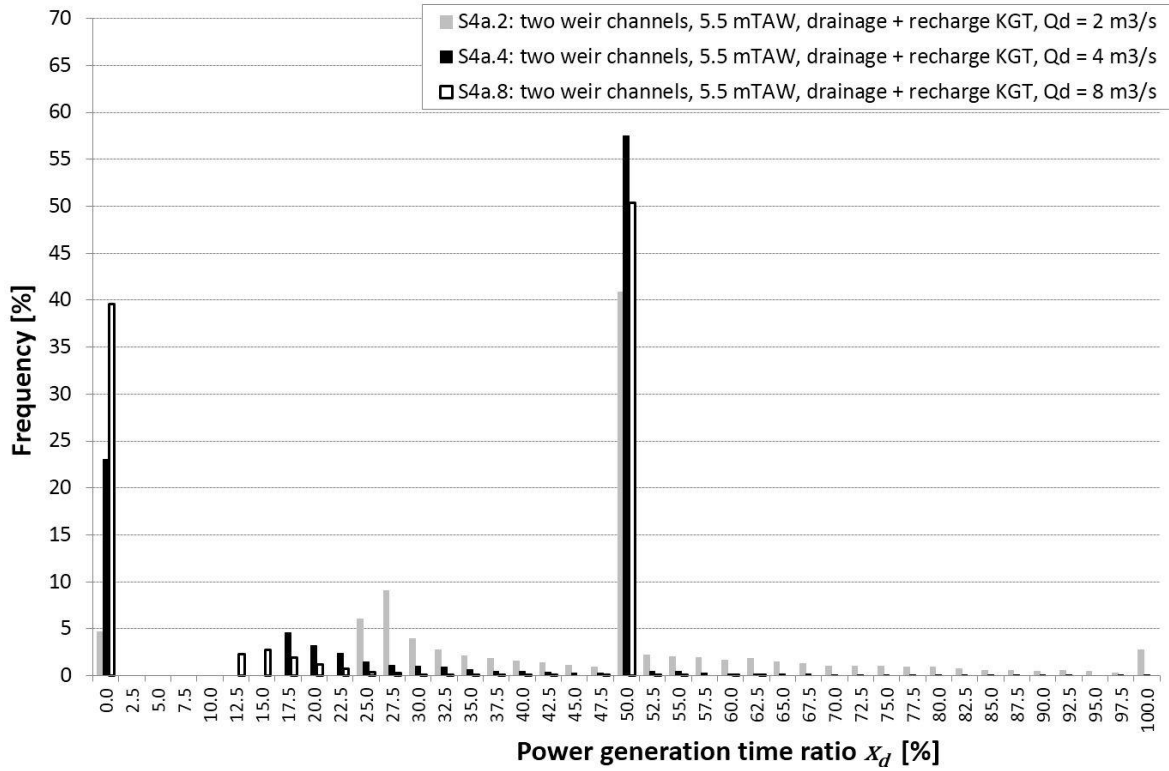


Figure 4-21: Frequency distribution of the power generation time ratio when combining flow drainage from and active recharge to KGT, and a gate closure level of 5.5 mTAW (S4a.2, S4a.4 and S4a.8).

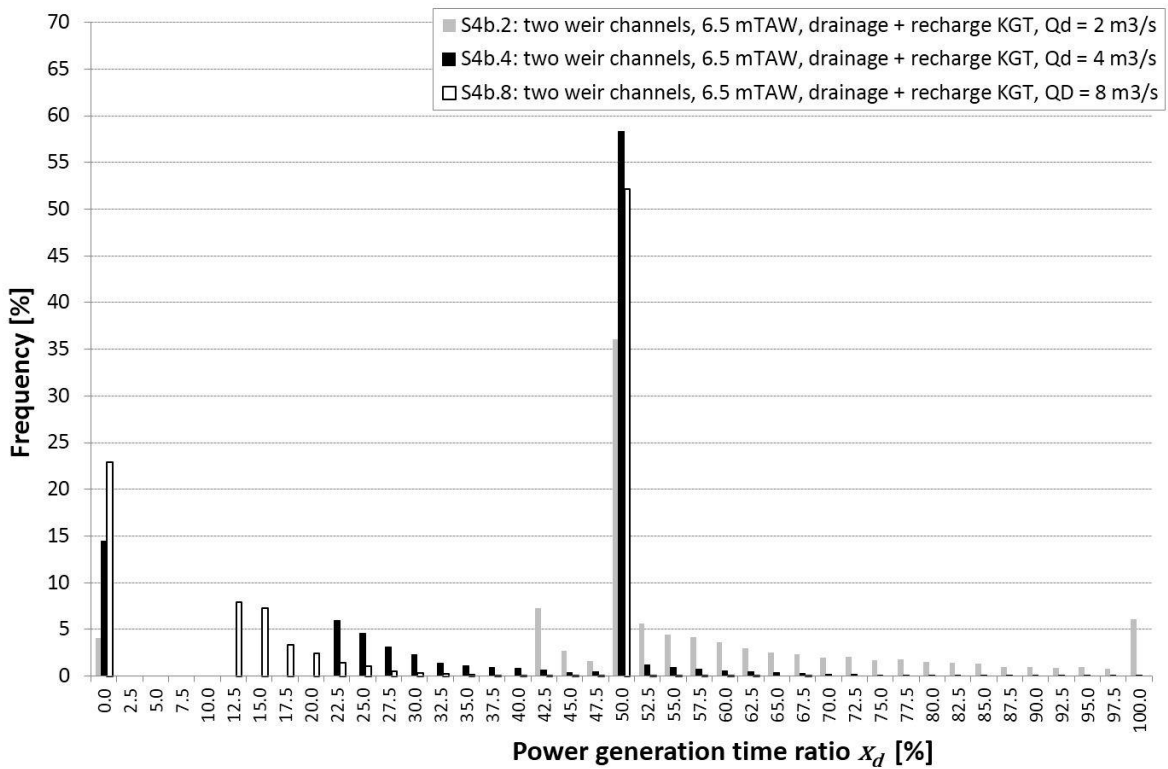


Figure 4-22: Frequency distribution of the power generation time ratio when combining flow drainage from and active recharge to KGT, and a gate closure level of 6.5 mTAW (S4b.2, S4b.4 and S4b.8).

In Figure 4-23, the duration curves of the flow drained from KGT for all S4-scenarios are shown. Compared to the curves in the S3-scenarios (Figure 4-15), it is clear that the amount of days with drainage from KGT is larger (mind the scale of the horizontal axis). The pressure on the water balance hence appears to be higher, but it should be stressed that the active recharge enables this additional usage.

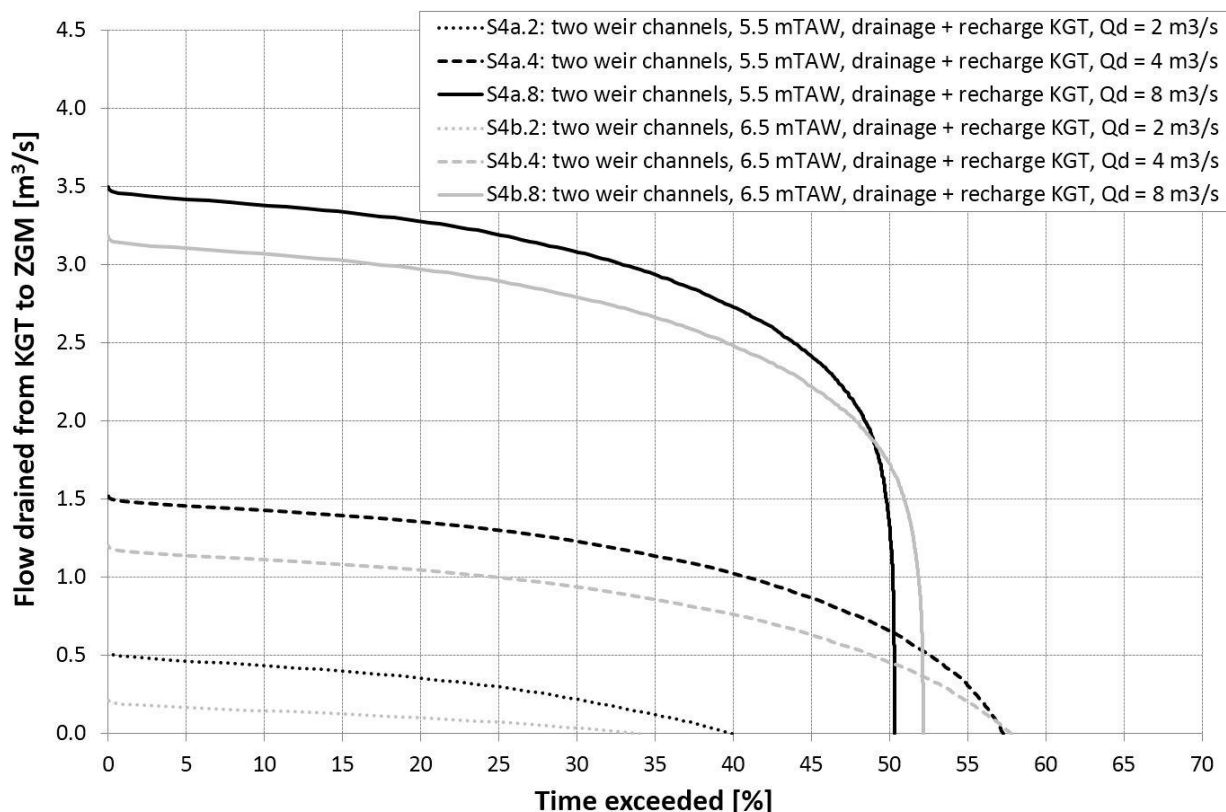


Figure 4-23: Duration curve of the drained flow, daily averaged, from KGT to ZGM when combining flow drainage from and active recharge to KGT (S4).

The effect on the 2-monthly averaged daily simulated flow passing Evergem – which is considered representative for the flow going to KGT – can be seen in Figure 4-24. The figure shows an example of three years (from 1996 to 1998). The combination of active recharge and drainage results in a decrease of the flow when the 2-monthly average is above the threshold value of 13 m³/s, while there is an increase when the 2-monthly is below this threshold value. So there is some kind of general decrease in ‘amplitude’ of the time series, closer towards the threshold value – except for the first months below the threshold. Also there is a shift in the dry period – i.e. the period during which the flow is below the threshold –, as can be seen in Figure 4-25. The dry period in the situation with active recharge and drainage starts earlier than in the current situation, but it ends earlier as well.

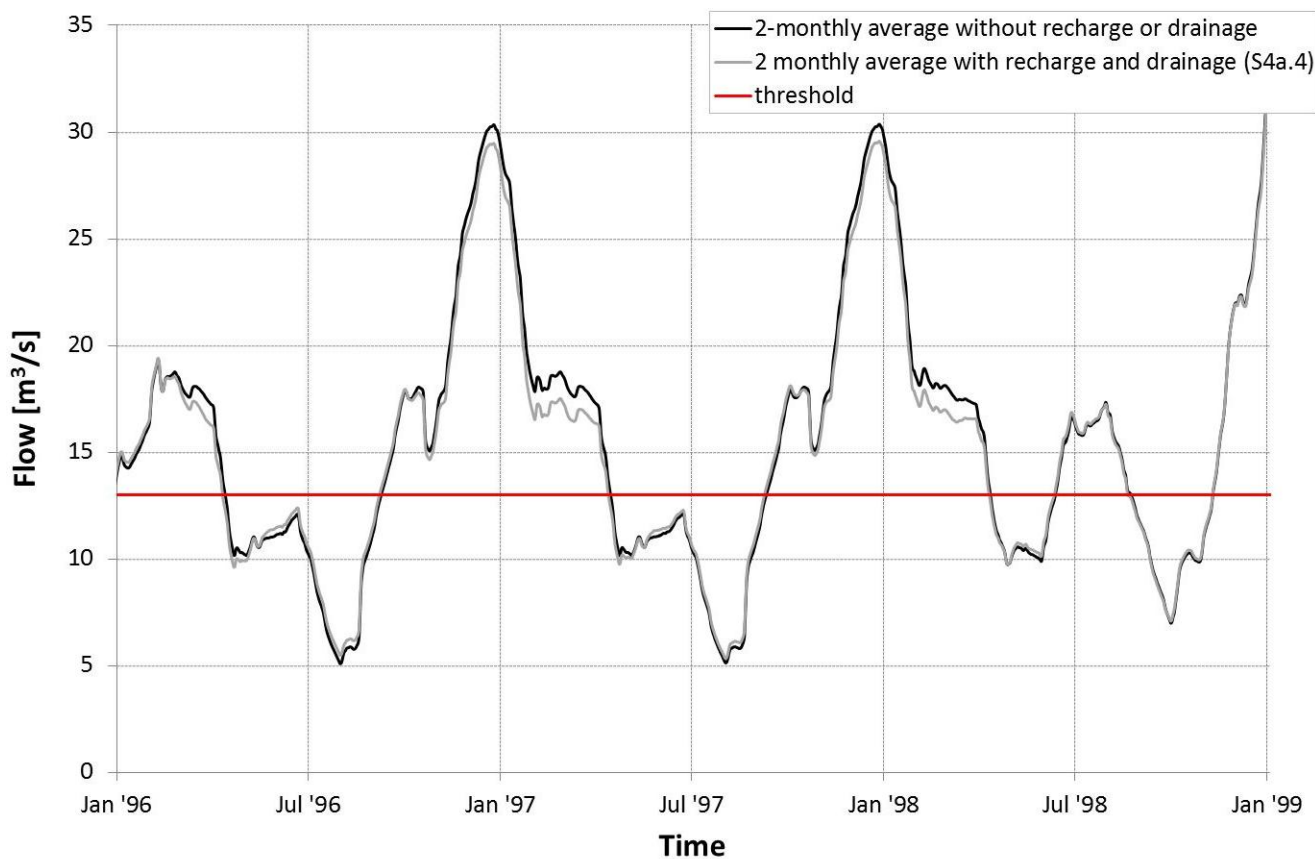


Figure 4-24: Two-monthly averaged simulated daily flow passing Evergem, for the current situation (without recharge or drainage) and the situation with active recharge and drainage (and a closure level of the weir channels gates of 5.5 mTAW, S4a.4), for the years 1996-1998.

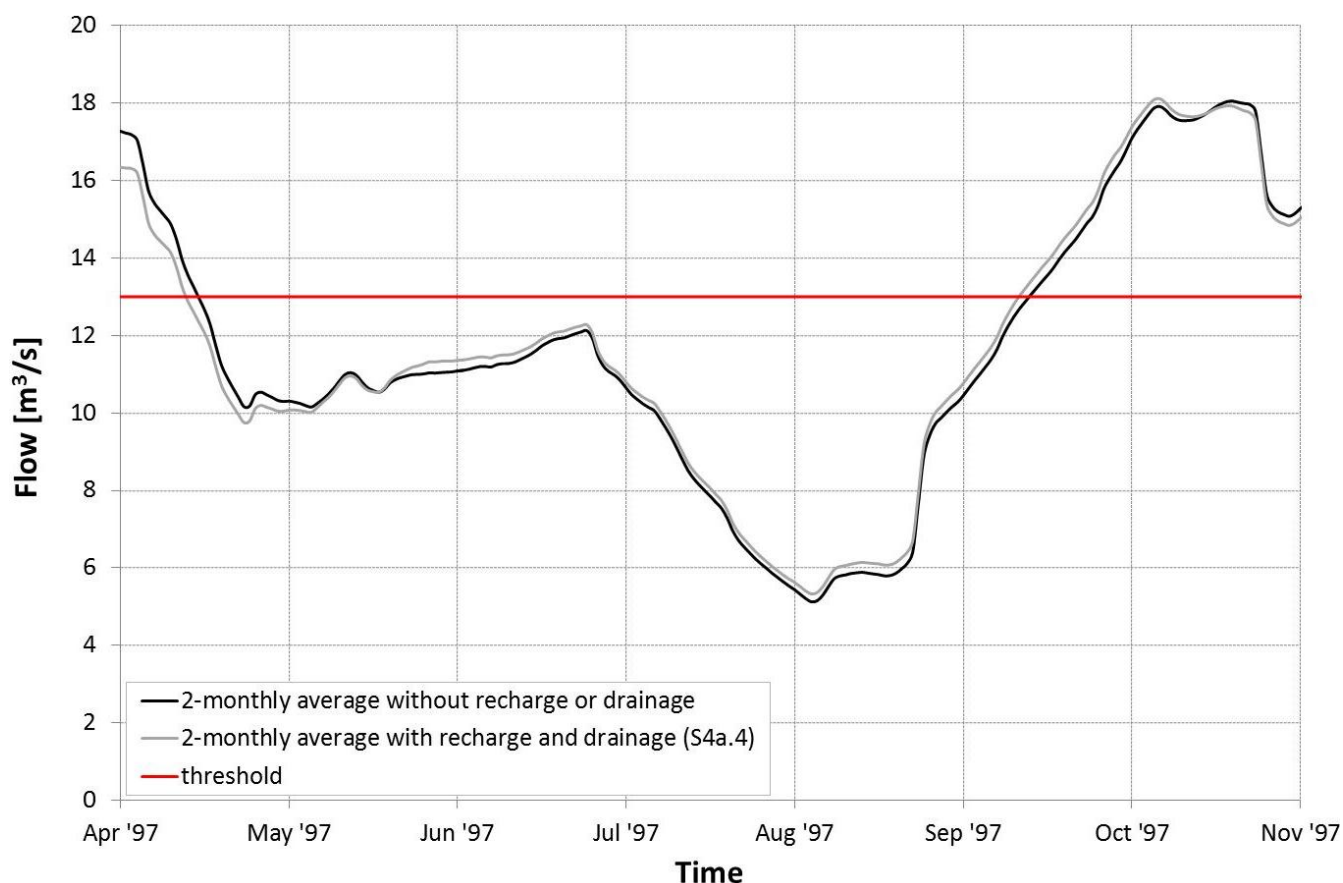


Figure 4-25: Two-monthly averaged simulated daily flow passing Evergem, for the current situation (without recharge or drainage) and the situation with active recharge and drainage (and a closure level of the weir channels gates of 5.5 mTAW, S4a.4), for the period April–October 1997.

### 4.3.3 S5: COMPROMISE BETWEEN POWER GENERATION AND WATER USAGE

In scenario 4, the channel between Ghent and Terneuzen is actively recharged during dry periods, when a minimal power generation time ratio  $x_{d,min}$  would not be met, even when flow from KGT could be used. This  $x_{d,min}$ -value, together with the threshold value  $Q_{KGT,th}$  to decide whether drainage is possible, are given values which put no extra pressure on the water balance than currently is the case, i.e. the frequency of non-exceedance of the value 13 m<sup>3</sup>/s does not increase. In other words, the power generation is given sole priority within the boundaries of the treaty.

Another possibility is to optimize these parameters taking both the power generation and the water scarcity around Ghent into account. For instance, by setting the minimal  $x_d$ -value equal to the target level while keeping the same values for  $Q_{KGT,th}$ <sup>10</sup>, thus  $x_{d,min} = 49.5\%$ . This way, more recharge flow becomes available, and the exceedance

<sup>10</sup> In principle, the values for  $Q_{KGT,th}$  could be lowered, since  $x_{d,min}$  increases. This however is not investigated because the S5 scenarios explicitly aim at an improvement of the water shortage in dry periods. Finding the most 'desirable' compromise between power generation and water usage is a political choice rather than a technical one.

frequency of 13 m<sup>3</sup>/s will increase. The drawback of this scenario is – inevitably – a lower energy yield. The values used for  $x_{d,min}$  and  $Q_{KGT,th}$  are shown in Table 4-4, together with the impact on the water balance around Ghent. To compare, the exceedance frequency of 13 m<sup>3</sup>/s in the current situation, calculated from the available model results, is 78.71%. All scenarios result in a higher exceedance frequency.

Table 4-4: Water balance parameters for the scenarios with active recharge of KGT, with increase of the exceedance frequency of 13 m<sup>3</sup>/s.

WATER BALANCE PARAMETERS FOR THE SCENARIOS WITH ACTIVE RECHARGE OF KGT, WITH INCREASE OF THE EXCEEDANCE FREQUENCY OF 13 M <sup>3</sup> /S								
Scenario	$Q_{KGT,th}$ [m <sup>3</sup> /s]	$x_{d,min}$ [%]	Mean drained flow <sup>a</sup> [m <sup>3</sup> /s]	Percentage of days			Impact on treaty	
				with drainage [%]	without drainage or recharge [%]	with active recharge [%]	Exceedance frequency of 13 m <sup>3</sup> /s [%]	Relative decrease of dry period average length [%]
S5a.2	17.4	0.495	-0.03	40.4	24.2	35.4	79.67	4.5
S5a.4	16.6	0.495	0.47	57.9	2.6	39.5	79.28	2.7
S5a.8	17.5	0.495	1.31	50.67	0.04	49.29	78.98	1.3
S5b.2	13.7	0.495	-0.09	34.3	49.4	16.3	79.41	3.3
S5b.4	16.2	0.495	0.23	59.1	5.6	35.3	80.04	6.2
S5b.8	17.2	0.495	1.09	53.50	0.05	46.45	79.73	4.8

<sup>a)</sup> Taking into account recharge flow as well. Hence negative means a net recharge.

The scenarios with a negative mean flow from KGT, i.e. S5a.2 and S5b.2, have a net recharge of the channel. Consequently, these scenarios have a pronounced impact on the water balance. However, a high positive mean flow from KGT does not necessarily mean a smaller impact, as can be seen when comparing the exceedance frequency of 13 m<sup>3</sup>/s of scenarios S5a.2 and S5b.8. Although the latter has a net positive mean flow from KGT, it has a comparable impact – even slightly higher. This is because in S5a.2, drainage occurs more often and closer to the dry period, due to the lower demand. In other words, although S5b.8 has a high percentage of days with drainage, this drainage mainly occurs in periods with ample discharge. Moreover the recharge through the weir channels is higher, due to the higher gate closure level.

The time series of the flow available for power generation in scenarios S5a.2 and S5b.2 are shown in Figure 4-26, Figure 4-27 shows the time series for scenarios S5a.4 and S5b.4, and Figure 4-28 for scenarios S5a.8 and S5b.8.

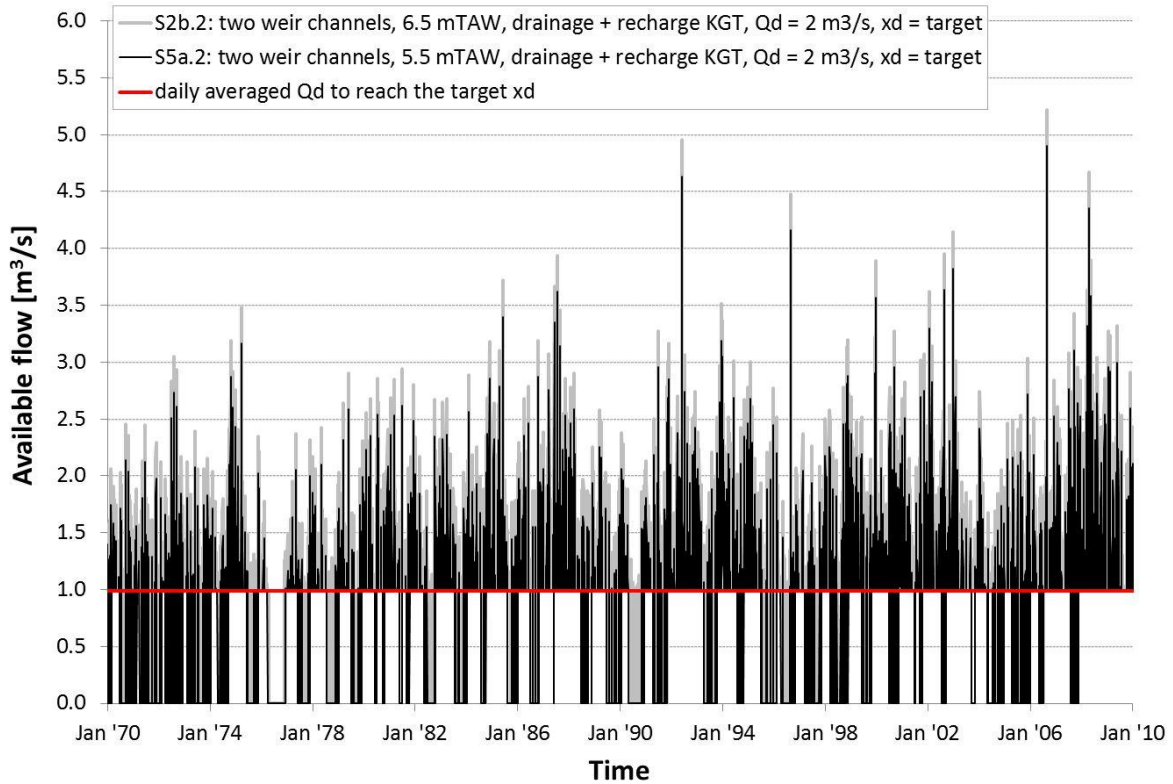


Figure 4-26: Time series of the available flow when combining flow diversion from and active recharge to KGT, whilst also improving the water balance, for a design flow of 2 m<sup>3</sup>/s (S5a.2 and S5b.2).

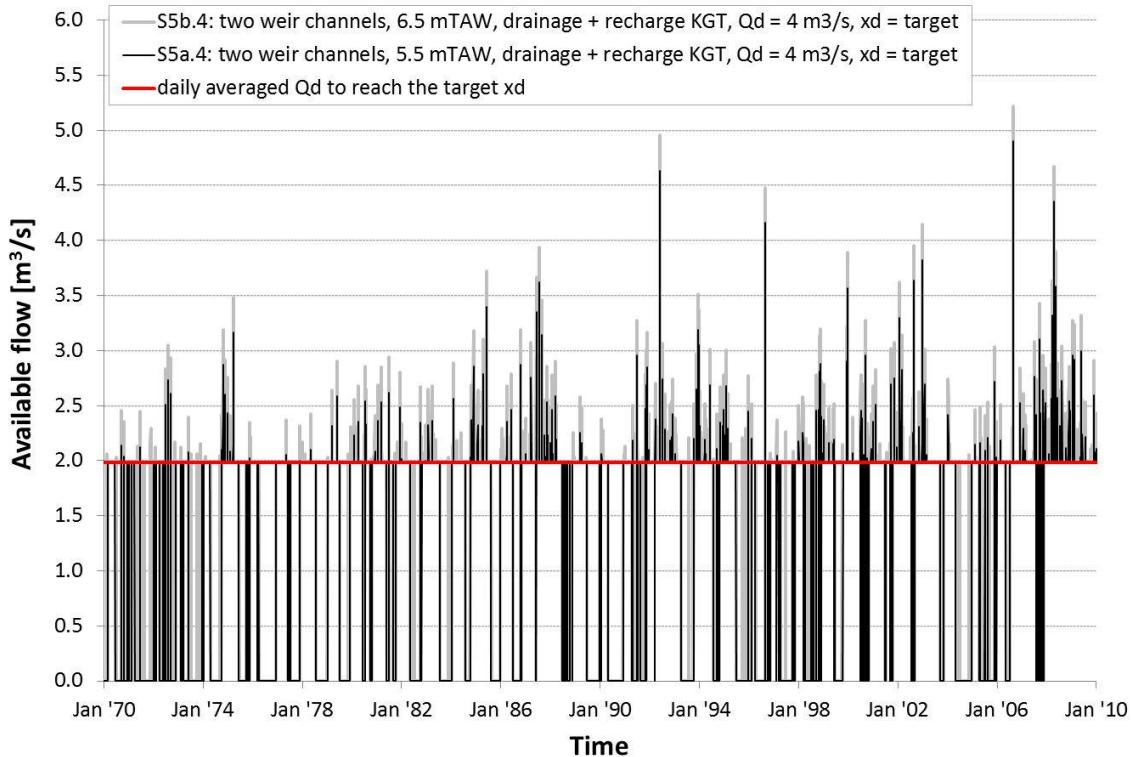


Figure 4-27: Time series of the available flow when combining flow diversion from and active recharge to KGT, whilst also improving the water balance, for a design flow of 4 m<sup>3</sup>/s (S5a.4 and S5b.4).

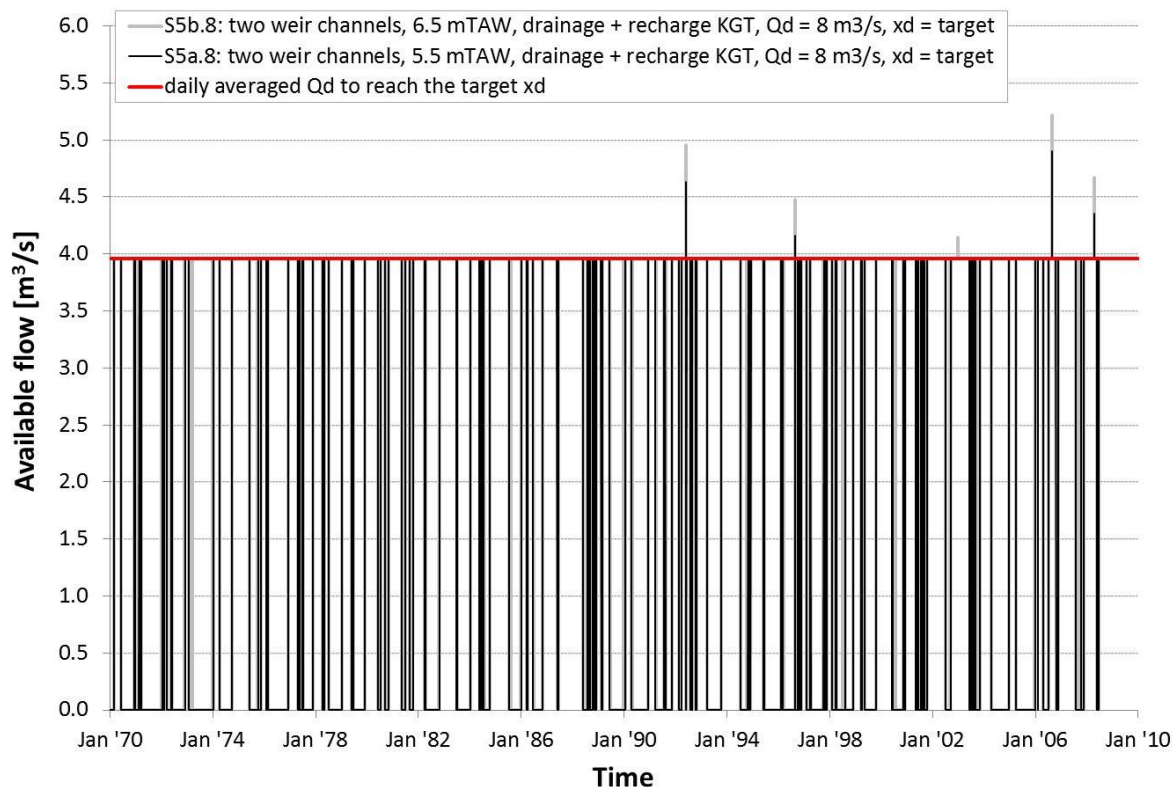


Figure 4-28: Time series of the available flow when combining flow diversion from and active recharge to KGT, whilst also improving the water balance, for a design flow of 8 m³/s (S5a.8 and S5b.8).

The corresponding duration curves are depicted in Figure 4-29 and Figure 4-30. In the frequency distribution of the power generation time ratio (Figure 4-31), it can again be seen how the frequency values for  $x_d$ -values below the target level drop to zero. The sum of all these frequency values in S4-scenarios is now equal to the frequency of  $x_d = 0\%$  in the corresponding S5-scenario, while the frequency around the target level remains the same (in practice a small difference might exist, but this is due to the discretization into classes).

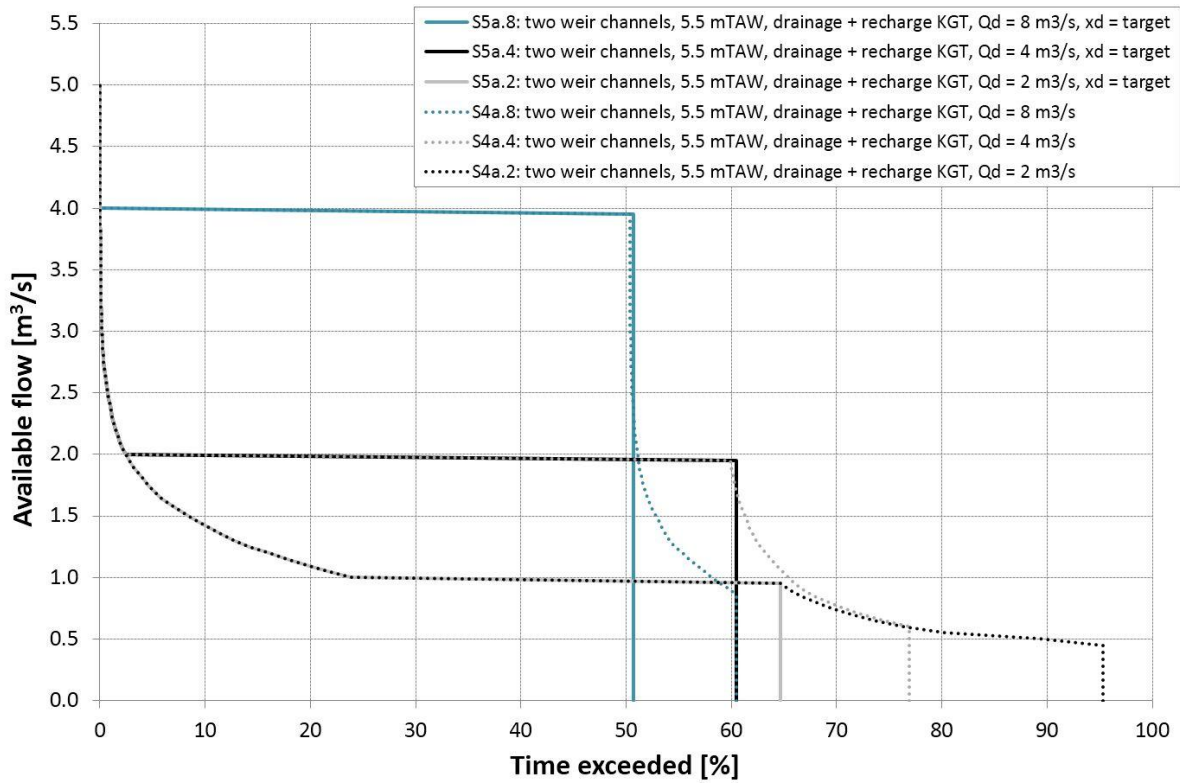


Figure 4-29: Duration curve of the available flow when combining flow diversion from and active recharge to KGT, whilst also improving the water balance, and a gate closure level 59 of 5.5 mTAW (S5a.2, S5a.4 and S5a.8).

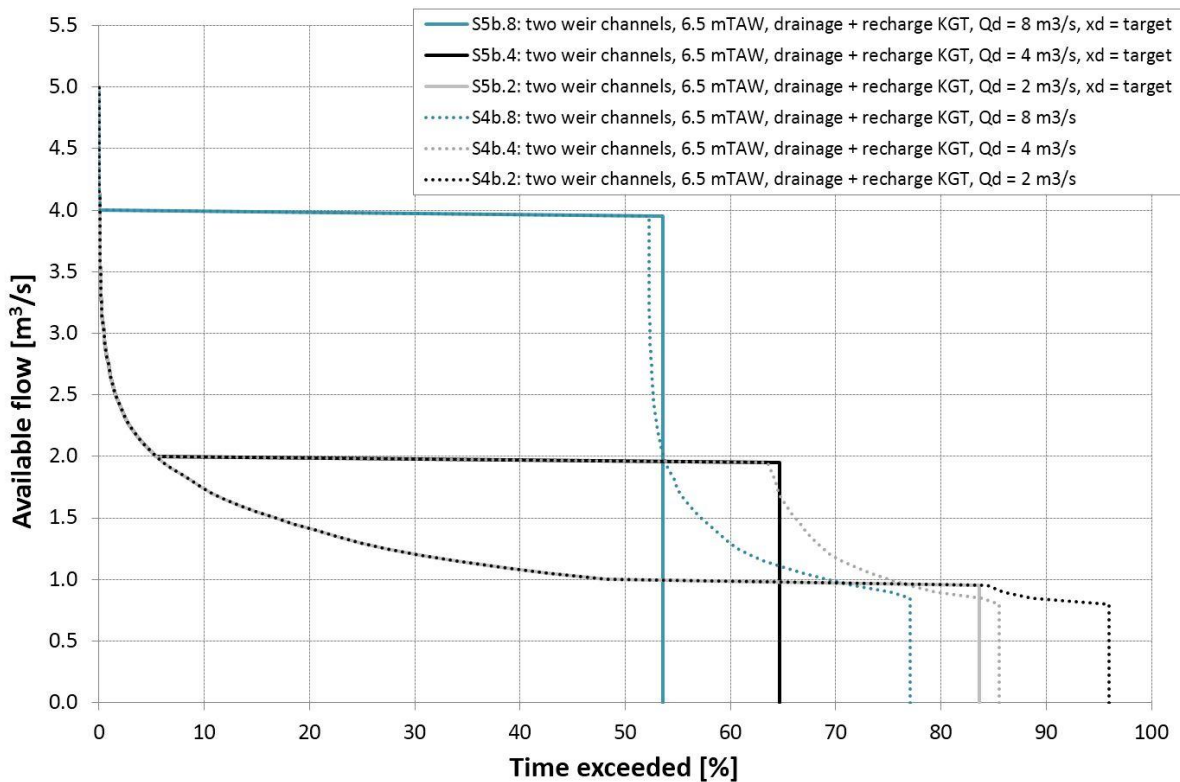


Figure 4-30: Duration curve of the available flow when combining flow diversion from and active recharge to KGT, while also improving the water balance, and a gate closure level of 6.5 mTAW (S5b.2, S5b.4 and S5b.8).

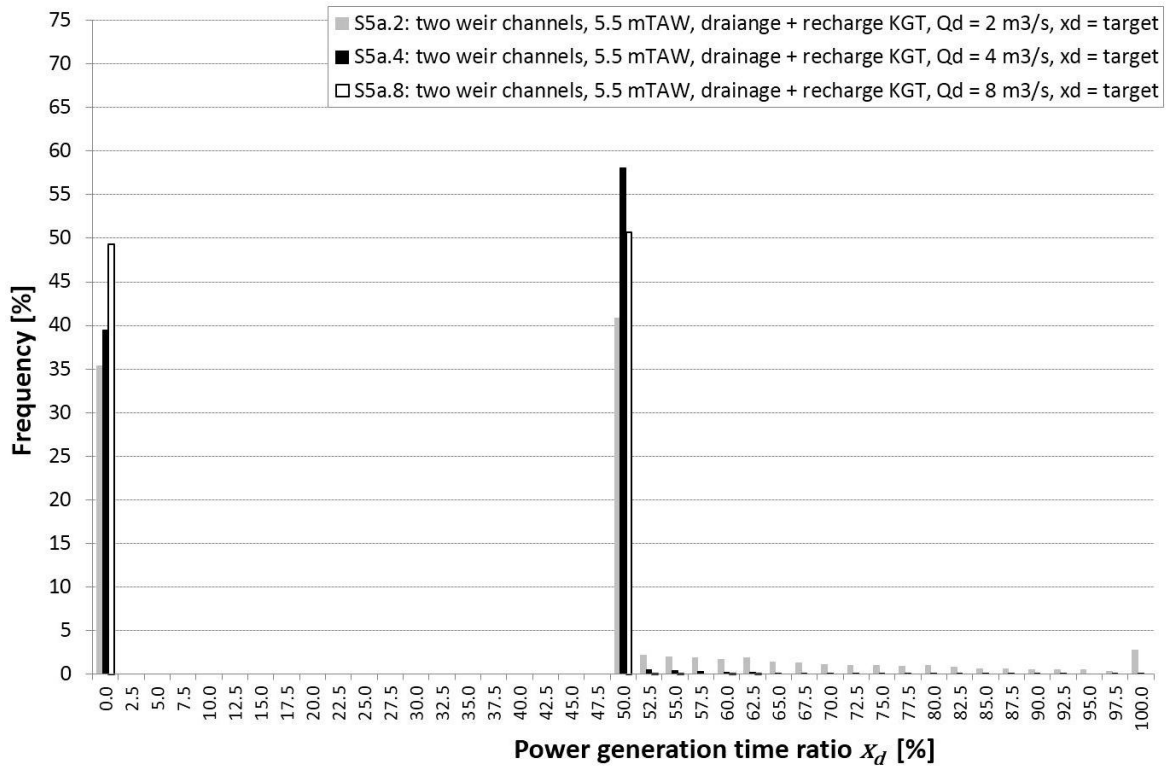


Figure 4-31: Frequency distribution of the power generation time ratio when combining flow diversion from and active recharge to KGT, whilst also improving the water balance, and a gate closure level of 5.5 mTAW (S5a.2, S5a.4 and S5a.8).

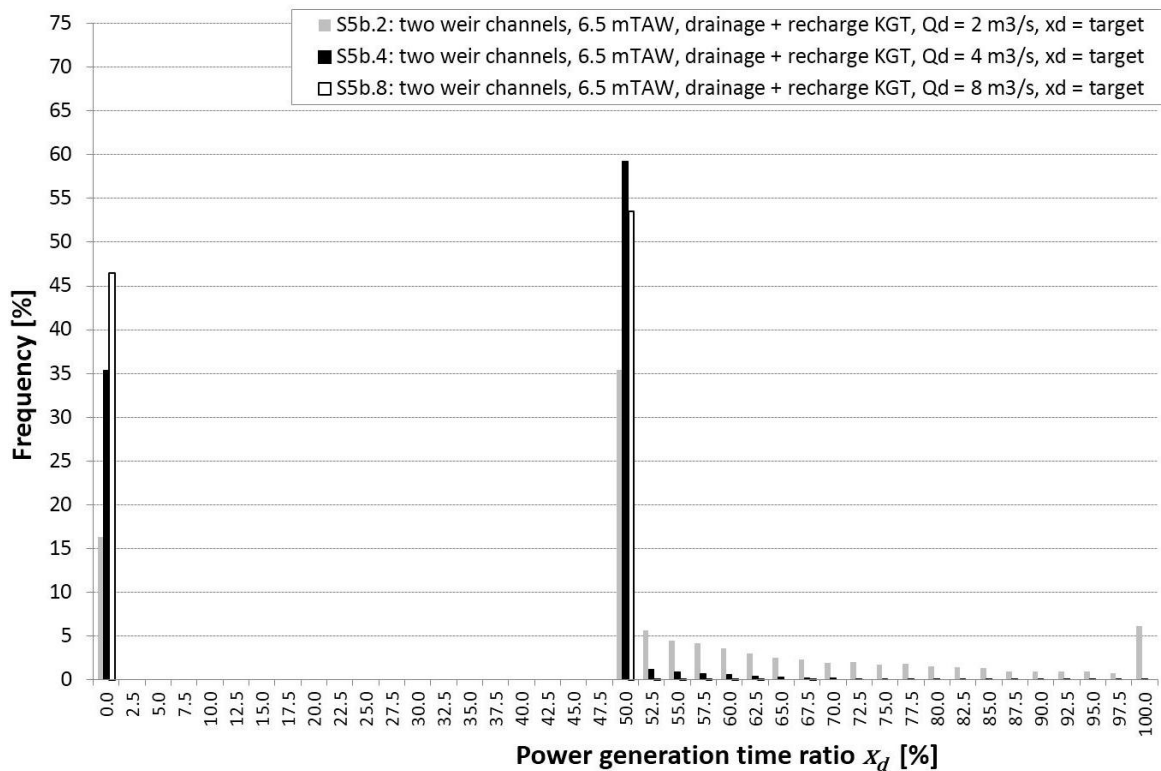


Figure 4-32: Frequency distribution of the power generation time ratio when combining flow diversion from and active recharge to KGT, whilst also improving the water balance, and a gate closure level of 6.5 mTAW (S5b.4 and S5b.8).

Figure 4-33 depicts the duration curves of the drained flow from KGT to ZGM, for the S5-scenarios. For comparison, the curves of the corresponding S4-scenarios are shown as well. Remarkably, the amount of flow drained is slightly higher. This is possible because of the higher amount of recharge volume towards KGT.

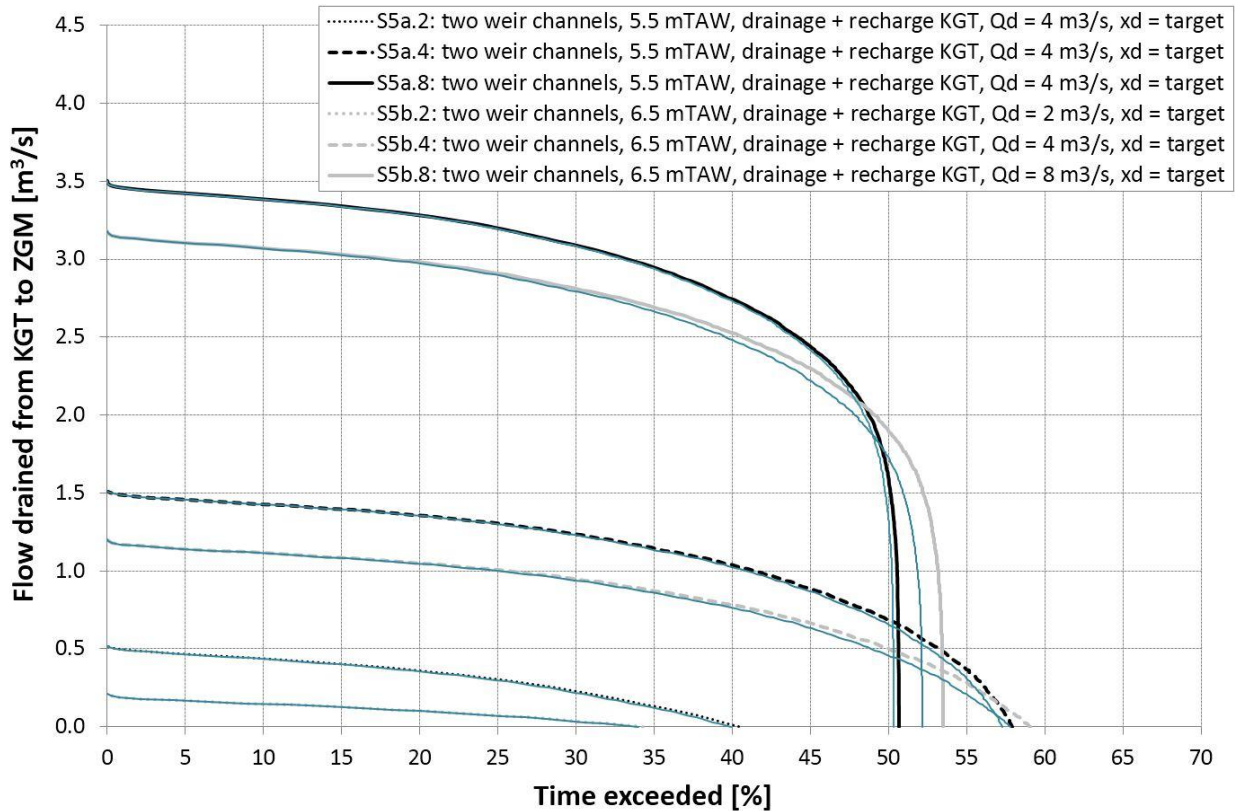


Figure 4-33: Duration curve of the diverted flow, daily averaged, from KGT to ZGM when combining flow diversion from and active recharge to KGT, whilst also improving the water balance (S5). The green lines are the curves of the corresponding S4-scenarios.

Finally, as an example, the difference between S4b.4 and S5b.4 – i.e. between maximum power generation and compromise between power generation and water usage – can be seen in Figure 4-34, that shows the 2-monthly averaged simulated daily flow passing Evergem for the current situation and the two scenarios. For S5b.4 – the compromise scenario – the dry period is shorter compared to S4b.4 or the situation without recharge or drainage. In other words, the S5-scenarios clearly are beneficial for the water shortage in the region during dry periods.

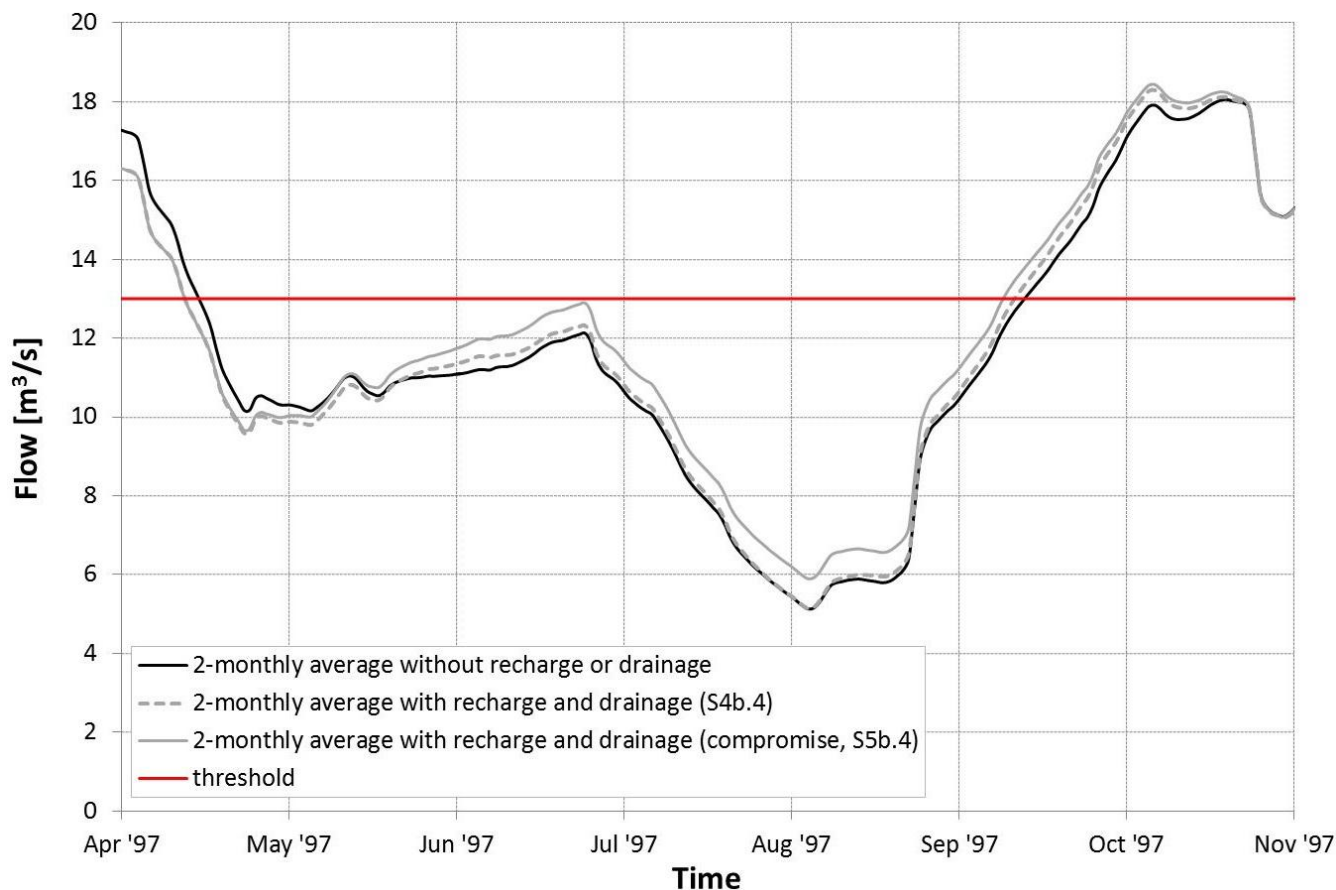


Figure 4-34: Two-monthly averaged simulated daily flow passing Evergem, for the current situation (without recharge or drainage), the situation with active recharge and drainage (S4b.4), and the compromise between power generation and water usage (S5b.4), for the period April–October 1997.

## 5 ENERGY YIELD

*In Chapter 4, several scenarios regarding available flow have been developed. In this chapter, the average yearly energy yield will be calculated, according to the methodology explained in §2.4. First an overview of all scenarios is given. After that, the energy yields are compared.*

### 5.1 TYPE OF TURBINE

At the site in Heusden, the available head and discharge vary considerably through one tidal cycle. Hence a possible turbine should be able to provide a high efficiency for a wide range of operating conditions. In IMDC (2011), an overview of the turbine types that can be applied at the tidal lock in Heusden is given. It was concluded that the most suitable types were a Kaplan turbine, a bulb turbine, or a cross flow turbine. Examples of efficiency curves can be seen in Figure 2-2. *Due to the limited head available here, a Kaplan or bulb turbine is preferred over a cross flow turbine.*

In this study, no specific choice is made for either of the two suitable options, but instead it is conceptualized as having a fixed design flow and corresponding efficiency. Indeed, Kaplan and bulb turbines have comparable efficiencies around the design point. Moreover, the main objective of this study is to investigate the feasibility of harvesting energy at the tidal lock in Heusden, and both the Kaplan or the bulb turbine can be technically 63 implemented in a possible hydropower scheme. The final selection of a turbine is part of a detailed design study.

### 5.2 CALCULATIONS

The average yearly energy yield is calculated with Equation (18) and Equation (19), in which the efficiencies are given the following values:  $\eta_{gen} = 0.90$ ,  $\eta_{trans} = 0.97$  (ANRE & ODE-Vlaanderen, 1999) and  $\eta(Q_d) = 0.85$  (Figure 2-2), resulting in a total efficiency of 0.74.

For the calculation of the yearly average energy yield, the frequency distributions of  $x_d$ , as defined in Chapter 4, serve as input. Since it is only possible to generate power for  $\Delta H$  above 1 m, the maximum power generation time ratio is  $x_d = 49.5\%$ . Hence in the calculations, days with  $x_d$ -values above 49.5% the energy yield remains the same as that for a day with an  $x_d$ -value of 49.5%. The surplus volume is considered to be unusable for power generation because of the limited design discharge of the turbine.

### 5.3 RESULTS

Table 5-1 shows an overview of the scenarios considered, 26 in total. All scenarios use the hydrological flow to ZGM (S0). Gradually additional flows are considered, making more flow available for power generation. First flow through two weir channels (S2) is additionally considered, with the level in the Sea Scheldt at which the gates are closed as an additional parameter. Then, a diverted flow from KGT is considered as well (S3), which

is a unidirectional volume exchange from KGT to ZGM. The next step considers bidirectional volume exchange between KGT and ZGM (S4), combining active recharge of KGT during dry periods, which allows for longer periods of drainage as well. These S4-scenarios aim at a maximization of the energy yield. Finally, a balanced scenario, in which the water scarcity is alleviated compared to the current situation, at the expense of the energy yield, is considered as well (S5).

The energy yield is calculated as explained in §2.4, taking into account the smaller hydraulic head range (§2.5). The results are given in Table 5-1. The results from Table 5-1 can also be seen in Figure 5-1, expressed in number of households. In Flanders, the average yearly amount of electric energy consumed by a household is 3 500 kWh (VREG, 2014).

For comparison, the energy yield results can be compared to the energy yield of the *fictitious* situation where an average head of 2 m is available all the time (halfway between 1 m and 3 m), as well as the design discharge of 4 m<sup>3</sup>/s. Equation (2) then results in a yearly energy yield of 510 MWh, or about 146 households.

Table 5-1: Overview of average yearly energy yield of the considered scenarios.

OVERVIEW OF AVERAGE YEARLY ENERGY YIELD OF THE CONSIDERED SCENARIOS										
Drainage from KGT	Recharge to KGT	no. of weir channels [-]	Gate closure level [mTAW]	Design flow $Q_d$ [m <sup>3</sup> /s]	$X_{d,min}$ [%]	$Q_{KGT,th}$ [m <sup>3</sup> /s]	Scenario	$E_{year}$ [MWh]	$E_{year}$ [hhs <sup>a)</sup> ]	
no	no	-	-	2	-	-	S0.2	44.5	13	
				4	-	-	S0.4	54.0	15	
		2	5.5	2	-	-	S2a.2	90.2	26	
				4	-	-	S2a.4	115.2	33	
				8	-	-	S2a.8	128.9	37	
			6.5	2	-	-	S2b.2	108.5	31	
				4	-	-	S2b.4	150.6	43	
				8	-	-	S2b.8	173.2	49	
		yes	no	2	5.5	2	-	30.6	S3a.2	92.4
4	-					30.1	S3a.4	131.7	38	
8	-					28.5	S3a.8	189.9	54	
6.5	2				-	24.2	S3b.2	109.1	31	
	4				-	30.3	S3b.4	161.1	46	
	8				-	28.8	S3b.8	224.5	64	
yes	2			5.5	2	24	17.4	S4a.2	97.2	28
					4	15	16.6	S4a.4	157.3	45
					8	11	17.5	S4a.8	247.1	71
				6.5	2	40	13.7	S4b.2	106.9	31
					4	21	16.2	S4b.4	176.2	50
					8	11	17.2	S4b.8	282.1	81
2	5.5		2	49.5	17.4	S5a.2	72.6	21		
			4	49.5	16.6	S5a.4	136.5	39		
			8	49.5	17.5	S5a.8	229.1	65		
	6.5		2	49.5	13.7	S5b.2	94.1	27		
			4	49.5	16.2	S5b.4	145.9	42		
			8	49.5	17.2	S5b.8	241.8	69		

<sup>a)</sup> In Flanders, the average yearly amount of electric energy consumed by a household is 3500 kWh (VREG, 2014).

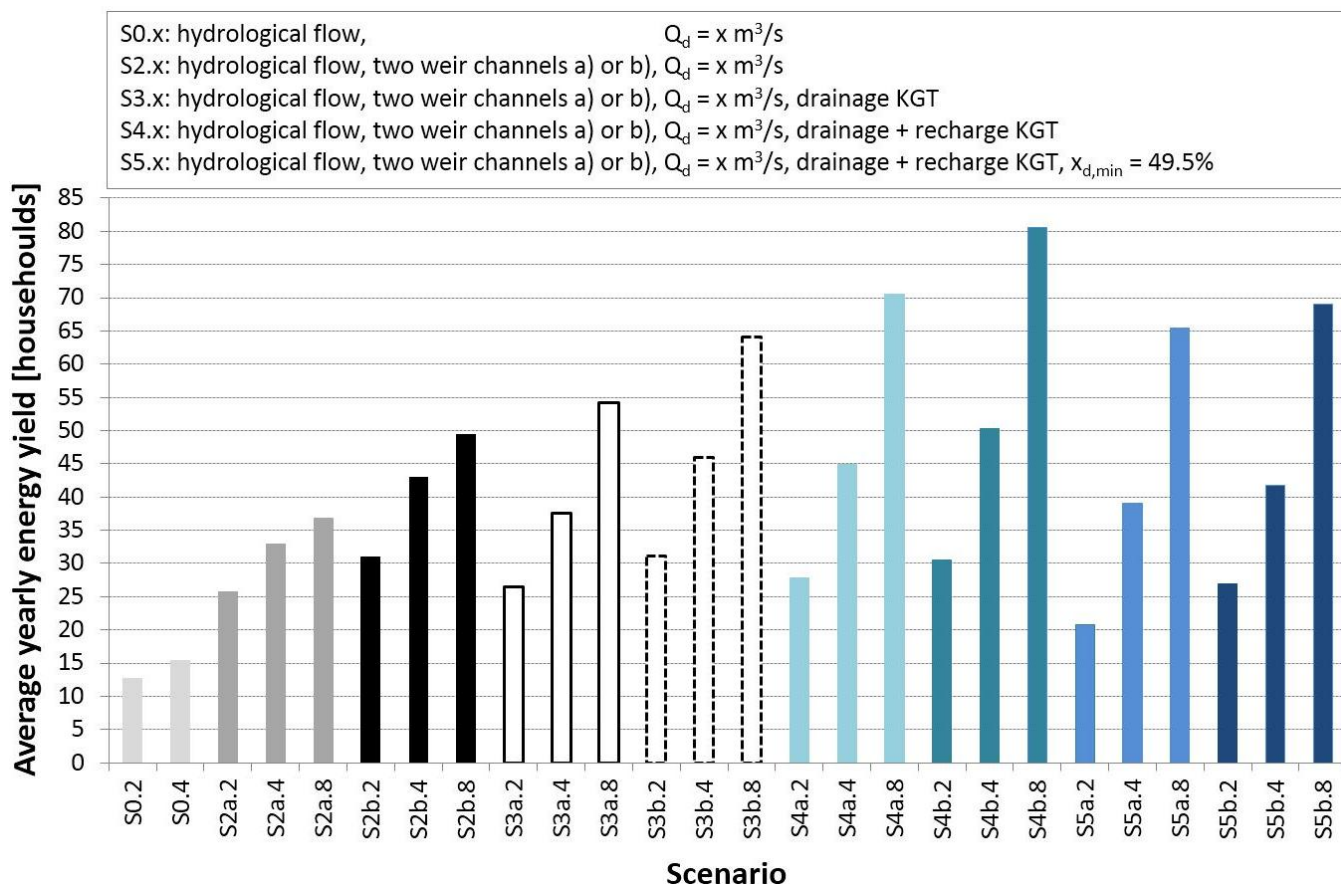


Figure 5-1: Average yearly energy yield for the different considered scenarios.

## 5.4 DISCUSSION

From the results it is clear that a 'b'-scenario always generates a higher energy yield than an 'a'-scenario, for the same design flow and water balance parameters. This is of course logical, since closing the gates at a higher level results in a larger volume flowing from the Sea Scheldt to ZGM, that can be used for power generation.

A next notable result is the energy yield of S2b.4, which is comparable to that of more complex scenarios for the same design flow, i.e. S3b.4 and S4.b4. About 43 households could be served, without the need to invest in the implementation of complex control algorithms, together with the required measurement devices. Moreover, this scenario can be regarded as more 'robust', because it is not susceptible to failure of electronic equipment.

On the other hand, for decision makers the energy yield might not be the only objective: alleviating the water scarcity around Ghent can be considered important as well. If an alleviation is aimed at, together with a reasonable energy yield, the implementation of control rules is inevitable and an S5-scenario should be considered.

All S4-scenarios aim at a maximization of the energy yield. This is also visible in the results: an S4-scenario will always give a higher energy yield compared to its counterpart-scenarios. S4b.8 gives the highest energy yield, being 81 households.

In principle, the design flow could be increased to obtain higher yearly energy yields, but the investment cost will increase as well. Moreover, after a certain value for the design flow, the additional increase in energy yield becomes lower, due to the shorter time period during which power can be generated. In other words, the increase in flow is counteracted more and more by the decrease in time period during which power generation is possible (Equation (2)). As an example, the average yearly energy yield in scenario S2b has been calculated for different values of the design flow (Figure 5-2). There is a steep rise for the smaller values of the design flow (1-10 m<sup>3</sup>/s), but after that, increasing the design flow results in a smaller increase of the energy yield, and the curve becomes almost horizontal. Of course, for other scenarios the design flow values that define this transition will vary, but a flattening of the curve is expected anyhow, even in the scenarios with water exchange between KGT and ZGM.

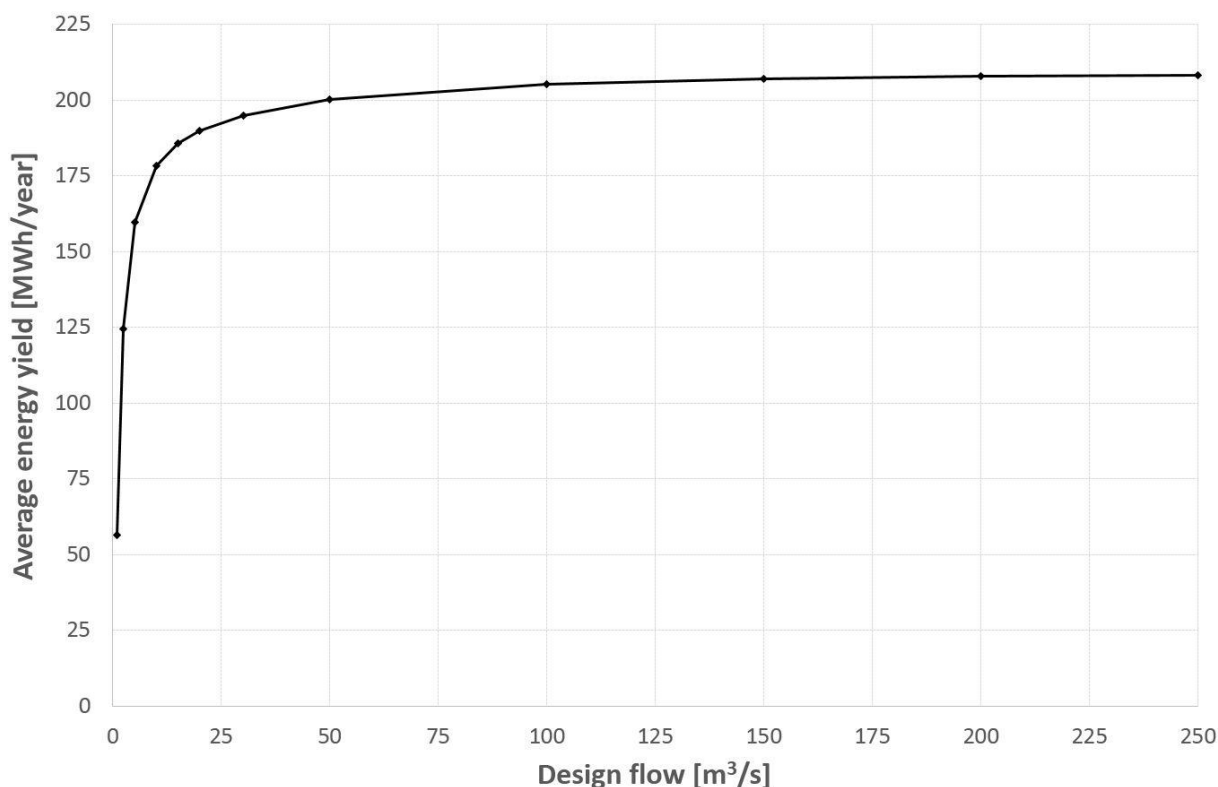


Figure 5-2: Variation of the average yearly energy yield with design flow, in scenario S2b.

## 6 CONCEPTUAL DESIGN

*This chapter outlines the conceptual design. Once the basic geometry is known, the total investment cost of the proposed conceptual design is estimated. It should be noted that the main goal of the conceptual design and the cost estimate is to deliver input for the cost-benefit analysis in the next chapter, and not to have a fully optimized design.*

### 6.1 HYDRAULIC DESIGN

The useful head difference is equal to the geometric head difference – i.e. the water level difference between upper and lower reach – minus the total hydraulic losses over (i) the intake from the upstream reach to the turbine, (ii) the turbine itself, (iii) and the outflow from the turbine into the Sea Scheldt. The conceptual design aims at minimizing these hydraulic losses. In addition this optimization was iterated taking cost aspects into account.

#### 6.1.1 GEOMETRIC BOUNDARY CONDITIONS

A first important geometric boundary condition is defined by the distance between the upper reach and the lower reach, the Sea Scheldt, on the location of the new lock. The overall length of the lock is 100 m.

Whether tidal energy harvesting will be implemented at the location of the lock or not, a weir channel will be constructed on each side of the lock parallel to its longitudinal axis (Figure 1-3). The main function of the two weir channels is drainage of rainwater from the upper reach to the Sea-Scheldt. The channels, each 3 m wide by 2.2 m high, are placed below the future ground level. Both channels have a horizontal bed slope. One channel is modified to facilitate fish migration.

The second boundary condition results from the head difference between the upper reach and the Sea Scheldt. The upper reach is characterized by a quasi-constant water level of 4.50 mTAW. The design value for low tide on the Sea Scheldt is 2.00 mTAW. The top of the turbine outflow has to be situated under this level of 2.00 mTAW, to assure that the circuit remains pressurized.

Dimensions related to the turbine are based on typical drawings.

#### 6.1.2 ELEMENTS OF THE HYDRAULIC CIRCUIT

From upstream to downstream, three main elements can be identified: intake - turbine - outfall. Given a total length of the circuit of 100 m, the length to the turbine and outfall (10 to 20 m) is small in relation to the intake length. Construction costs and ease of maintenance are more favourable in case of a long intake on a high level and a short outfall on a low level, instead of another configuration.

The outfall length is minimized due to the higher depth under future ground level (8.00 mTAW). Given a level of 0.00 mTAW for the outfall axis and an assumed

downstream diameter of 2 m, top and bottom of the outfall lie on +1.00 mTAW and -1.00 mTAW respectively. The outfall is conceived as a divergent to obtain an as smooth as possible transition of the flow lines between the exit of the turbine and the Sea Scheldt, to minimize head losses at the outfall. A control valve on the outfall is foreseen. The outfall has no trash rack. The length of the outfall is determined by the upstream diameter (1000 mm), the downstream diameter (2000 mm) and the maximum opening angle (13°). A total length of 5 m is set for the outfall, that is composed of a 4 m divergent and a 1 m tube transitional section with constant diameter. This transitional section also is provided with a control valve.

The maximum intake invert level is at most equal to the upstream water level minus the necessary vertical dimension of the intake. In a downstream direction the intake consists of a connection from the upper reach to the turbine, a convergent diameter reduction and a control valve. The level of the connection channel's axis can decrease gradually – i.e. hydraulically profiled – or can have a distinguished drop on one location. Somewhere on the connection channel a trash rack has to be installed. A convergent diameter reduction is necessary at the upstream end of the turbine to connect the intake (diameter to be determined) to the turbine entrance (diameter 1000 mm). Given a length of the outfall of 5 m and an assumed length of the turbine of 3 m, the intake connection channel has a length of about 90 m.

### 6.1.3 HYDRAULIC CONSIDERATIONS

Given the levels and lengths from §6.1.2, hydraulic losses are calculated for the intake and the outfall. The total head loss consists of friction losses and local losses, calculated using the following formula:

$$\Delta F = K \cdot L \cdot Q^2 + K' \cdot \zeta \cdot Q^2 = Q^2 (K \cdot L + K' \cdot \zeta) \quad (25)$$

in which:

$\Delta F$	=	total head loss	[m]
$K$	=	friction loss factor	[s <sup>2</sup> /m <sup>6</sup> ]
$L$	=	total length of the conduit	[m]
$Q$	=	discharge through the conduit	[m <sup>3</sup> /s]
$K'$	=	local head loss geometric factor	[s <sup>2</sup> /m <sup>5</sup> ]
$\zeta$	=	local head loss coefficient	[-]

The friction loss factor  $K$  and the local head loss geometric factor  $K'$  are calculated as follows:

$$K = \frac{4^{10/3} \cdot n^2}{\pi^2 \cdot D^{16/3}} \quad (26)$$

$$K' = \frac{8}{g \cdot \pi^2 \cdot D^4} \quad (27)$$

with  $n$  [ $\text{sm}^{-1/3}$ ] the Manning roughness coefficient,  $D$  [m] the conduit diameter and  $g$  [ $\text{m/s}^2$ ] gravitational acceleration.

For concrete  $n = 0.013 \text{ sm}^{-1/3}$  and with a nominal turbine design flow of  $4 \text{ m}^3/\text{s}$  the total head loss can be calculated. Local losses are taken into account on the following locations: entrance from the upper reach into the intake channel, trash rack on the intake channel, convergent diameter reduction between intake channel and turbine entrance, angular deflection of intake channel, divergent outfall between turbine exit and Sea Scheldt, and the exit from the outfall into the Sea Scheldt. Losses over the turbine itself and over control valves are neglected at this stage.

A classical circular penstock of 1000 mm as intake channel would lead to a total head loss over the intake and outfall of more than 3 m, which is – of course – not acceptable. Enlarging the intake channel diameter with increments of 200 mm gives the following results for the total head loss over the circuit: 1.4 m ( $\varnothing$  1200 mm), 0.8 m ( $\varnothing$  1400 mm), 0.5 m ( $\varnothing$  1600 mm), 0.4 m ( $\varnothing$  1800 mm), 0.3 m ( $\varnothing$  2000 mm). The outfall parameters ( $\varnothing$  1000 mm to  $\varnothing$  2000 mm under  $8^\circ$ ) are fixed and lead to a head loss of 0.2 m (included in the total loss mentioned above).

Take a rectangular intake channel with dimensions 3 m wide x 2.2 m high. The hydraulic radius  $R_{hyd}$  is calculated as the wetted section  $A$  divided by the wetted perimeter  $P$ . The  $R_{hyd}$  of a 3 m x 2.2 m intake channel is 0.63 m. If the water level in the intake channel does not reach up to the ceiling of the channel (unpressurized flow), the hydraulic radius becomes 0.75 m for a water level of 1.5 m and 0.86 m for a water level of 2 m in the intake channel. The diameters of a circular tube with an equivalent hydraulic radius are 2500 mm ( $R = 0.63$  m), 3000 mm ( $R = 0.75$  m) and 3400 mm ( $R = 0.85$  m). From these calculations it is clear that it would be difficult to limit the head losses – in an economical way – using a classical circular penstock.

From these calculations it can be concluded that the intake diameter, due to the length of 90 m, is decisive to obtain acceptable head losses. A shortening of the intake channel length, by for example and open excavation in the future ground level, is not considered. A larger intake channel on the other hand, leads to increasing construction costs. At this point the weir channel, that will be constructed regardless of the decision to implement a hydropower scheme at the lock, provides an interesting opportunity to minimize construction costs.

## 6.2 GEOMETRIC DESIGN

### 6.2.1 LAYOUT

From the above hydraulic considerations it is clear that it is beneficial to let the intake from the upstream part to the turbine coincide with the weir channel on the same bank (Figure 6-1). Hydraulically speaking, the 3 m x 2.2 m channel is certainly sufficient to limit head losses to an acceptable level. To be able to feed the turbine with a discharge of 4 m<sup>3</sup>/s the water depth in the intake channel has to be 1.5 m. Since the upstream water level is fixed, the bottom level of the intake channel, originally foreseen at 4.00 mTAW, is adapted to 4.50 mTAW - 1.5 m = 3.00 mTAW.

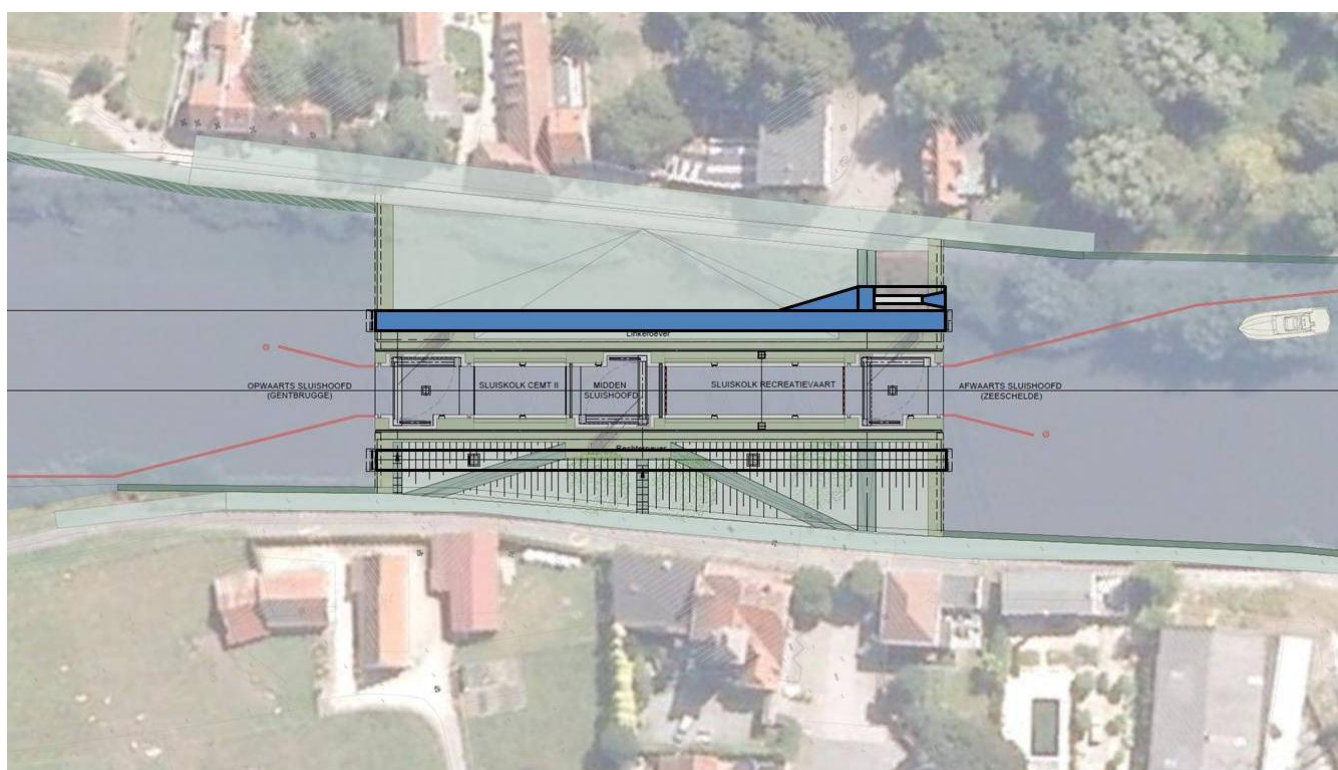


Figure 6-1 : Integration of the hydropower station into the design of the lock.

At the downstream end of the intake/weir channel a connection needs to be made to the turbine and the outfall. In principle the turbine and outfall, with axis level at 0.00 mTAW, can be installed underneath the intake/weir channel. For ease of construction however, the turbine and outfall are foreseen next to the intake/weir channel on the side of the intake/weir channel opposite the lock (Figure 6-2). In that configuration the installation and possible removal – for maintenance – of the turbine does not interfere with the intake/weir channel. Another advantage is that the outfall is situated further away from the lock entrance, lowering the possible interference of the outfall jet on vessels manoeuvring to or from the lock's entrance.

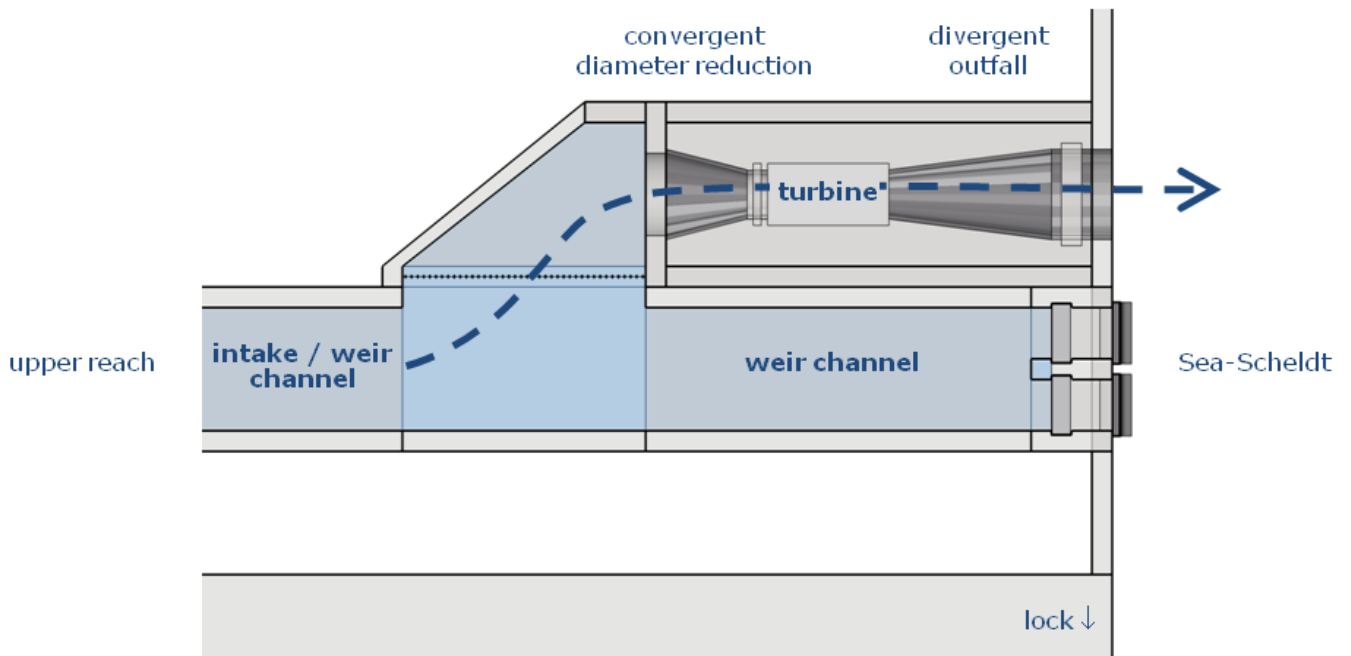


Figure 6-2: Geometric design of the hydropower station – top view.

Both the turbine and the convergent diameter reduction and divergent outfall are placed in a dry basement (Figure 6-3). The floor level of the basement (-1.50 mTAW) is determined by the turbine axis level of 0.00 mTAW minus the radius of the outfall diffuser (1000 mm) and an extra margin of 0.5 m. Placing the outfall in the dry basement makes <sup>72</sup> inspection and maintenance easier. For the same reason the most downstream part of the intake, the convergent diameter reduction, is also situated inside the dry basement.

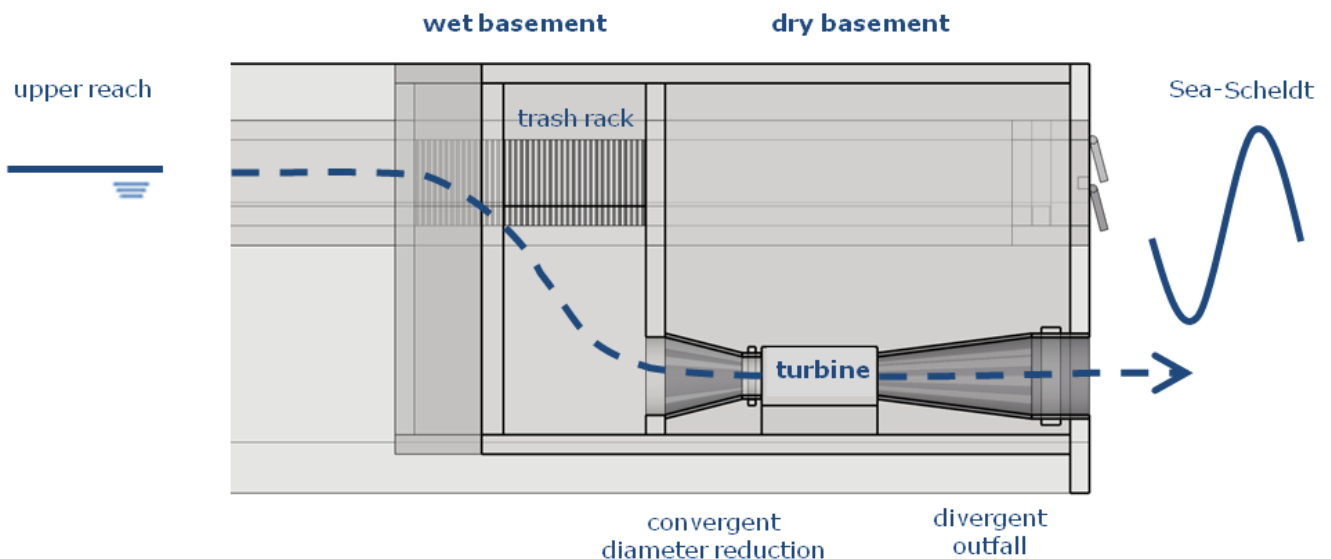


Figure 6-3: Geometric design of the hydropower station – side view.

The connection between the intake/weir channel and the dry basement is made by a wet basement, in-line with the dry basement and adjacent to the intake/weir channel. An opening in the intake/weir channel's wall leads to the wet basement, after passing through a trash rack. Preliminary hydraulic calculations of the connection indicate that a width of 6 m should suffice for this opening, for a design discharge of 4 m<sup>3</sup>/s. In the lower

part of the wet basement the intake flow enters the dry basement through the convergent diameter reduction.

Another cost reduction is obtained by combining the wall between the turbine basement and the Sea Scheldt as wing wall of the lock, retaining the backfill next to the lock. The turbine basement's longitudinal wall is not combined with the lock wall.

An estimation of the flow velocity profile due to the outfall in the Sea Scheldt is made. Governing parameters are discharge ( $4 \text{ m}^3/\text{s}$ ) and outfall diameter (2 m). The initial exit velocity of  $1.3 \text{ m/s}$  propagates to a distance of circa 7 times the outfall diameter. From that point on, the velocity decreases inversely proportional to the distance from the outfall. At a distance of 20 m flow velocity is approximately  $0.8 \text{ m/s}$  and  $0.4 \text{ m/s}$  at 40 m. These values need to be taken into account during detailed design of the berthing places. An erosion protection is applied in the immediate vicinity of the outfall.

Considering the configuration of the excavation pit for the turbine basement, at least one sheet pile wall (wing wall of the lock) can be omitted when the construction of the turbine basement and the lock are synchronised – which is recommended to save costs. At the backside of the lock wall another sheet pile wall can possibly be saved.

The floor slab of the turbine basement has a different foundation level compared to the floor slab of the lock; hence no synergetic effect can be obtained.

### 6.2.2 HIGHER DESIGN FLOW

73

The above exercise has been repeated for a higher design flow, i.e.  $8 \text{ m}^3/\text{s}$ . The main differences, compared to a set-up for a design flow of  $4 \text{ m}^3/\text{s}$ , are the larger dimensions of the turbine, and hence the civil works. Also, the weir channel that serves as intake for the flow has to be enlarged, which is not required when considering  $4 \text{ m}^3/\text{s}$ .

More details on the resulting dimensions of both the  $4 \text{ m}^3/\text{s}$  and  $8 \text{ m}^3/\text{s}$  can be found in the Bill of Quantities (BoQ) in Annex 1.

### 6.2.3 COST ESTIMATE

A sound cost estimate of the total investment cost is necessary for the cost-benefit analysis in Chapter 8. In this paragraph the initial investment cost is calculated for the layout described in §6.2.1. The main components to estimate are:

- 💡 civil works (wet and dry basement)
- 💡 convergent diameter reduction
- 💡 energy production and transport (turbine, voltage transformer...)
- 💡 divergent outfall.

Table 6-1 summarizes the bill of quantities, unit prices and the resulting cost estimate, for both a design flow of  $4 \text{ m}^3/\text{s}$  and  $8 \text{ m}^3/\text{s}$ . The civil works are estimated from the BoQ of the conceptual design (see Annex 1 for an elaborated BoQ). The cost estimate from the electromechanical equipment is based on contacts with suppliers.

Table 6-1: Estimate of initial investment cost.

ESTIMATE OF INITIAL INVESTMENT COST			
component	element	4 m <sup>3</sup> /s cost [EUR]	8 m <sup>3</sup> /s cost [EUR]
<b>basement</b>	(dry and wet basement)	<b>112,500</b>	<b>160,000</b>
	sheet piles for construction pit	30,000	40,000
	foundation and floor slab in reinforced concrete	10,000	17,500
	walls in reinforced concrete	40,000	60,000
	removable ceiling in reinforced concrete	20,000	30,000
	access ladder	2,500	2,500
	winch 1 ton	10,000	10,000
<b>intake</b>	(additional civil works compared to lock)	<b>10,000</b>	<b>44,000</b>
	trash rack: 6 m x 2.2 m / 6 m x 3.3 m	3,000	5,000
	connection to dry basement: Ø 2000 mm / Ø 3500 mm	1,500	2,500
	diameter reduction: Ø 2000 to 1000 mm / Ø 3500 to 1400 mm	3,000	5,000
	control valve Ø 1000 mm / Ø 1400 mm	2,500	3,500
	enlargement weir channel from 2.2 m to 3.3 m	-	28,000
<b>energy production and transport</b>		<b>175,000</b>	<b>230,000</b>
	turbine, generator and frequency regulator	165,000	220,000
	current transformer	2,500	2,500
	connection to power grid	5,000	5,000
	minor connections and small equipment	2,500	2,500
<b>outfall</b>		<b>17,500</b>	<b>35,000</b>
	divergent outfall piece: Ø 1000 to 2000 mm / Ø 1750 to 3500 mm	5,000	12,500
	connection to Sea-Scheldt Ø 2000 mm / Ø 3500 mm	5,500	10,000
	control valve: Ø 2000 mm / Ø 3500 mm	3,000	8,500
	erosion protection 50-400 kg	4,000	4,000
<b>SUBTOTAL</b>		<b>315,000</b>	<b>469,000</b>
	5% margin for known but not detailed costs	15,750	23,450
	10% margin for unknown costs	31,500	46,900
<b>OVERALL TOTAL</b>		<b>362,250</b>	<b>539,350</b>

It should be noted that the above cost estimation does not include any measures related to fish migration (see Chapter 7). Possible measures are to be installed in the upper and lower reach itself, and do not influence the above estimated costs. When fish migration measures are foreseen, the cost for this can be added to the overall total.

### **6.3 RECOMMENDATIONS FOR DETAILED DESIGN**

A preliminary hydraulic and geometric design is performed in §6.1 and §6.2. A possible next step in the design should focus on the aspects below:

- detailed hydraulic design of the hydraulic circuit dimensions, the turbine details and a control system;
- detailed structural design of the basement, based on a survey of soil conditions and a pursued far-reaching synergy with the construction of the lock.

## 7 FISH MIGRATION ASPECTS

*The presence of the weir-lock complex could be a fish migration bottleneck, if no additional measures are taken. The original lock design already included a fish passage. This chapter will mainly focus on the impact on fish migration of the extension of the complex with a power plant. Also, possible mitigating measures are discussed.*

### 7.1 INTRODUCTION

As the lock will create a migration obstruction for fish, a fish passage has already been foreseen in the concept of the lock, i.e. the stop logs of the western weir channel will provide a weir level that is about 50 cm lower than the target level in the upper channel. This way, a small flow is available for fish to migrate from the upper channel to the lower channel during low tide conditions. During high tide conditions, migration can occur in both directions.

If a turbine is included in the design as well, an additional possibility of fish passing through the turbine must be considered and evaluated. First, an inventory of the fish species living in the Sea Scheldt is made. Then, the options for fish to pass the weir-lock-power plant complex are discussed.

### 7.2 SPECIES TO CONSIDER

In the freshwater zone of the Zeeschelde, 33 species were collected between 1997 and 2008 (Table 7-1) (Breine, 2009). Freshwater species comprised 69.7% of the total species richness and contributed 78.9% to the total number of individuals recorded. The marine migrants contributed only 0.04% to the total number caught and were only recorded during 2008. Diadromous species, i.e. species migrating between fresh and marine habitats, make up 18.2% of the species richness and 19.3% of the individuals recorded and are potentially vulnerable to being caught up in water intakes, particularly when their life cycle involves lengthy migrations up or down river. In 1997 only a few diadromous specimens were caught but this guild was well represented from 2005 onwards. Two estuarine species (common goby *Pomatoschistus microps* and sand goby *P. minutus*) have been encountered yearly in the freshwater zone since 2006. They were already occasionally recorded in 1997 and 2004. Estuarine species contributed 1.7% to the total number of individuals caught.

In a highly polluted river like the Sea Scheldt, oxygen deficiency strongly affects the fish community structure. However, over the years a gradual improvement in species richness is observed. A significant and steady increase in species richness and number of individuals is noted since 2004, the worst year observed being 2003. At present the most abundantly caught species are flounder, common goby, pike-perch, roach and white bream. Another indication of the water quality improvement is the presence of twaite shad, recorded in spring 2007.

An important factor to consider is the swimming speed of the fish present in the Sea Scheldt. This speed depends on the size and shape of a fish, but also on the water temperature and the general fitness of a fish. Table 7-1 gives an overview of the known sprint speeds of a number of fish (Kroes & Monden, 2005). The *sprint speed* is defined as an elevated speed that can be maintained for no longer than 15 seconds and that can be used to pass obstacles. Swimming upstream through certain structures costs a lot of energy and since rivers in Belgium are mostly quite slow, fish are not adjusted to high velocity circumstances. Therefore, when designing fish passages in Belgium and the Netherlands it is generally considered that the maximum water velocity should not exceed 1 m/s (Coenen et al., 2013).

Table 7-1 : Catch frequency for fish species, expressed as percentage, for the freshwater zone of the Zeeschelde between 1997 and 2008 (Breine, 2009) and sprint speed (Kroes & Monden, 2005).

CATCH FREQUENCY AND SPRINT SPEED FOR FISH SPECIES			
Scientific name	Common name	Catch frequency (%)	Sprint speed (m/s)
<i>Abramis brama</i>	Bream	63.3	0.9-1.0
<i>Alburnus alburnus</i>	Bleak	16.3	?
<i>Alosa fallax</i>	Twaite shad	2	?
<i>Anguilla anguilla</i>	European eel	85.7	0.5-1
<i>Blicca bjoerkna</i>	White bream	79.6	?
<i>Carassius carassius</i>	Crucian carp	2	?
<i>Carrasius gibelio</i>	Prussian carp	81.6	2-2.2
<i>Clupea harengus</i>	Herring	2	?
<i>Cottus gobio</i>	Bullhead	4.1	?
<i>Cyprinus carpio</i>	Carp	73.5	0.6-1.7
<i>Dicentrarchus labrax</i>	Seabass	2	?
<i>Esox lucius</i>	Pike	14.3	3-6.9
<i>Gasterosteus aculeatus</i>	Three-spined stickleback	73.5	1.5
<i>Gymnocephalus cernuus</i>	Ruffe	59.2	1.3
<i>Lampetra fluviatilis</i>	River lamprey	16.3	?
<i>Lepomis gibbosus</i>	Pumpkinseed	28.6	?
<i>Leucaspis delineatus</i>	Belica	6.1	?
<i>Leuciscus cephalus</i>	Chub	2	0.5-3.8
<i>Leuciscus idus</i>	Ide	22.5	?
<i>Liza ramado</i>	Thinlip mullet	8.2	?
<i>Osmerus eperlanus</i>	Smelt	8.2	?
<i>Perca fluviatilis</i>	Perch	71.4	1.45
<i>Platichthys flesus</i>	Flounder	61.2	?
<i>Pomatoschistus microps</i>	Common goby	20.4	?
<i>Pomatoschistus minutus</i>	Sand goby	12.2	?
<i>Pseudorasbora parva</i>	Stone moroko	77.6	?
<i>Pungitius pungitius</i>	Nine spine stickleback	20.4	?
<i>Rhodeus sericeus</i>	Bitterling	51	?
<i>Rutilus rutilus</i>	Roach	93.9	2.1-4.5
<i>Sander lucioperca</i>	Pike-perch	61.2	?
<i>Scardinius erythrophthalmus</i>	Rudd	81.6	1.74
<i>Silurus glanis</i>	Wels catfish	12.2	?
<i>Tinca tinca</i>	Tench	8.2	?

## 7.3 FISH PASSAGE ROUTES AT THE LOCK IN HEUSDEN

In this section the different possible routes for fish to pass the lock in Heusden – voluntary or not – are described. Passage in the landward direction is from the lower to the upper channel, and vice versa for passage in the seaward direction.

### 7.3.1 PASSAGE IN THE LANDWARD DIRECTION

#### 7.3.1.1 Through the provided fish passage of the lock system

Fish migrating in a landward direction can pass through the fish passage 7% of time when the current is going in an upstream direction, 3% of time in when it is going in a downstream direction (IMDC in association with Technum and University of Antwerp, 2013).

However, the water current in the fish passage is not as strong as the one flowing out of the turbine outlet. Generally, fish will follow the strongest current present, until this current becomes too strong compared to their swimming capacities. When reaching this threshold – which is species dependent – they will follow it until they find a possible migration route (Coenen et al., 2013). During high tide the turbine will be inactive while the fish passage becomes accessible, allowing fish to find the other current created by the fish passage.

In principle, the eastern weir channel can be used as well. The weir level however is set 79 higher, so this is not explicitly taken into account.

#### 7.3.1.2 Through the lock

Passage through the lock will be possible several times a day when the doors of the lock are opened. Fish that have gathered in front of the lock are likely to find their way through the open doors. To increase the time that migration is possible, it can be suggested to leave the doors of the lock open during high tides. Especially bottom-dwelling fish species are likely to pass through the lock doors as they will not use the fish passage that is located quite high in the water column.

#### 7.3.1.3 Through the turbine by-pass

Fish should be discouraged from using the outlet of the turbine due to the increased risk of injuries and mortality. Fish friendly turbines, such as the one manufactured by Pentair Fairbanks Nijhuis/FishFlow Innovations, have for the moment only been tested in a downstream direction (Winter et al., 2012) and it remains uncertain if fish can pass unharmed when trying to pass upstream. In addition, the water velocities can reach 5 m/s or more inside the turbine during peak moments, which is too fast for most species of fish (Table 7-1), so it is highly unlikely that fish will migrate in a landward direction through an operating turbine. Nevertheless, a barrier could be provided. Techniques of repelling fish to enter the tunnel with the turbine are described in §7.4.

## 7.3.2 PASSAGE IN THE SEAWARD DIRECTION

### 7.3.2.1 Through the provided fish passage

Passage in a seaward direction is always possible as the water levels on the landward side of the lock are at a constant level. Depending on the tide, the fish might drop up to a maximum height of 2 m but will not be harmed.

In principle, the eastern weir channel – with the turbine by-pass – allows fish passage as well. The weir level of the stop logs will be higher however, so in general there will be no current over this weir, except during periods of high rainfall, in which a higher water level can be expected in the upper channel.

### 7.3.2.2 Through the lock

As described in §7.3.1.2.

### 7.3.2.3 Through the turbine by-pass

If a fish friendly turbine is installed, fish are very likely to pass unharmed, either by going through the trash rack and turbine or by passing by the rack and exiting through the tunnel.

However, as mentioned in §7.3.1.3, fish cannot be guaranteed to pass safely in a landward direction, so some type of barrier would have to be provided at the turbine outlet. If a barrier is installed at the seaward side to block this passage, a barrier should be installed at the inlet of the weir channel as well. After all, if fish would pass through the - possibly fish friendly – turbine, they become trapped between the turbine outlet and the barrier at the outlet. 80

## 7.4 BARRIERS

As the outlet of the turbine creates a current which will attract fish, a barrier will need to be installed on both sides. Two types of barriers exist: physical barriers and behavioural barriers. A behavioural barrier can be defined as any stimulus or non-solid obstruction that discourages or prevents a selected species from passing through a target region. The advantage of the latter is that they do not constrain water flow or restrict navigation, which are requirements for the design of the lock in Heusden.

### 7.4.1 PHYSICAL BARRIERS

Physical barriers are not preferable as they change the efficiency of the turbine. For preventing fish to move in a landward direction, a screen would have to be placed at a large distance of the turbine outlet in order not to lose efficiency, resulting in an obstruction of navigation and the installation of a large and therefore costly barrier.

The screen inside the tunnel, preventing debris from entering the turbine, could be adapted to exclude fish as well. However, in order to exclude all fish, including juveniles, the mesh size would have to be so small that the operational efficiency will not be optimal

anymore. Therefore, physical barriers are not recommended for the Heusden site. However, the interested reader can find more information in e.g. EA (2012).

## 7.4.2 BEHAVIOURAL BARRIERS

Experiments show that there is a large response variation between species, life stage, individual fish and water quality conditions. Therefore, it cannot be predicted that a fish will always move toward or away from a certain stimulus. Even when such a movement is desired by a fish, it often cannot perceive the source or direction of the signal and choose a safe escape route. Another concern is repeated exposure: a fish may no longer react to a signal that initially was an attractant or repellent. In strong or accelerating water velocity fields, the swimming ability of a fish may prevent it from responding to a stimulus even if it attempts to do so. Other environmental cues, such as pursuing prey, avoiding predators or an attractive habitat, may also cause a fish to ignore the signal. A solution to these problems might be to combine stimuli, by combining different techniques.

### 7.4.2.1 Electric fish barriers

Electric barrier technology has evolved over time. In the past, alternating current (AC) was used to keep fish out, but is now known to cause injuries, unlike direct current (DC). Also abrupt deterrence-type fields have been used, which are still used in certain applications, but nowadays the creation of a graduated field is more common (Burger et al., 2012).

81

While each application is designed to achieve a specific barrier/guidance objective, a system generally consists of a series of electrodes (cables or metal bars) attached to the bottom of the channel, often in grooves in a concrete sill, rising up the sides of the channel to accommodate higher water levels. However there are many other types of configurations including vertical pile-mounted and suspended vertical electrodes. Different configurations produce different fields, some uniform, some graduated, some more intense close to the bottom.

The *Graduated Field Fish Barrier (GFFB)* is an electrical barrier producing a graduated, pulsed field of direct current in the water, that affects muscular control in fish (Figure 7-1). The animal feels uncomfortable in the field and moves in the direction that reduces this discomfort. A graduated field can be specifically designed to meet the needs of each site in terms of its physical configuration, water depth and conductivity, the size and species of fish for which behaviour modifications are required to be changed, and the objective (e.g. total blocking, guidance of adults, barrier to adults only, etc.).

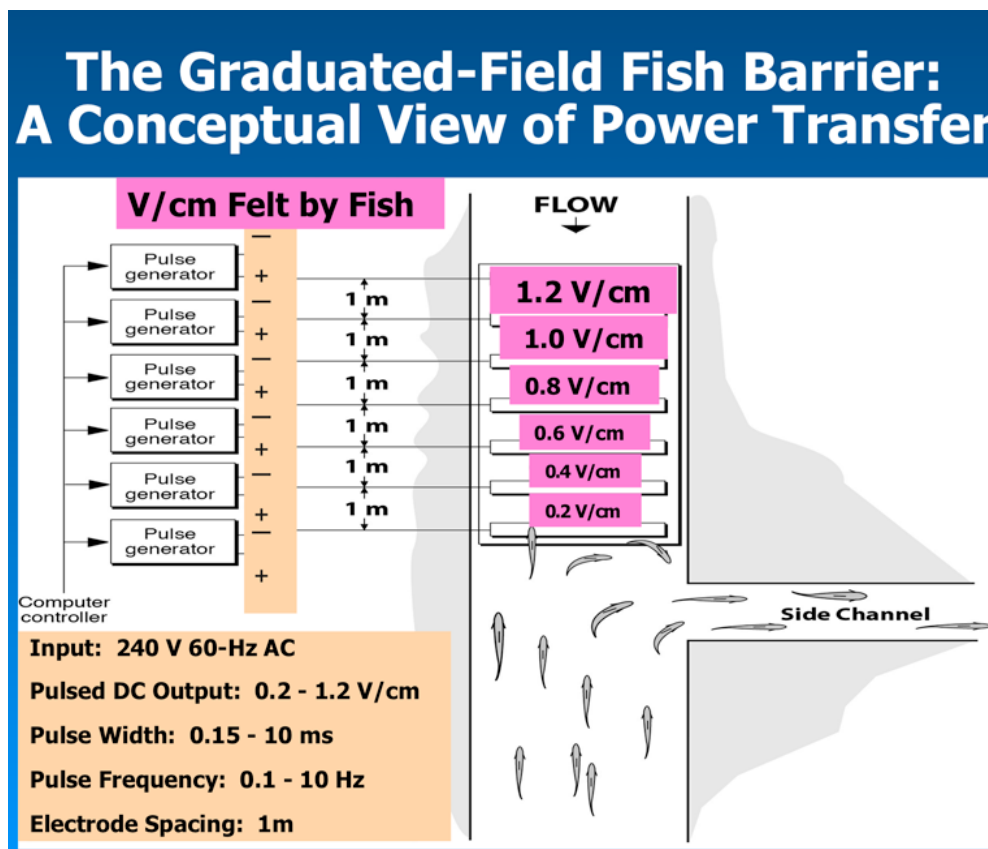
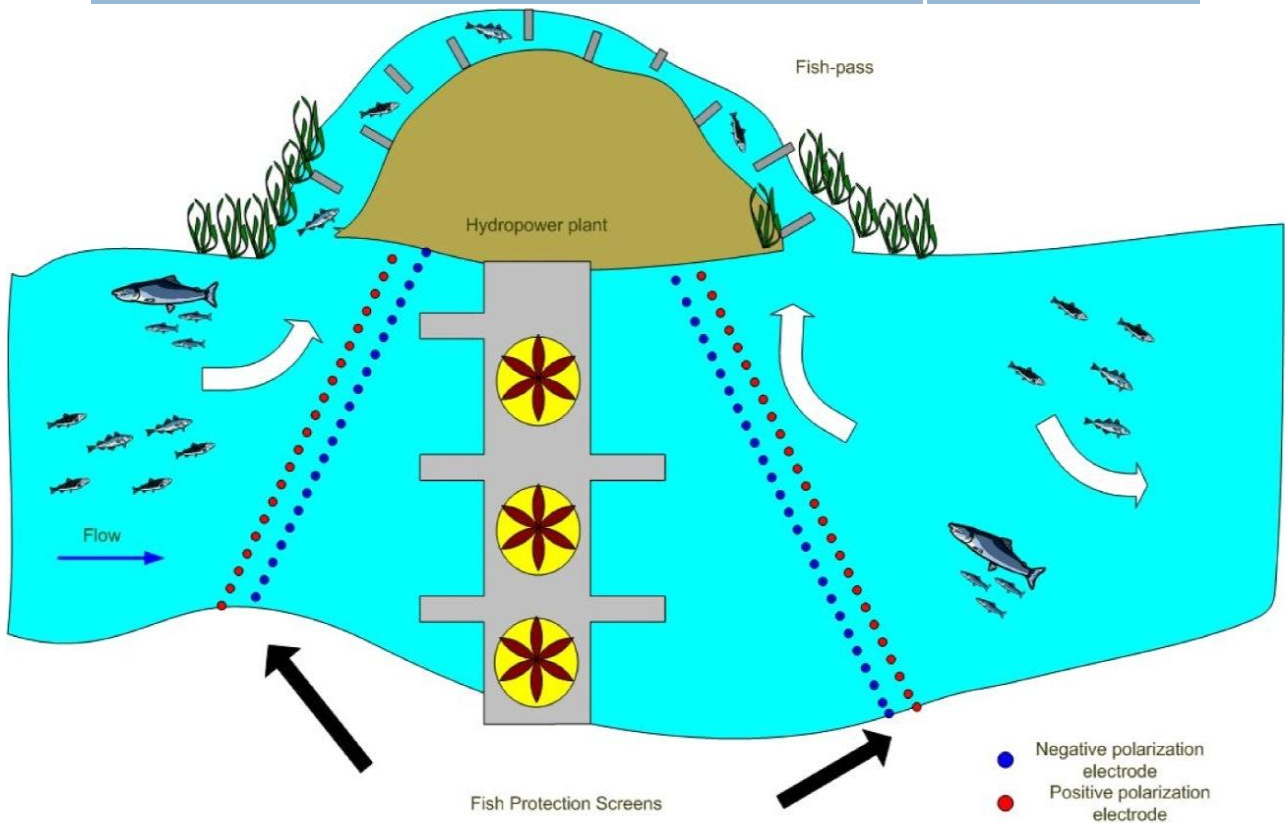
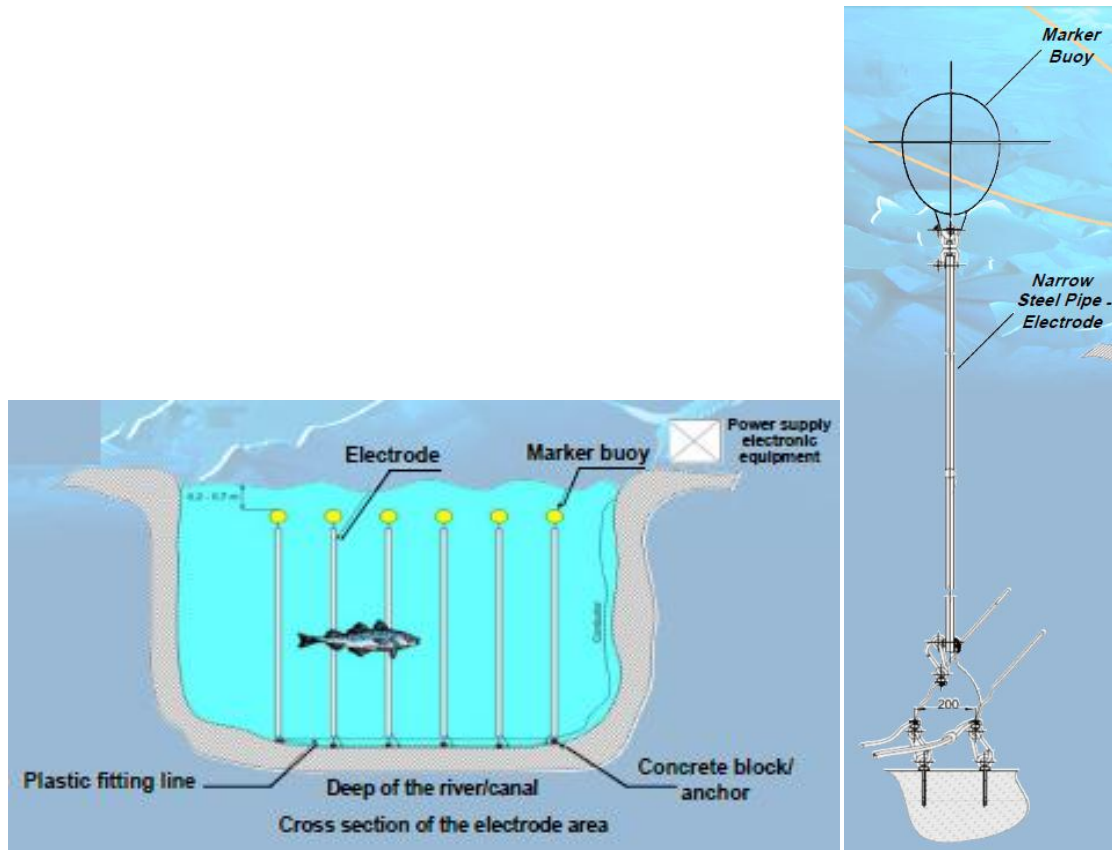


Figure 7-1 : Concept diagram of the graduated output of a GFFB electric deterrence array to guide upstream-moving fish into a diversion channel. The gradient [V/cm] increases as fish move upstream (taken from Burger et al., 2012).

Literature review shows that electric barriers can safely guide, control or deter upstream fish migrations in many different applications, including those required for hydropower application. These upstream-deterrence control barriers can be quite effective in environments that range from small culverts to transportation canals and major rivers (Burger et al., 2012).

The NEPTUN electrical fish barrier has been developed by the Polish company PROCOM SYSTEM (PROCOM SYSTEM, 2013). The NEPTUN barrier generates a progressive electric gradient between the positive and negative electrodes installed (Figure 7-2). The current used is low voltage (60 V), which reduces the risk of electrocution associated with this barrier, as opposed to more traditional systems which use several hundreds of volts. The system uses very little energy, and requires only light maintenance. Initial biological results obtained at a hydro-electric plant on a reservoir in Poland showed a level of effectiveness approaching 100%. Other tests are under way in the USA, involving various species and applications, with promising results.



EXAMPLE OF THE ELECTRONIC FISH PROTECTION SCREENS APPLICATION FOR HYDROPOWER STATION WITH FISH-PASS

Figure 7-2: Pictorial diagram of the electrode spacing (top left), a single electrode (top right) and an example of a possible set up (under) (taken from Fishways Global, 2013).

The advantages are (Fishways Global, 2013):

- 💡 Dynamic electric field designed to divert, not stun fish
- 💡 Random alternating electric field prevents acclimation
- 💡 Vertical control of electric field with virtually no depth limitation
- 💡 Electric field does not disperse into the ground
- 💡 Size flexibility and easy installation
- 💡 Durable and resistant to icing and debris
- 💡 Low energy consumption (solar panels may be practical)
- 💡 Low operating and maintenance costs
- 💡 Remote control
- 💡 Limited effect on navigation

Profish (2013) is a Belgian provider of the technology. The Profish Technology price depends on the water velocity, salinity, water current direction and the neighbouring structures where the electrodes can be attached. The cost could be € 30,000 to € 50,000 per system. Very little maintenance is required.

#### 7.4.2.2 Light barriers

Strobes and lighting systems use light to either attract or repel fish. They can be used either to drive fish away from water diversions and intakes, thus excluding fish from the diversion, or to attract or guide fish to a desired location or elicit some desired response. Lighting systems offer a low capital and operation and maintenance cost option for fish control. They can be applied at difficult sites that are either very large, pass large flows that would be difficult or expensive to screen, or that are inaccessible. Lighting systems might also be considered for application at sites where cost would otherwise not allow installation of fish exclusion devices.

The primary drawback of lighting systems is their inconsistency in excluding or guiding fish. They have proven effective at some sites with specific fish species and life stages and ineffective at other sites. The performance of lighting systems, particularly when applied at shallower depths, is also strongly influenced by the daylight or ambient sun lighting which will dominate over any artificial lighting effects. Consequently, lighting systems, when applied at shallower sites, are typically effective only at night.

Strobe or flashing lights have been shown to be more effective than continuous lighting in repelling fish. Response however depends on fish species, fish life stage, and as addressed above, on the influence of ambient lighting (McLean, 2008). Studies have also shown that flashing rate (number of flashes per minute) and flash intensity influence the fish response to the particular light source. While there is evidence to suggest that fish do not exhibit short-term habituation to sustained strobe light exposure (Hamel et al., 2008), studies to date do not suggest that strobe lights employed as a stand-alone method of deterrence could provide complete security in situations where total deterrence is the

objective. Strobe lights may be more effective when used as part of an integrated deterrence system, with for example bubble barriers or sound (Noatch & Suski, 2012).

In conclusion, this type of barrier can be used at the Heusden site to prevent fish from entering the turbine by-pass from both the intake and the outlet, when combined with other systems, such as a sound barrier (§7.4.2.3) or a bubble curtain (§7.4.2.4).

### 7.4.2.3 Sound barriers

#### 7.4.2.3.1 Infrasound

Infrasound systems have demonstrated a strong directed flight reaction in fish, as opposed to other stimuli which totally disorient the fish. All species of fish are sensitive to infrasound; however the intensity used in the generator and the frequencies emitted (5-16 Hz) basically target fish of less than 20 cm.

The first definitive installations and the various tests conducted during the past few years have led to validate an effectiveness in the order of 80% in cooling water intakes located on rivers (Sonny et al., 2006). As things stand, this technology cannot generally be applied reliably in the water intakes of hydro-electric plants. An application specific to eels remains at the study stage.

Both the fact that the system mainly targets fish of less than 20 cm and that the effect on eels is still unclear, make this system less suitable for the Heusden site.

#### 7.4.2.3.2 Acoustic fish deterrents

Similar to visual deterrents, the reported effectiveness of sound as a fish deterrent has varied considerably (Noatch & Suski, 2012), and the effectiveness of acoustic fish deterrents (AFD) systems can be influenced by bottom morphology, hydraulics, and angle of the sound waves. Maes et al. (2004) investigated an acoustic deterrent system producing 20-600 Hz to deter estuarine fishes away from the water inlet of a power station. Total fish impingement decreased by 60% during sound emission, but the avoidance response varied amongst species. The effectiveness of the acoustic system appeared to depend on whether the fish had an accessory structure that would increase hearing abilities; those fish without swim-bladders generally showed no or little response, whereas the intake rates were significantly reduced in species with swim-bladders.

Low-frequency sound waves, though effective deterrents in some studies, propagate poorly in shallow water and across hard substrates. Successful treatment levels can occur in the ranges of acoustic sound (20 Hz to 20 kHz) and infrasound (0.01 Hz to 20 Hz). In addition to variation in frequency, sound intensity (amplitude) can be increased in an effort to induce avoidance behaviours (Noatch & Suski, 2012).

As with light systems, sound systems are a fish control option with low capital and operation & maintenance costs. Sound systems can be applied at difficult sites that are either very large, pass large flows that would be difficult or expensive to screen, or are inaccessible. Sound systems might also be considered for application at sites where cost would otherwise not allow installation of fish exclusion devices.

However, at the Heusden site an AFD barrier would be less recommendable because fish might be deterred from the fish passage or lock itself as well. After all, sounds are hard to direct in a certain direction so the zone of influence is hard to determine.

#### 7.4.2.4 Bubble curtains

Bubble curtains or bubble screens are one of the most basic forms of behavioural barrier. A curtain of bubbles is produced by a submerged, perforated tube, through which compressed air is released. The wall of bubbles that is released is used to guide approaching fish into a by-wash. Bubble curtains are most effective when combined with other deterrent systems, such as sound and/or (strobe) lights, e.g. the Bio-Acoustic Fish Fence (BAFF) of Fish Guidance Systems Ltd. (FGS, 2013). Figure 7-3 shows the principle of a BAFF.

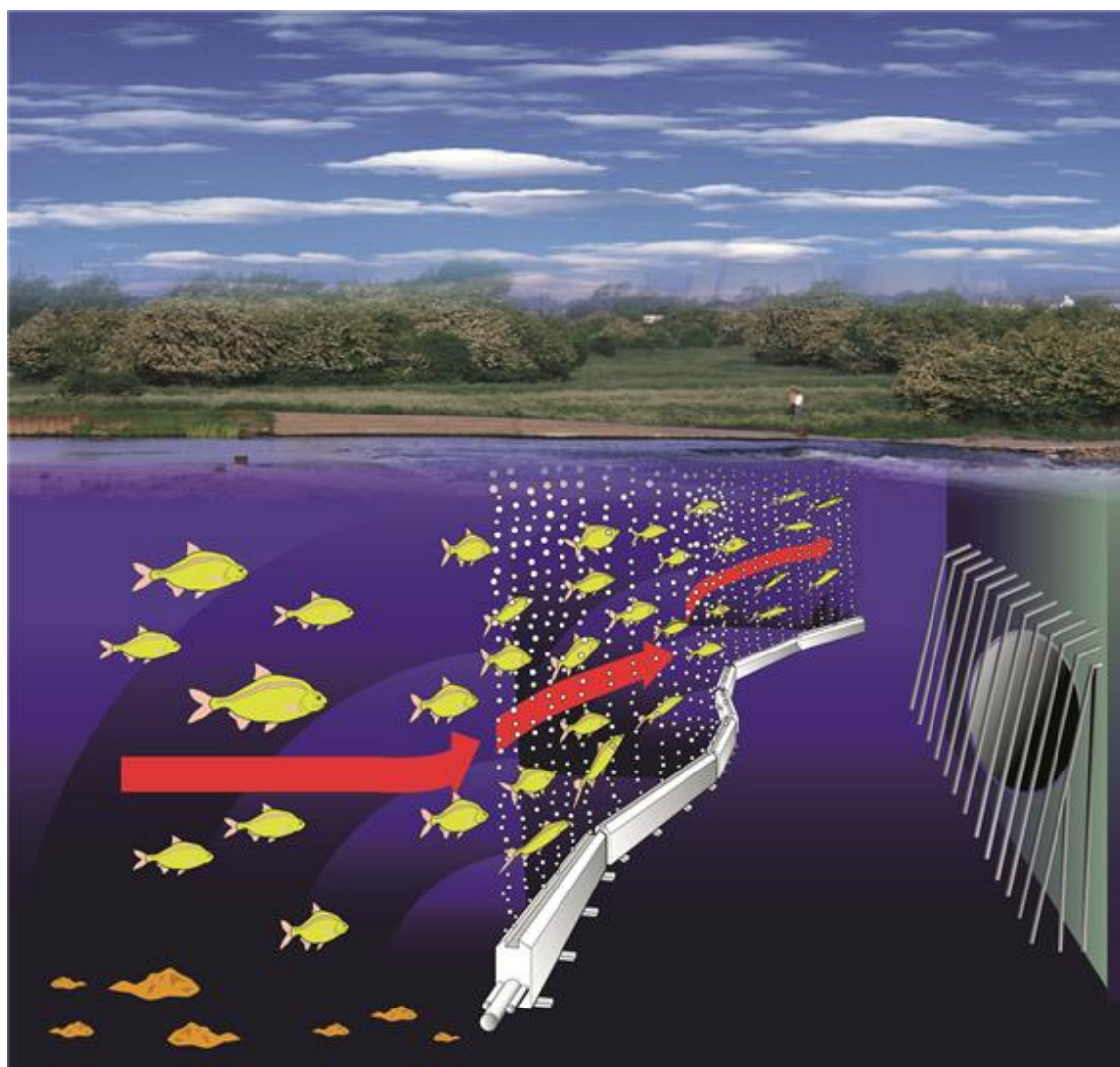


Figure 7-3: Bio-Acoustic Fish Fence (taken from Ovivo, 2013).

Physically, a BAFF comprises of a pneumatic sound transducer coupled to a bubble-sheet generator, causing sound waves to propagate within the rising curtain of bubbles. The sound is contained within the bubble curtain as a result of refraction, since the velocity of sound in a bubble-water mixture differs from that in either water or air alone. The sound

level inside the bubble curtain may be as high as 170 dB re 1 mPa, typically decaying to 5% of this value within 0.5-1 m from the bubble sheet. It can be deployed in much the same way as a standard bubble curtain, but its effectiveness as a fish barrier is greatly enhanced by the addition of a repellent sound signal.

The sound which is encapsulated within the bubble curtain, allows a precise linear wall of sound to be developed. Effectively, this creates a "wall of sound" (an evanescent sound field) that can be used to guide fish around river structures by deflection into fish passes. The alignment of the bubble curtain determines the guidance line for the fish. The trapping of the sound signal within the air curtain prevents contamination of the surrounding area by sound which typically falls to ambient levels at a range of 3 m from the bubble curtain axis. The acoustic stimulus is produced by electromechanical sound projectors that generate frequencies within the range of 5-600 Hz at source levels of around 160 dB re 1  $\mu$ Pa @ 1 m.

Linear arrays of intense flashing lights can be used to generate the visual stimulus. The lights are LED powered devices that create white light in a vertically orientated beam. The bubble curtain reflects the beam and improves the visibility from the direction of approaching fish. The BAFF system can either be mounted directly on to the river or lake bed, or it can be located on a horizontal framework supported by columns.

The main disadvantage of a BAFF, next to the higher capital and O&M costs, is that it is not applicable in strong currents. Hence it is likely that the strong currents generated by 87 the outlet will affect the efficiency of a bubble curtain.

### 7.4.3 LOUVRE SCREENS

Louvre Screens are semi-physical barriers that offer low resistance to flow but high fish deflection efficiency for fish moving in an upstream direction. The deflection principle is that current vortices are created between slats so that an approaching fish senses a shearing flow and avoids it. The fish exclusion performance is variable though: exclusion performance varies depending on fish species, size, life stage, and swimming strength.

This type of screen is not applicable at the Heusden site, since the direction of current changes almost twice a day because of the tide.

## 7.5 CONCLUSION AND RECOMMENDATIONS

Although a separate fish passage has been included in the design of the lock, the currents generated by the turbine will create a higher attraction for fish wanting to migrate past the lock/turbine system.

Fish friendly turbines have been successfully developed (e.g. by Pentair Fairbanks Nijhuis together with FishFlow Innovations) but thus far have only been tested in a downstream direction. As safe passage cannot be guaranteed in the upstream direction, and fish will have to be discouraged from using the passage through the turbine in both directions, the fish friendliness of the turbine becomes of secondary importance.

A wide range of fish barriers has been developed, but few systems are able to exclude all species and life stages of fish. From a turbine efficiency point of view the use of physical barriers is discouraged. Hence behavioural barriers are a more preferred alternative. Light and sound barriers alone have a variable deflection efficiency, but show good results when used in combination with a bubble screen (a Bio-Acoustic Fish Fence). However, as currents can locally become strong, the wall of bubbles will be disrupted. It seems that the only barrier that could provide the highest efficiency is an electric barrier. This barrier should be installed on both sides of the lock near the turbine intake/outlet, but should not obstruct passage through the lock and the fish passage.

It remains unclear if fish, being attracted to the strong current of the turbine but also being repelled from this side of the lock, will be able to find their intended fish passage on the other side of the lock. The further the barrier is installed from the turbine intake and outlet, the easier it will be for fish to find the smaller current of the fish passage. This will of course make the installation of the barrier more costly, because the barrier has to be installed over a greater length.

## 8 COST-BENEFIT ANALYSIS

*In this chapter the costs and benefits of a potential hydropower plant at the lock in Heusden are compared. In principle all possible costs and benefits should be monetized, i.e. quantified in currency. For some costs and benefits, this is very cumbersome, if not impossible, and this would require a serious amount of additional effort. So in this study the cost-benefit analysis (CBA) will be limited purely to financial costs and benefits. The outcome of this CBA therefore should be considered as only one aspect in the decision making process, rather than the decisive factor.*

### 8.1 IDENTIFICATION OF THE COSTS AND BENEFITS

#### 8.1.1 COSTS

The total cost breaks down in two major components: investment costs at the beginning of the project (capital expenditures, CAPEX) and operational costs during the lifetime of the project (operational expenditures, OPEX).

##### 8.1.1.1 CAPEX

For hydropower generation at the tidal lock in Heusden, the CAPEX include:

- 💡 civil works: power house, intake, outlet, possibly fish migration facilities;
- 💡 electromechanical equipment: turbine, control, voltage convertor, connecting cables.

89

In principle, additional costs can be considered, such as costs related to the design (including development of control procedures when drainage and active recharge are to be considered), permitting and additional infrastructure, e.g. an access road or fencing. However these costs are less straightforward to assess, and generally only contribute to a small extent in the CAPEX. Therefore, first only the civil works and electromechanical equipment are considered, to verify the financial feasibility.

According to SPLASH (2005), the costs for electromechanical equipment increase almost linearly with the power output, while the costs for the civil works depend strongly on the project site. In IMDC (2011), the CAPEX was estimated using values from literature (Montanari, 2003; Penche, 2004; SPLASH, 2005). These values generally express the investment cost per unit of installed power [€/kW], i.e. the specific cost. Figure 8-1 and Figure 8-2 illustrate the expected range of this specific cost.

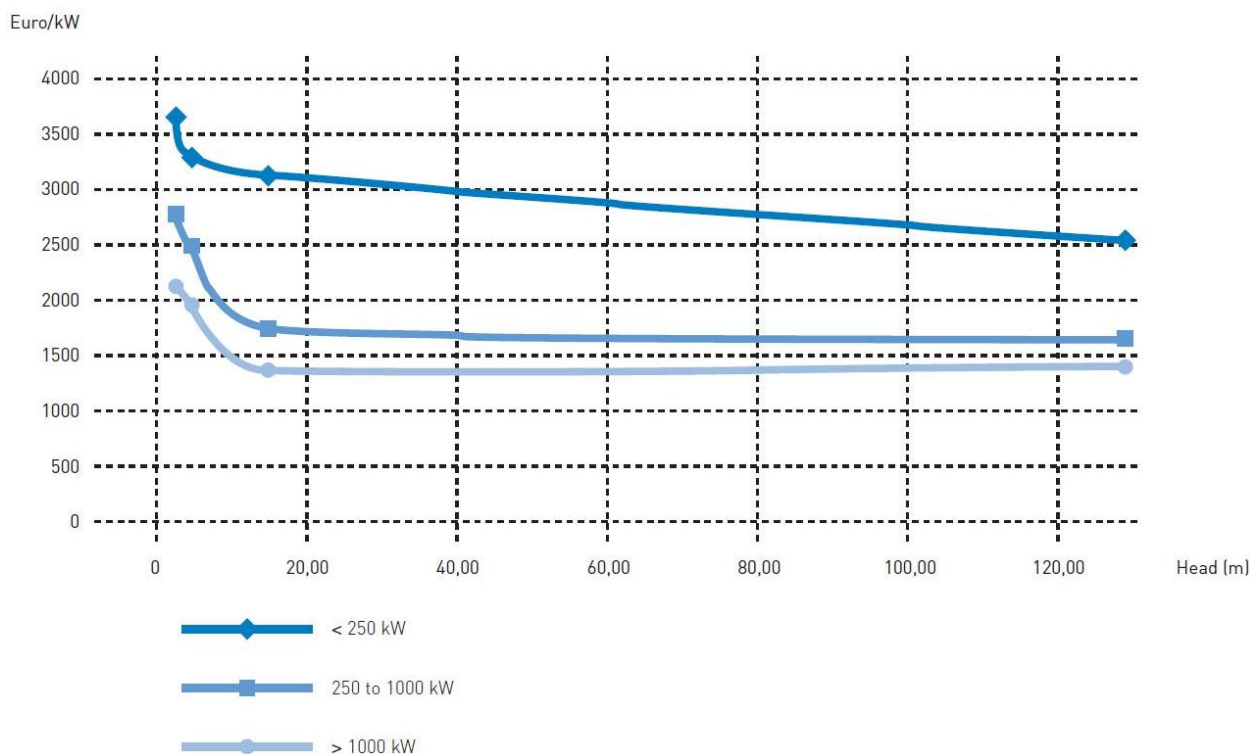


Figure 8-1: Specific cost of installed power as a function of head<sup>11</sup>.

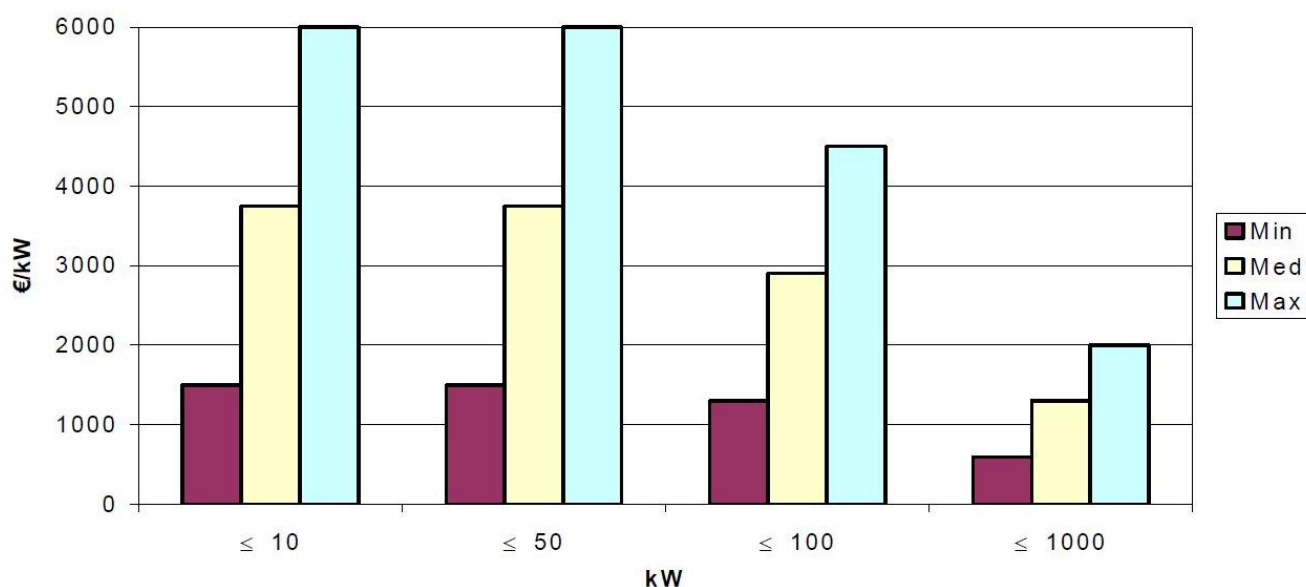


Figure 8-2: Typical turn-key investment costs for small hydropower plants<sup>12</sup>.

The above figures enable a first assessment of the potential of a site. However, in IMDC (2011) it was already recommended to base investment costs on a conceptual design, due to the large spread of the specific cost. Therefore, since this is a follow-up study of IMDC (2011), the CAPEX is estimated based on the conceptual design in the previous chapter,

<sup>11</sup> Source: European Commission, Directorate-General for Energy and Transport, Brussels, 2001. Taken from SPLASH (2005).

<sup>12</sup> Source: Scientific and Technological References Energy Technology Indicators (<http://www.cordis.lu/eesd/src/indicators.htm>). Taken from Penche (2004).

and the results are given in Table 6-1. This also enables to isolate the costs related to development of the hydropower plant from the costs for civil works related to the construction of the lock.

For comparison, the specific cost of the project can be calculated. Taking into account the investment costs from Table 6-1, and calculating the installed capacity from Equation (1) – with  $\eta = \eta_{turb} * \eta_{gen} * \eta_{trans} = 1.0$  and  $\Delta H = 2.26$  m, (this is the value that is exceeded 10% of time) the results are as follows: for S2b.4, an installed capacity of 89 kW results in a specific cost of about € 4070 per kW; for S4b.8 an installed capacity of 177 kW would result in a specific cost of about € 3047 per kW. Compared to the numbers in Figure 8-1 and Figure 8-2, these values fall well within the values given in literature. Taking into account that, in Figure 8-1, a curve for a power output of let's say 100 kW would be situated above the current one for '< 250 kW', it is clear that the specific costs of the two considered scenarios are below average. This is because part of the civil works are – rightfully – attributed to the lock. Still, despite this synergy with the lock, the specific cost remains quite high; this however is due to the very limited head available (Figure 8-1).

#### 8.1.1.2 OPEX

The OPEX are mainly maintenance costs, related to the electromechanical equipment but also the intake and outlet, e.g. removal of rubbish, but also possibly insurance or financing costs. In this study, a yearly operational cost of 1% of the total investment cost is assumed. An increase of the OPEX during the lifetime of the project could be expected, <sup>91</sup> although hydropower turbines generally do not require extensive maintenance.

It is possible to consider a different lifetime for the electromechanical equipment compared to the civil works. However, since the investment cost for the civil works is made at the beginning, it is recommended to extend the lifetime of the electromechanical part of the project to the same extent as that of the civil costs – to maximize the return on investment –, for instance by replacing the equipment. In this study, the lifetime of the project is set to 50 years – the lifetime of the lock – and after 25 years the electromechanical equipment is replaced.

In principle, the cost for demolition and recycling, the so-called decommissioning cost, should be taken into account when the full lifecycle is considered. However these costs are sometimes difficult to assess, and effort to estimate this cost should only be made when the result of the CBA is positive, to verify the solidity of the conclusions.

#### 8.1.2 BENEFITS

The economic benefits come from the sales of the generated electricity. An estimate for the selling price per MWh can be derived from Belpex. Belpex is the Belgian Power Exchange for anonymous, cleared trading in day-ahead electricity, providing the market with a transparent reference price (Belpex, 2013b). The price fluctuates heavily on a daily and weekly basis, as can be seen in Figure 8-3. On a monthly scale, the variation is less pronounced (Figure 8-4). A reasonable value to assume throughout the year appears to

be € 50 per MWh. On the long-term, an increase in this price can be expected, or at least a long-term increase is more likely than a long-term decrease.

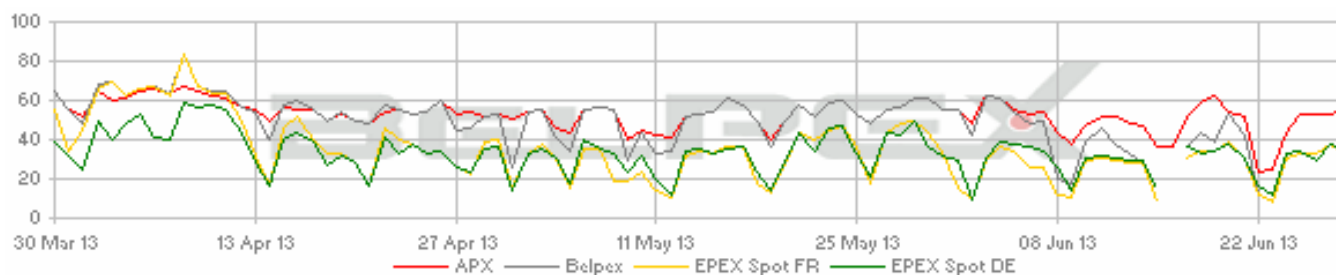


Figure 8-3: Evolution of the price of electricity [€/MWh] between 30/03/2013 and 28/06/2013, on the Belgian stock exchange and that of its neighbouring countries The Netherlands (APX), France (EPEX Spot FR) and Germany (EPEX Spot DE) (Belpex, 2013a).



Figure 8-4: Monthly average of the daily averaged Belpex index [€/MWh], for the year 2013 (Source: Belpex, 2013b).

Besides selling the electricity, governmental support is available in Belgium as well. In 2002, the federal government developed a system of 'green power certificates' (GPCs) to encourage renewable energy production<sup>13</sup>. The implementation of this system for the Flemish Region is described in the so-called Energy Decree<sup>14</sup>. For each MWh produced using renewable resources, a green certificate is awarded. This certificate is tradable, for instance it can be sold to suppliers of electricity. After all, they have to provide a minimal amount of certificates to the government. If they do not meet their quota, a fine of € 100 per missing certificate must be paid.

<sup>13</sup> Royal Order of 16 July 2002 regarding the establishment of mechanisms for the promotion of electricity produced from renewable energy sources, Belgian Official Journal of 23 August 2002.

<sup>14</sup> Decree of 8 May 2009 concerning general conditions regarding the energy policy, Belgian Official Journal of 7 July 2009.

When the fine was € 125, the average market price was above € 105 per certificate (Figure 8-5). Since the recent lowering of the fine<sup>15</sup>, the average market price is more difficult to estimate, because the markets require some time to adjust to the new situation. A first estimate can be made by applying the same ratio between the fine and the market price. This results in a selling price of € 84 per certificate.

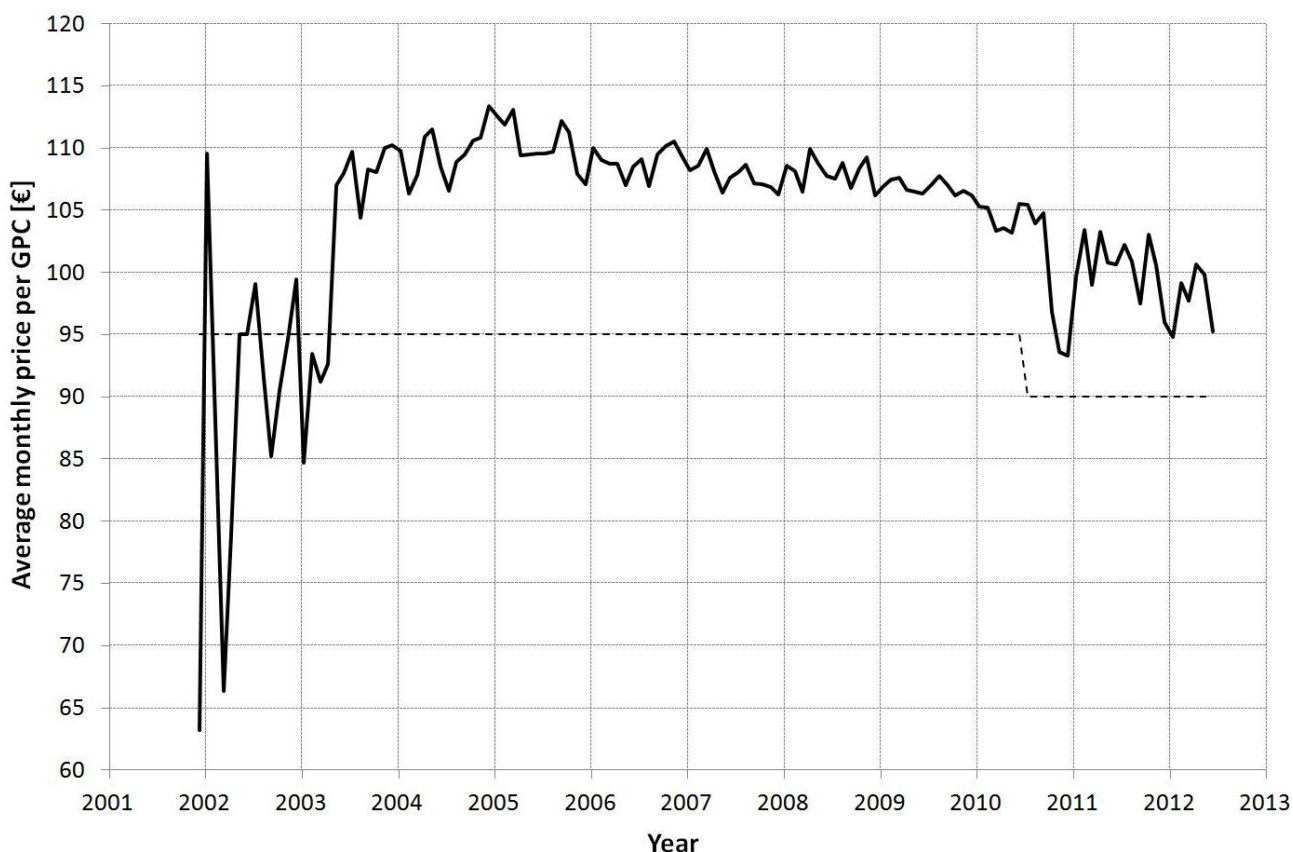


Figure 8-5 : Evolution of the average monthly price per green power certificate (GPC) (Source: VREG, 2014).

Finally, other benefits are related to the production of renewable energy as well. For example, the efforts of W&Z regarding renewable energy, being a governmental entity, serve as an example towards society. Other examples are: lower CO<sub>2</sub>-emissions, the decrease of dependency on fossil, nuclear or foreign power. Since these benefits are difficult – if not impossible – to monetize, they are not considered further. However, they should be accounted for in the decision-making process.

<sup>15</sup> This fine was recently lowered from € 125 (before 31 March 2012) to € 118 (before 31 March 2013) to € 100 (after 31 March 2013). Lowering the fine results in a decrease of the market price of a green certificate. The relevant legislation: Decree of 6 May 2011 for amending the Energy Decree of 8 May 2009, Belgian Official Journal of 10 June 2011.

## 8.2 ECONOMIC EVALUATION

The classical method to perform a CBA is to bring all costs and benefits at a moment in time  $t$ ,  $X_t$ , to their present value  $PV[X_t]$  :

$$PV[X_t] = \frac{X_t}{(1+r)^t} \quad (28)$$

In this equation,  $r$  is the discount rate. The higher the discount rate, the higher the depreciation of future costs and benefits, i.e. less value is given to costs and benefits in the future, and they will be less determinative for the final balance. A common value for the discount rate is 4%.

When the present value of all benefits  $B_i$  and all costs  $C_j$  are calculated, the net present value of an investment  $NPV$  can be calculated as the difference between the total of the present value of all benefits minus the total of the present value of all costs:

$$NPV = \sum_i \left\{ \sum_{t=0}^T PV[B_{t,i}] \right\} - \sum_j \left\{ \sum_{t=0}^T PV[C_{t,j}] \right\} \quad (29)$$

In this equation,  $T$  is the lifetime of the project. When comparing several possible investments, the ratio of the NPV with the initial investment  $I_0$  of the different options should be compared. The project with the highest value for  $NPV/I_0$  is, financially speaking, the most profitable.

## 8.3 RESULTS

Two of the scenarios from §5.3 will be investigated further: S2b.4 and S4b.8. The first scenario is considered because of its relative simplicity. After all, no complex controls have to be implemented, and the additional energy yield is negligible for the corresponding more complex scenarios, i.e. S3b.4 and S4b.4. The second one is considered because that scenario has the highest energy yield, and hence the highest revenue. Conversely, the investment costs will be higher.

The results will be analysed using graphs showing the course of the  $NPV/I_0$  ratio through time. A lifetime of 50 years for the entire project is considered, and it is assumed that the electromechanical equipment is replaced after 25 years.

### 8.3.1 FULL IMPLEMENTATION

First, the CBA is performed when considering a full implementation of the entire power generation scheme, i.e. all investments for the facilities for generating power are made, including the electromechanical equipment. In other words, all costs listed in Table 6-1 are considered for the initial investment. The results can be seen in Figure 8-6.

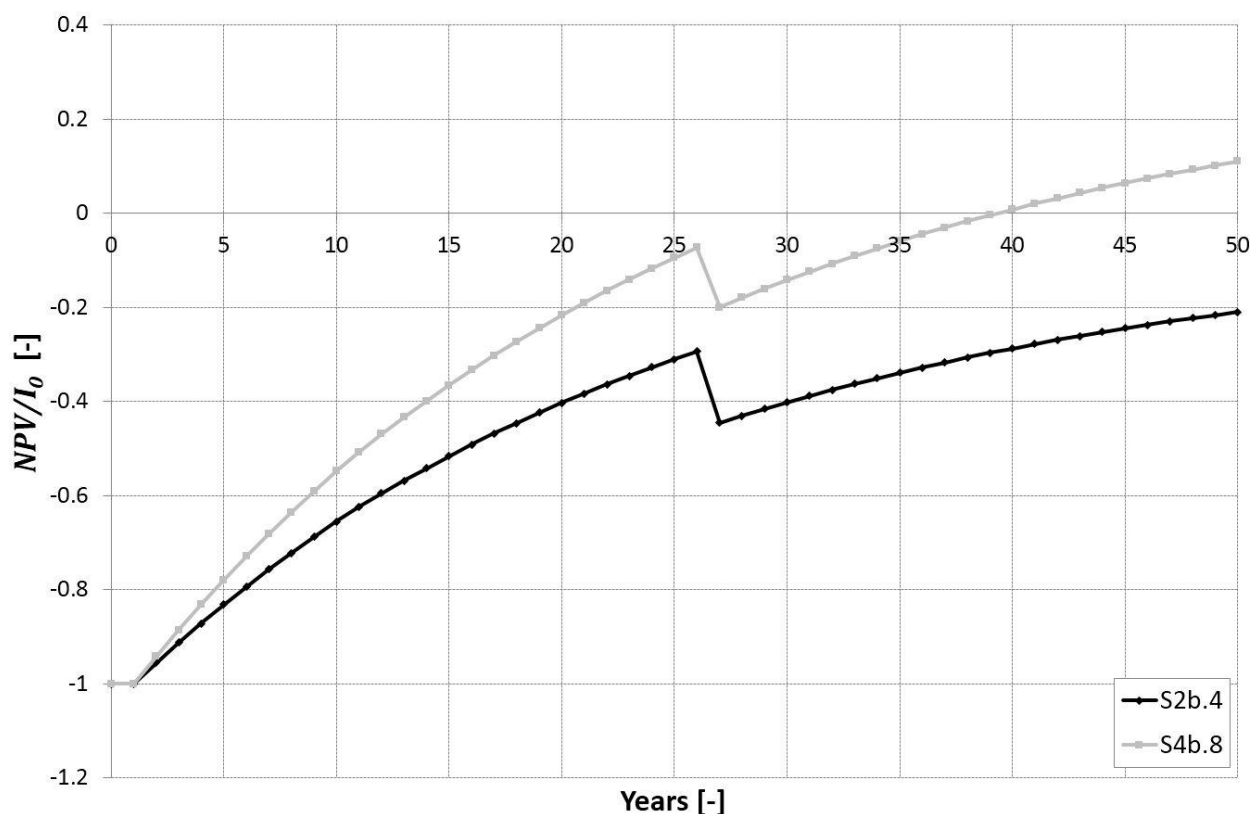


Figure 8-6: Ratio of net present value to initial investment through time, for S2b.4 and S4b.8.

Purely financially speaking, S4b.8 would be a viable project. This is mainly due to the governmental support through the GSC-system. Unfortunately the Flemish government decided to drastically reform this system, resulting in no support for hydropower projects. The results of this analysis are described in §8.3.2 below.

### 8.3.2 WITHOUT GOVERNMENTAL SUPPORT

On 21 December 2012, the Flemish government decided to drastically reform the then governing regulations for awarding green power certificates<sup>16</sup>. Due to that decision, all renewable energy classified as 'hydropower', is no longer considered eligible for governmental support through the system of green power certificates (specific cases can deviate from this, but these are not applicable for the project in this study). Therefore, the above CBA is repeated without considering the benefits from GPCs. The results, which are dramatically more negative, can be seen in Figure 8-7.

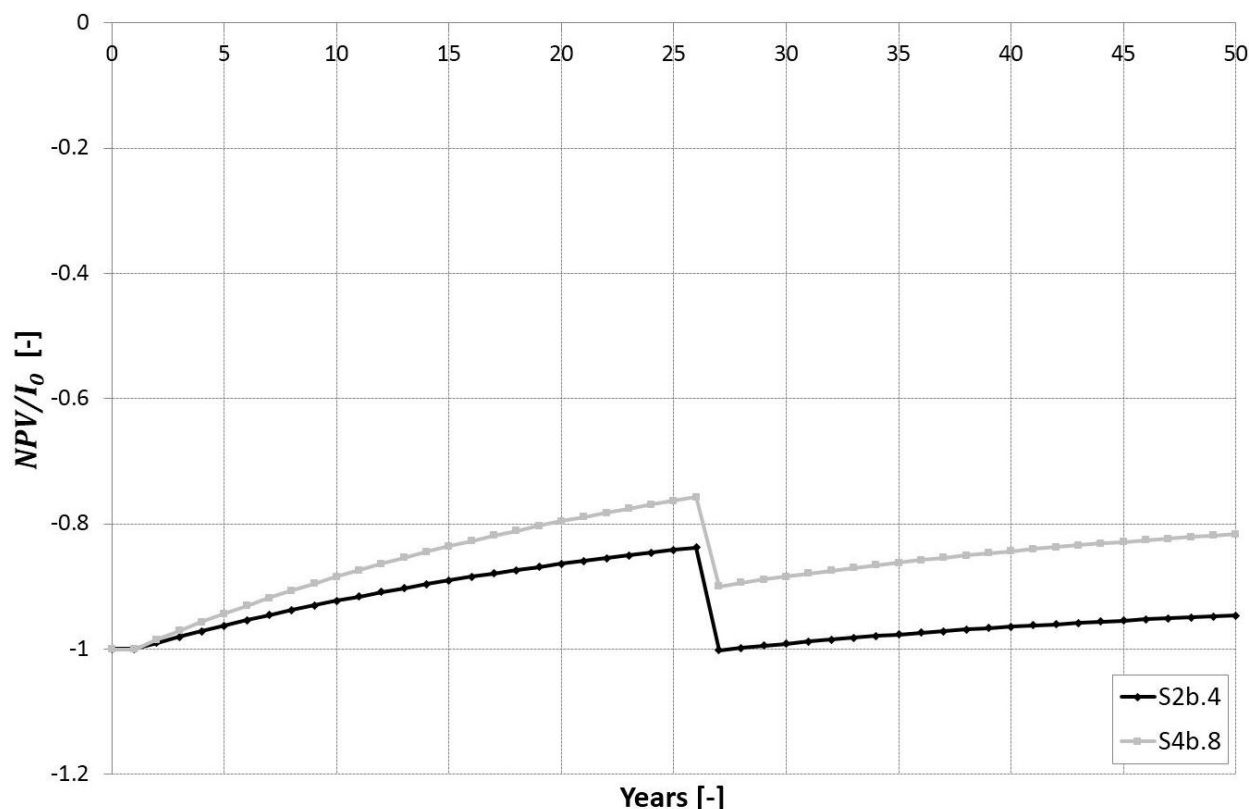


Figure 8-7: Ratio of net present value to initial investment through time, for S2b.4 and S4b.8, without green power certificates.

To conclude, the fictitious situation where power generation is possible all the time at an average head of 2 m and a design discharge of 4 m<sup>3</sup>/s, can be considered as well. The energy yield in this situation would be 510 MWh per year, as calculated in §5.3. Even then, the project would only be profitable after 43 years, when no green power certificates are awarded. With GPCs, the project would already be profitable after 8 years. This emphasizes the importance of governmental support of a possible hydropower project at the tidal lock in Heusden.

<sup>16</sup> Decision of the Flemish Government of 21 December 2012.

### 8.3.3 PHASED IMPLEMENTATION

Since a full implementation at the start of the project does not appear to be profitable, a phased implementation could be considered. In this phasing, the basement (Table 6-1) would be constructed during the construction of the lock, while the intake, the energy production and the outfall are considered as a separate project, to be executed in the future. Hence the costs for construction of the basement are excluded from the analysis.

The course of the ratio  $NPV/I_0$  can be seen in Figure 8-8. Although the curves shift upwards for both S2b.4 and S4b.8, the ratio remains negative for both scenarios.

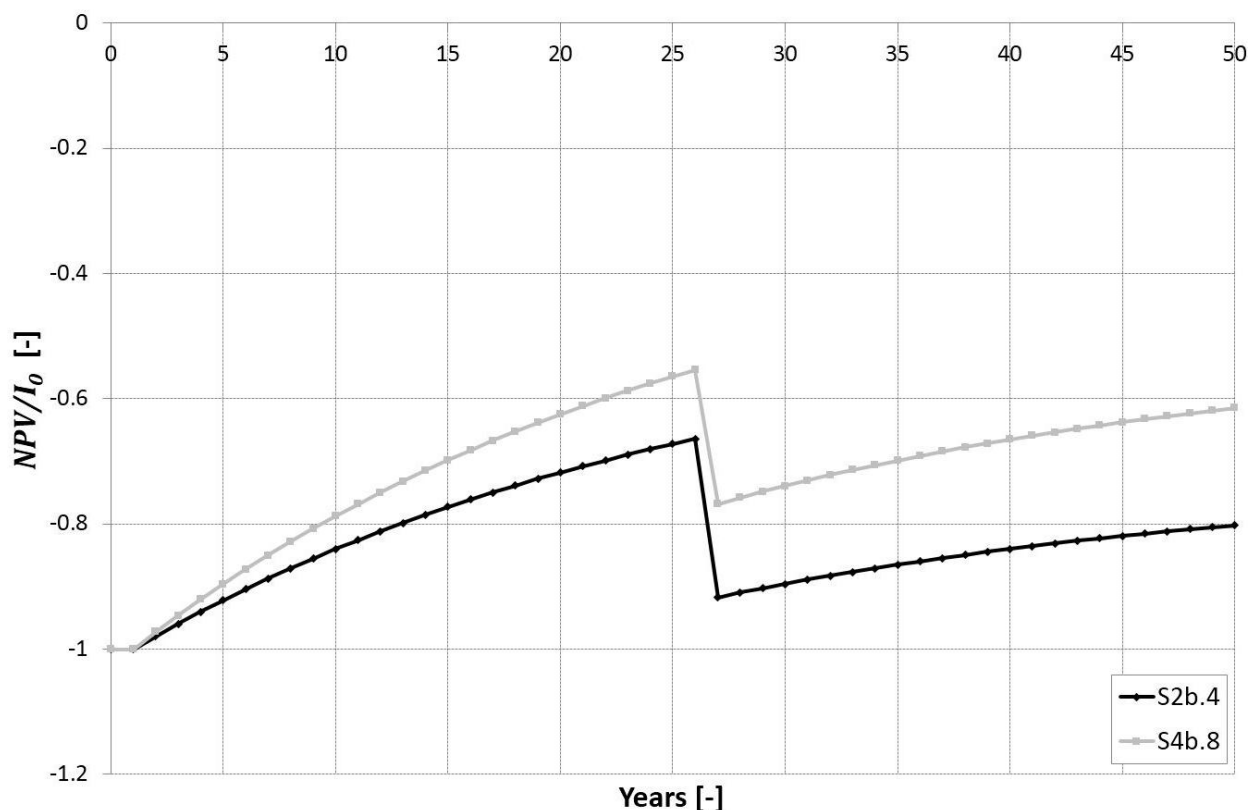


Figure 8-8: Ratio of net present value to initial investment through time, for S2b.4 and S4b.8, when only the costs for intake, energy production and outlet are considered.

### 8.3.4 LEVELIZED COST OF ELECTRICITY

To finalize, a levelized cost of electricity can be calculated within the above described economic framework. The levelized cost of electricity is the price at which the generated energy should be sold, to turn break-even during the lifetime of the project. *No subsidies are taken into account when calculating this cost.* Practically, the calculation is done by trial-and-error, until the curves in Figure 8-6 reach a zero value for  $NPV/I_0$  at 50 years. For S2b.4, this results in a levelized cost of € 161 per MWh, while this is € 126 per kW for S4b.8. For comparison, Figure 8-9 shows estimated levelized costs of new electric generating technologies in 2018, calculated by the U.S. Energy Information Administration. Based on this figure and using an exchange rate of 1.36 \$/€, the levelized cost for hydropower generation at the lock in Heusden is between that of solar photovoltaic and offshore wind. From the figure, it is also clear the levelized cost of hydroelectric power generally is lower than in Heusden. This is expected because of the resource limitations at Heusden.

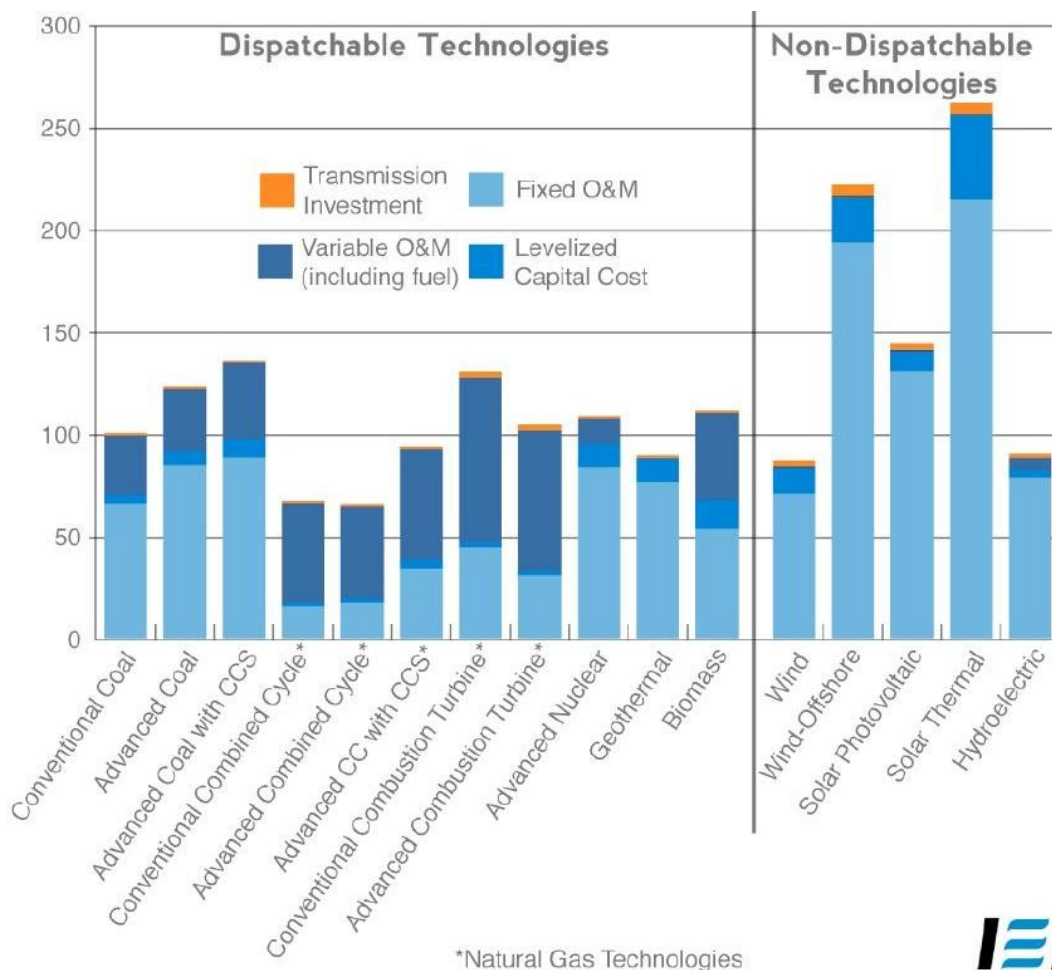


Figure 8-9: Estimated levelized cost of new electric generating technologies in 2018 [2011 \$/MWh]<sup>17</sup>.

<sup>17</sup> Source: Energy Information Administration, Annual Energy Outlook 2013. [http://www.eia.gov/forecasts/aeo/er/electricity\\_generation.cfm](http://www.eia.gov/forecasts/aeo/er/electricity_generation.cfm). Taken from the Institute for Energy Research, <http://www.instituteforenergyresearch.org/levelized-costs-of-new-electricity-generating-technologies>.

### 8.3.5 CONCLUSION

It is clear that constructing a hydropower plant at the tidal lock in Heusden does not result in a profitable investment, given the assumptions made. Then again, it should be noted that in this analysis, only the easily monetized costs and benefits were considered.

The unprofitability results from the small energy yield compared to the required CAPEX. The energy yield is low because of the combination of the following three reasons:

- 💡 The available discharge is limited in magnitude. There also exists a limitation regarding the amount of time a certain discharge is available, but this can be coped with by intelligently controlled drainage from and recharge to KGT.
- 💡 The available head is limited in magnitude. On average, a maximum head of about 2.8 m is reached every day. Due to the tidal variation in water level in the Sea Scheldt, power generation occurs on average with a head of 2 m, which is very low.
- 💡 The available head is limited in time. Due to the tide, only about 50% of time the head is sufficiently large to generate power.

Hence the available resources appear to be the limiting factor. Hypothetically speaking, if it was possible to change only one of these three limitations, it would be most interesting to have the head available during a longer period of time, since increasing the design flow would increase the CAPEX as well, while an increased time frame for power generation does not affect the required investment costs.

## 9 CONCLUSIONS

Waterwegen en Zeekanaal NV – Department Sea Scheldt is investigating the feasibility of tidal energy harvesting in the Sea Scheldt, on the one hand using potential energy at the to-be-constructed tidal lock in Heusden, and on the other hand kinetic energy at different locations in the Sea Scheldt. This report describes the results of the detailed feasibility study of tidal energy harvesting using potential energy at the tidal lock in Heusden.

At Heusden, a new tidal lock will be constructed, its main objectives being (i) safety against flooding from the Sea Scheldt during extreme events (ii) re-enabling navigability of the Sea Scheldt towards Gentbrugge for recreational shipping (iii) enhance the natural environment (iv) enable recreation along the river banks.

The site will be characterized by a maximum head difference of about 2 m, however due to the tide in the lower reach, i.e. the Sea Scheldt, the available hydraulic head varies considerably during the day. Taking into account that power can only be generated with a certain minimum head, e.g. 1 m, only 49.5% of time power generation is possible (only unidirectional turbines are considered here). Moreover, there exists a high pressure on the water use in the region around Ghent. For the channel between Ghent and Terneuzen (The Netherlands), a treaty between both countries exists, posing a limit on the water usage during dry periods.

These limitations of 'resource' – small, variable head and limitations on the flow to be used – renders energy harvesting at this location challenging. Due to these strong variations in both available head and flow, a methodology has been developed to estimate the average yearly energy yield. After that, several flow scenarios have been defined, in which different possibilities have been investigated to maximize the water volume available for power generation. 100

From these scenarios it becomes clear that, when applying suitable technology – i.e. low-head turbines – and controlling the surrounding hydraulic structures – to actively recharge to and drain from the upper reach – energy harvesting becomes technically feasible, although large yields should not be expected. Depending on the flow scenario considered (starting from S2a), the average yearly energy yield varies between 85-280 MWh, or electric energy for about 25 to 80 households.

After estimating the energy yield, a conceptual design has been made, together with a cost estimate, which served as input for a cost-benefit analysis. The specific cost – i.e. the investment cost per installed kW – agreed with values found in literature.

From the cost-benefit analysis, it can be stated that – purely financially speaking – it will be very difficult to obtain a profitable project, at least within the assumptions made. A levelized cost of around € 150 per kW is expected, a number comparable to that of offshore wind. This is mainly due to the limited resources available. Nonetheless, other factors could lead to the decision of continuing the efforts for energy harvesting at this location, such as the pioneering role of Waterwegen en Zeekanaal nv, the continually increasing demand for renewable energy, or changes in economic factors, e.g. electricity price increase or more efficient and cheaper technology.

## 10 REFERENCE LIST

- Afdeling Kust – Vlaamse Hydrografie (2012). Getijtafels (in Dutch). IVA Maritieme Dienstverlening en Kust, Brussel. Depotnr. D/2012/3241/222.
- ANRE & ODE-Vlaanderen (1999). Kleine waterkracht (in Dutch). Ministry of the Flemish Community.
- Belpex (2013a). Consulted on 28 June 2013. <http://www.belpex.be>.
- Belpex (2013b). Consulted on 28 October 2013. <http://www.belpex.be>.
- Breine J. (2009). Fish assemblages as ecological indicator in estuaries: the Zeeschelde (Belgium). PhD theses of the Research Institute for Nature and Forest 2009 (INBO.T.2009.1). PhD thesis, Instituut voor Natuur- en Bosonderzoek/Katholieke Universiteit Leuven, Leuven. ISBN 978-90-103-0299-2.
- Burger C.V., Parkin J.W., O'Farrell M., Murphy A. and Zeligs J. (2012). Non-Lethal Electric Guidance Barriers for Fish and Marine Mammal Deterrence: A Review for Hydropower and Other Applications. *HydroVision Brazil*, 25-27 September 2012, Rio de Janeiro, Brasil.
- Coen L., D'Haeseleer E., Peeters P. and Mostaert F. (2012). Studie ten behoeven van aanleg van overstromingsgebieden en natuurgebieden in het kader van het Sigmaplan: Ondersteunende studies: sluis Heusden (in Dutch). Version 2\_0. 101 WL Reports, 713\_15m. Flanders Hydraulics Research, Antwerp, Belgium.
- Coenen J., Antheunisse M., Beekman J. and Beers M. (2013). Handreiking Vispassages in Noord-Brabant (in Dutch). Water board De Dommel, Water board Aa and Maas and Water board Brabantse Delta.
- De Boeck K., Michielsen S., Pereira F. and Mostaert F. (2012). Opmaak van modellen voor onderzoek naar waterbeschikbaarheid en -allocatiestrategieën in het Scheldtestroomgebied: Deelrapport 4 – Modellerings van de huidige toestand op regionaal niveau (in Dutch). Version 3\_0. WL Reports, 724\_04. Flanders Hydraulics Research, Antwerp, Belgium.
- EA (2012). Hydropower Good Practice Guidelines: Screening requirements. Environmental Agency, December 2012.
- Fishways Global (2013). Fishways Global, LLC. Consulted on 27 March 2013. <http://www.fishwaysglobal.com>.
- FSG (2013). Fish Guidance Systems Ltd. Consulted on 27 March 2013. <http://www.fish-guide.com>.
- Hamel M.J., Brown M.L. and Chipps S.R. (2008). Behavioral responses of rainbow smelt to in situ strobe lights. *N. Am. J. Fish. Manage.*, 28(2), 394-401. doi: 10.1577/M06-254.1.

- IMDC (2011). Getijdenenergie op de Zeeschelde – dossier Interreg: Haalbaarheidsstudie (in Dutch). Final report. Study commissioned by Waterwegen en Zeekanaal NV, Department Sea Scheldt. I/RA/11372/11.071/TGO.
- IMDC (2012). 11372 – Sluis te Melle: vismigratie (in Dutch) (Note on fish migration through the weir channels at the lock). 23 April 2012. I/NO/11372/12.111/MOE.
- IMDC in association with Tritel, Technum and Ecobe (2011). Zeeschelde Gentbrugge-Melle en Bastenakkers: Voorontwerp sluis (in Dutch). I/NO/11372/11.056/JVB.
- IMDC in association with Technum and Universtiy of Antwerp (2013). Bevaarbaarheid Boven-Zeeschelde: Studie en technische ontwerpen Scheldemeander Gentbrugge-Melle: Hydraulische studie ZGM (in Dutch). For Waterways and Seacanal – Sea Scheldt Division. I/RA/11372/12.039/MOE.
- Kroes M.J. & Monden S. (Eds.) (2005). Vismigratie; een handboek voor herstel in Vlaanderen en Nederland (in Dutch). Ministry of the Flemish Community, AMINAL Department Water, Brussels, Belgium. Organisation for the Improvement of the Inland Fishery, Nieuwegein, The Netherlands. ISBN 90-803245-6-6.
- Maes J., Turnpenny, A.W.H., Lambert D.R., Nedwell J.R., Parmentier A. and Ollevier F. (2004). Field evaluation of a sound system to reduce estuarine fish intake rates at a power plant cooling water inlet. *J. Fish Biol.*, 64(4), 938-946. doi: 10.1111/j. 1095-8649.2004.00360.x.
- McLean A.R. (2008). Strobe lights as a fish deterrent. MSc thesis, Royal Roads University, Victoria, British Columbia, Canada.
- Montanari R. (2003). Criteria for the economic planning of a low power hydroelectric plant. *Renewable Energy*, 28, 2129-2145.
- Noatch M.R. & Suski C.D. (2008). Non-physical barriers to deter fish movements. *Environ. Rev.*, 20, 71-82.
- Ovivo (2013). Ovivo. Consulted on 24 October 2013. <http://www.ovivowater.nl>.
- Penche C. (2004). Guide on how to develop a small hydro site. European Small Hydropower Association (ESHA).
- PROCOM SYSTEM (2013). PROCOM SYSTEM S.A. Visited on 27 March 2013. <http://www.procomsystem.pl>.
- Profish (2013). Profish. Consulted on 27 March 2013. <http://www.profish-technology.be>.
- Sonny D., Knudsen F.R., Enger P.S., Kvernstuen T. and Sand O. (2006). Reactions of cyprinids to infrasound in a lake and at the cooling water inlet of a nuclear power plant. *J. Fish Biol.*, 69(3), 735-748. doi: 10.1111/j.1095-8649.2006.01146.x.
- SPLASH (2005). Guidelines for micro hydropower development. SPLASH Project, Altener Programme – European Commission.

VREG (2014). Vlaamse Regulator van de Elektriciteits- en Gasmarkt (Flemish Regulator of the Electricity and Gas market). Consulted on 7 January 2014. <http://www.vreg.be> (in Dutch)

Winter H.V., Bierman S.M & Griffioen A.B. (2012). Field test for mortality of eel after passage through the newly developed turbine of Pentair Fairbanks Nijhuis and FishFlow Innovations. For Pentair Fairbanks Nijhuis and FishFlow Innovations. Institute for Marine Resources and Ecosystem Studies (IMARES), Wageningen University. Report number C111/12.

## 11 ANNEXES

### ANNEX 1

### BILL OF QUANTITIES CONCEPTUAL DESIGN - CIVIL WORKS 4 AND 8 m<sup>3</sup>/s

#### ESTIMATE OF INITIAL INVESTMENT COST - 4 m<sup>3</sup>/s TURBINE

element	height [m]	width [m]	length [m]	quantity [unit]	unit	unit cost [EUR / unit]	cost [EUR]
<b>basement</b>							
sheet piles construction pit	12.50	-	15.00	187.50	m <sup>2</sup>	160.00	30,000
concrete - foundation	0.50	4.50	12.00	27.00	m <sup>3</sup>	100.00	2,700
reinforced concrete floor slab	0.50	4.50	11.50	25.88	m <sup>3</sup>	300.00	7,763
construction steel floor slab 50 kg/m <sup>3</sup>	-	-	-	1,293.75	kg	1.00	1,294
reinforced concrete - walls	9.00	0.50	30.00	135.00	m <sup>3</sup>	300.00	40,500
construction steel walls 50 kg/m <sup>3</sup>	-	-	-	6,7500	kg	1.00	6,750
precast concrete removable ceiling	-	4.50	11.50	51.75	m <sup>2</sup>	400.00	20,700
access ladder	18.00	-	-	18.00	m	150.00	2,700
winch 1 ton	-	-	-	1.00	-	10,000	10,000
<b>intake</b>							
trash rack 6 m x 2.2 m	-	-	-	1.00	-	3,000.00	3,000
connection dry basement - turbine	-	-	1.00	1.00	m	250.00	250
connection to dry basement Ø 800 mm	-	-	-	1.00	-	1,000.00	1,000
control valve Ø 800 mm	-	-	-	1.00	-	2,500.00	2,500
connection to wet basement	-	-	-	1.00	-	2,000.00	2,000

<b>outfall</b>								
connection turbine - diffuser Ø 1000 mm	-	-	1.00	1.00	m	350.00	350	
divergent outfall piece Ø 1000 to 2000 mm	-	-	3.00	2.28	m <sup>3</sup>	2,000.00	4,565	
connection diffuser - Sea- Scheldt Ø 2000 mm	-	-	1.50	1.50	m	1,000.00	1,500	
connection to Sea-Scheldt Ø 2000 mm	-	-	-	1.00	-	4,000.00	4,000	
control valve Ø 2000 mm	-	-	-	1.00	-	3,000.00	3,000	
erosion protection 50-400 kg	0.50	10.00	20.00	100.00	m <sup>3</sup>	40.00	4,000	

**ESTIMATE OF INITIAL INVESTMENT COST - 8 m<sup>3</sup>/s TURBINE**  
[changes in relation to 4 m<sup>3</sup>/s in red]

element	height [m]	width [m]	length [m]	quantity [unit]	unit	unit cost [EUR / unit]	cost [EUR]
<b>basement</b>							
sheet piles construction pit	12.50	-	<b>18.38</b>	<b>229.75</b>	m <sup>2</sup>	160.00	<b>36,760</b>
concrete - foundation	0.50	<b>4.63</b>	<b>16.75</b>	<b>38.73</b>	m <sup>3</sup>	100.00	<b>3,873</b>
reinforced concrete floor slab	0.50	<b>4.63</b>	<b>16.75</b>	<b>38.73</b>	m <sup>3</sup>	300.00	<b>11,620</b>
construction steel floor slab 50 kg/m <sup>3</sup>	-	-	-	<b>1,936.72</b>	kg	1.00	<b>1,937</b>
reinforced concrete - walls	9.00	0.50	<b>36.75</b>	<b>165.38</b>	m <sup>3</sup>	300.00	<b>49,613</b>
construction steel walls 50 kg/m <sup>3</sup>	-	-	-	<b>8,268.75</b>	kg	1.00	<b>8,269</b>
precast concrete removable ceiling	-	<b>5.63</b>	<b>13.75</b>	<b>77.34</b>	m <sup>2</sup>	400.00	<b>30,938</b>
access ladder	18.00	-	-	18.00	m	150.00	2,700
winch 1 ton	-	-	-	1.00	-	10,000	10,000

<b>intake</b>							
trash rack 6 m x 2.2 m	-	-	-	1.00	-	<b>5,000.00</b>	<b>5,000</b>
connection dry basement - turbine	-	-	1.00	1.00	m	<b>400.00</b>	<b>400</b>
connection To dry basement Ø 1,400 mm	-	-	-	1.00	-	1,000.00	1,000
control valve Ø 1,400 mm	-	-	-	1.00	-	2,500.00	2,500
connection to wet basement	-	-	-	1.00	-	<b>3,000.00</b>	<b>3,000</b>
<b>enlarging weir channel</b>	<b>2.2</b>	<b>0.5</b>	<b>86.58</b>	<b>95.24</b>	<b>m<sup>3</sup></b>	<b>300.00</b>	<b>28,570</b>
<b>outfall</b>							
connection turbine diffuser Ø 1800 mm	-	-	1.00	1.00	m	<b>800.00</b>	<b>800</b>
divergent outfall piece Ø 1800 to 3500 mm	-	-	3.00	<b>6.25</b>	m <sup>3</sup>	2,000.00	<b>12,504</b>
connection diffuser - Sea- Scheldt Ø 3500 mm	-	-	1.50	1.50	m	<b>2,500.00</b>	<b>3,750</b>
connection to Sea-Scheldt Ø 3500 m m	-	-	-	1.00	-	<b>5,000.00</b>	<b>5,000</b>
control valve Ø 3500 mm	-	-	-	1.00	-	<b>8,000.00</b>	<b>8,000</b>
erosion protection 50-400 kg	0.50	10.00	20.00	100.00	m <sup>3</sup>	40.00	4,000